The University of Hull

Computer simulation of the osteocyte and bone lining cell network and the effect of normal physiological changes in cellular functions on that network

A thesis submitted in fulfilment of the requirements for the degree of Doctor of Philosophy in the University of Hull

by

Masoumeh Jahani

April 2012

Abstract

Osteocytes play a critical role in the regulation of bone remodelling by translating strain due to mechanical loading into biochemical signals transmitted through the interconnecting lacuno-canalicular network to bone lining cells (BLCs) on the bone surface. This work aims to examine the effects of disruption of that intercellular communication by simulation of osteocyte apoptosis and microcrack in the bone matrix. A model of a uniformly distributed osteocyte network has been developed that stimulates the signalling through the network to the BLCs based on strain level. Bi-directional and asymmetric communication between neighbouring osteocytes and BLCs is included; with propagation of the signal through the network gradually decreasing by a calcium decay factor. The effect of osteocyte apoptosis and microcracks are then examined by preventing signalling at and through the affected cells. It is found that a small percentage of apoptotic cells and tiny microcracks both lead to a significant reduction in the peak signal at the BLCs. The simulation shows that either apoptosis of only 3% of the osteocyte cells or tiny microcrack of 42μm, 42μm below the surface leads to a significant reduction in the peak signal at the BLCs. Furthermore, experiments with the model confirm how important the location and density of the apoptotic osteocytes are to the signalling received at the bone surface. The result also shows the importance of the location and length of microcrack on the signalling of BLC. The first may explain a possible mechanism leading to increased remodelling activity observed with osteoporosis, and the second, the mechanism driving normal bone remodelling and maintenance.

Acknowledgments

There are so many people I would like to thank, both academically and personally. The greatest thanks go to my supervisor Professor Michael Fagan for his continual support and encouragement throughout this programme of study. I have been tremendously fortunate in having superb supervisor. His detailed and constructive feedback has been essential to the intellectual clarity and coherence of the thesis. My sincerest thanks also go to Dr Catherine Dobson for both the support and interest she has given me. I would like also to extend my special thanks to Prof Ron Patton for his support and motivation and also for his allowing me to get the insight that I needed to complete the thesis. I wish also to acknowledge the help, advice and support offered by my colleagues in Medical and Biological Engineering (MBE) research group - too numerous to mention here – who kept me going and provided moral assistance on the many occasions when pressure of work became hard to bear. I specially would like to thank Kathryn Hoyle. She read the first draft of the thesis, gave insightful advice and made excellent revision. Catharine you are a cherished friend. Sue Taft and the entire staff at MBE made me feel at home and gave me intellectual and physical space necessary to complete the thesis. I really appreciate it. I am immensely indebted to my family and friends for their constant love and support, particularly to my Mum and Dad for getting us to where we are now, without their courage, perseverance, independence and commitment to giving me and my sisters the best life, I really wouldn't be writing this now. Mum and Dad, thank you for being the best parents I could ask for. You are my rock. Faezeh my younger sister thanks for your continued support you offered to me

during the last three years. Razieh my older sister I appreciate your moral support and encouragement. Hussein Miri our family friend thank you for your general help with everything. Undoubtedly, I owe the greatest debt to my husband, Pedram. From the proposal's inception to the day I submitted this thesis, he provided the sustenance, intellectual and emotional, without which I could not have completed it. His contribution is on every page. Finally, and certainly by no means least I would like to mention, my little angel, Arina who arrived in the most critical time of my study (twenty months ago). The overwhelming self-motivation, commitment and most of all the sense of belief that told me never to give up all came from her. The sole reason I finished this thesis was to make her proud of having a well-educated Mum. I dedicate this study in its entirety to her.

Table of contents

List of figures

List of tables

Chapter 1 Introduction

Osteocytes are the most abundant cells in bone, accounting for more than 95% of all bone cells. They are osteoblastic cells that are left in the bone matrix after bone modelling and remodelling (Manolagas, 2006, Seeman, 2006), with a normal cell density between 20,000 and 80,000 cells/mm^3 (Marotti, 1996, Parfitt, 1990, Mullender et al., 1996) and a lifespan which is possibly up to 50 years, significantly longer than the typical 3 month lifespan of osteoblasts (Frost, 1966, Manolagas and Parfitt, 2010). Osteocytes are located in cavities (lacune) and are connected to each other by canals (canaliculi) (Palumbo et al., 1990b, Zhang et al., 2006b), which enable them to communicate with each other and with bone lining cells (BLCs) at the surface of bone (Figure 1-1) (Batra et al., 2011, Duncan and Turner, 1995, Ishihara et al., 2008, Kamioka et al., 2007, Yellowley et al., 2000, You et al., 2008). It is widely believed that this osteocyte-bone lining cell network controls the adaptive bone remodelling process through the sensing of mechanical loading on the bone and transmission of signals to BLCs at the bone surface (Burger and Klein-Nulend, 1999b, Bonewald, 2011, Guo et al., 2006, Tatsumi et al., 2007, Adachi et al., 2009b).

Although the importance of the osteocyte network in the mechanotransduction processes of bone is now well established, some of the mechanisms involved are still unclear. A recent study proposed that mechanotransduction in the osteocyte takes place in three steps: 1) stimulation of the osteocyte; 2) detection of the stimulation and 3) initiation of a signalling cascade (Rochefort et al., 2010). The

osteocyte senses mechanical strain (Adachi et al., 2009b, Wang, 2008, Weinbaum et al., 1994, Rubin, 1984, Turner et al., 1994, Han et al., 2004, Cowin, 2002) with functional gap junctions providing the intercellular communication between osteocytes and the transportation of signalling molecules such as calcium (Ishihara et al., 2008, Yellowley et al., 2000). Adachi et al. (2009a) identified asymmetric calcium signalling between osteocytes and BLCs, which they proposed may explain why the region close to the bone surface was mechanically sensitive to osteocytic mechanosensation and cellular communication. It was also observed that intercellular calcium rises in a stimulated bone cell and is propagated to neighbouring cells through gap junctions, but intercellular calcium signalling of bone cells declines when the stimulus is removed from the cell (Charras and Horton, 2002).

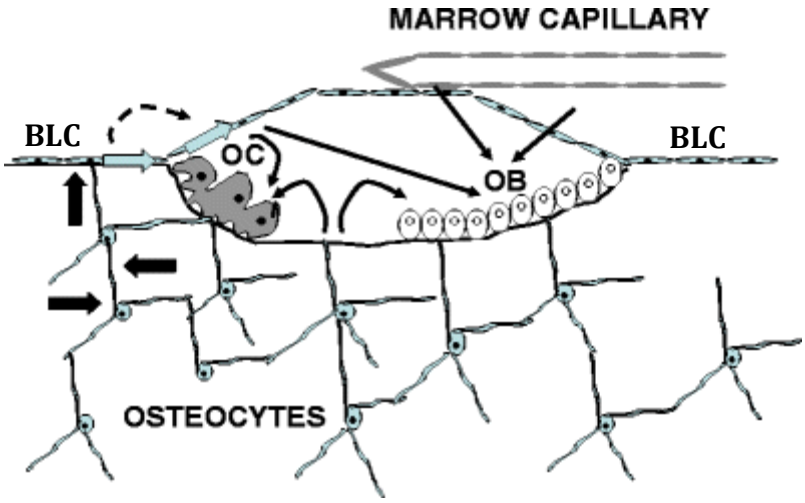

Figure 1-1: Connections between the bone lining cells (BLC), osteocyte network and the bone remodelling compartment. Gap junction provides connection between bone cells. It may also provide a pathway (*block arrows*), by that signals generated in deep bone reach the bone lining cells on the bone surface to initiate remodelling event by osteoclasts (OC) and osteoblasts (OB) in response to mechanical stimuli (Eriksen, 2010).

The formation of a microcrack which causes disruptions to the canalicular connections in the osteocytic network is a potential stimulus which initiates bone

remodelling. The rupture of cell processes by the microcrack also induces apoptosis in the osteocyte (Hazenberg et al., 2006, Taylor et al., 2007). Aging, loss of ability to sense microdamage signal, loss of mechanical strain and deficiency of sex hormones have all been shown to promote osteocyte death or apoptosis. Apoptotic osteocytes can also occur in association with pathologic conditions such as osteoporosis with 6% to 10% increase in cell apoptosis (Qiu et al., 2003, Almeida et al., 2007), and iliac cancellous osteocyte density is reported to decline in patients with a vertebral fracture (Qiu et al., 2003, Almeida et al., 2007).

In this study, we developed a simulation of cellular communication in the osteocyte-BLC network which was initiated by mechanical strain. Osteocyte signal propagation, the corresponding BLC signals, and the effect of osteocyte apoptosis and microcracks on that signalling were investigated.

Simulation of the osteocyte-bone lining cell network necessitates a fundamental knowledge of bone biology, for better understanding of the mechanotransduction mechanism and bone remodelling. These subjects are covered in Chapter 2, where bone cells, communication pathways between cells, particularly between osteocytes and bone lining cells, mechanotransduction in the osteocyte network and apoptosis in osteocytes and microcracks are outlined.

Previous theoretical and experimental investigations into the role of the osteocyte network are critically reviewed in Chapter 3. The various simulations and experiments are discussed individually with regard to their relevance to the

current work. Because the field is complex and the current process of mechanotransduction are still not unanimously agreed upon.

The development of the simulation algorithms of the simple osteocyte network are established in Chapter 4, it is extended to include bone lining cells and consider the effect of heterogeneity on cellular functions is examined.

The simulation is further extended to include asymmetric cellular communication in the osteocyte and BLC network with “calcium decay” in Chapter 5.

Chapter 6 considers the effect of apoptosis on signalling in the osteocyte-bone lining cell network. The simulation is extended further to investigate the effect of microcracks on this network.

The major findings of the research are highlighted and discussed in the relation to previous work reported in the literature and implications for further development and improvement of the work are also discussed in Chapter 7.

Finally Chapter 8 provides some brief conclusions about the work in this thesis and suggests for future research and development, which could be carried out in this area.

In brief, the main objectives of this work are:

1. To develop a basic simulation of cellular communication in the osteocyte and bone lining cell network and examine the effect of heterogeneity in cellular functions.

2. To integrate into the simulation, asymmetric communications between osteocytes and bone lining cells, and “calcium decay”.
3. To model the effect of apoptotic osteocytes on the signalling of the osteocyte-bone lining cell network.
4. To model the effect of microcracks with of various lengths and locations, in the signalling on the bone surface and osteocyte network.
5. Where possible, to validate the results obtained from these simulations.

Chapter 2 Literature review

2.1 Introduction

Bone is the key constituent of the musculoskeletal system and differs from the connective tissues in rigidity and hardness. The major cellular elements of bone include osteoclasts, osteoblasts, osteocytes, and bone-lining cells. An introduction to bone cells and their properties is presented in this chapter, with a special focus on the osteocyte. The key features of osteocytes such as their formation, death, and density are discussed, as well as the function and role of active osteocytes and apoptotic osteocytes in bone remodelling, mechanotransduction mechanisms and bone disease. Finally, communication mechanisms in the osteocyte network, such as gap junctions and hemichannels, are discussed.

2.2 Cortical bone

Cortical bone is a dense, compact tissue, which forms the diaphyses of long bones and outer shell of the metaphyses. Cortical bone accounts for 80% of the skeletal mass in the adult human skeleton, with the remaining 20% being cancellous bone. There are a number of differences between cortical and cancellous bone such as; bone development, architecture, and function, the blood supply, proximity to the bone marrow, rapidity of turnover and magnitude of age-dependent changes and fractures. At the tissue level, human cortical bone contains secondary osteons surrounding Haversian canals, enclosed in interstitial tissue, with cement lines separating the interstitial bone tissue from the osteons. Each osteon consists of

concentric lamellae, among which the osteocytes reside in cavities called lacunae (Figure 2-1).

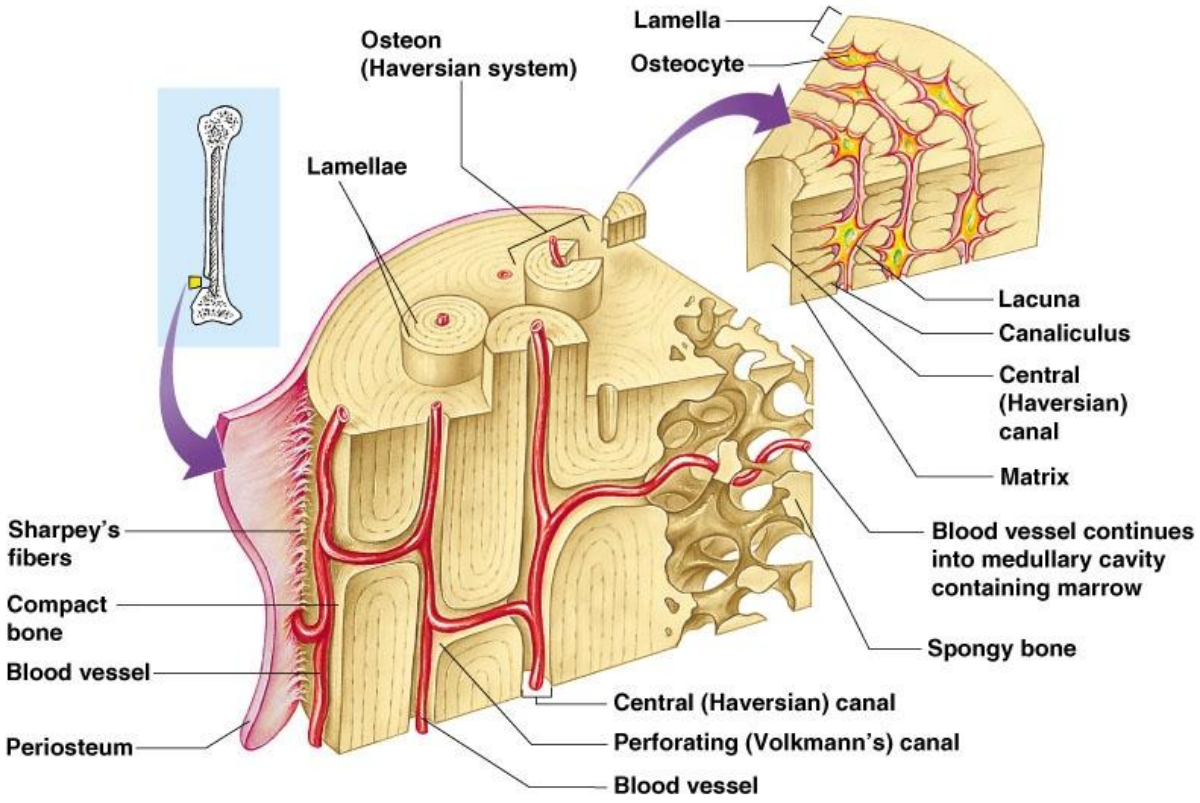

Figure 2-1: Diagram of the microstructure of cortical and cancellous bone (Marieb and Hoehn, 2010).

2.3 The osteocyte

2.3.1 The osteocyte and canalicular network

Osteocytes are dendritic cells that are embedded in lacunae within the lacuna-canalicular network. Long and slender, cytoplasmic processes radiate in all directions from the lacunae which contain the cell body of the osteocytes (Figure 2-2), the surface of bone has the highest density of these radiations. They pass through the bone matrix in very thin canals, called canaliculi, via gap junctions, and

are connected to cells in the bone surface and bone marrow. The length of canaliculi varies from 20 to 60μm, depending on the location within bone and the species of animals (Schneider et al., 2010, Wang et al., 2005a). Canaliculi provide the communication passages between osteocytes and their neighbours and between osteocytes and bone lining cells (Seeman, 2006, Seeman and Delmas, 2006) (Figure 2-3). However, Kamioka et al. (2001) observed that some of the canaliculi at the surface are not connected to the bone lining cells and suggested that there may also be a signalling system between osteocytes and the bone marrow.

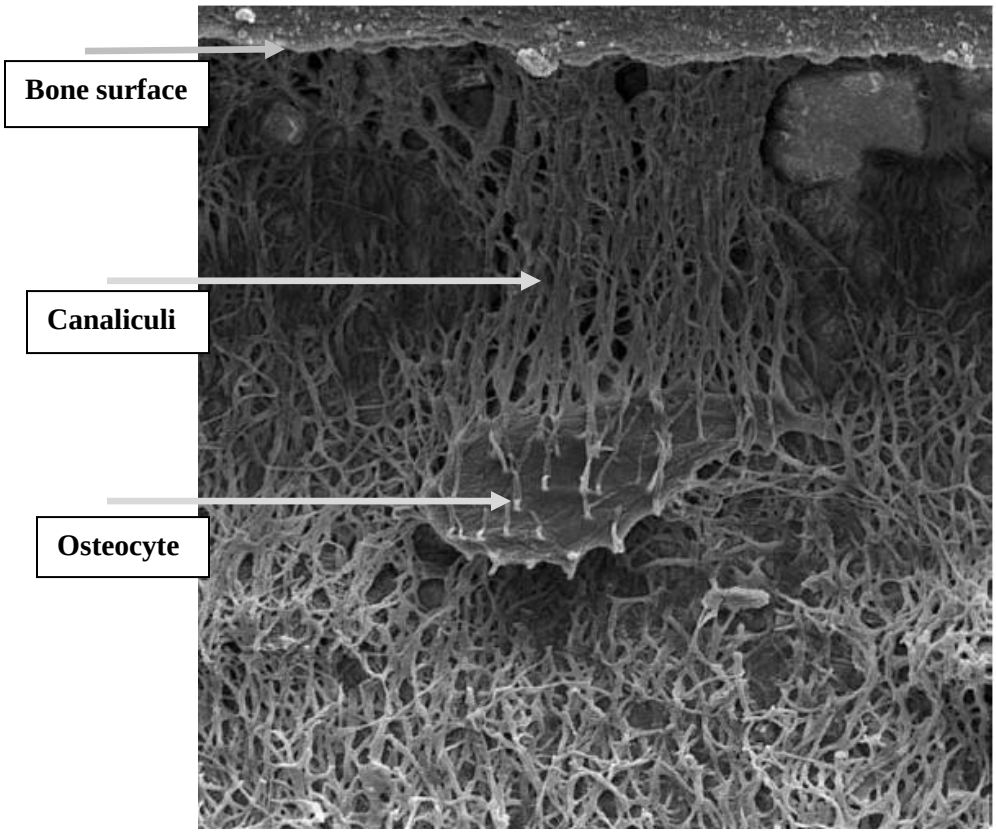

Figure 2-2: An image of a murine bone section by electron microscopy that shows that an osteocyte lacuna connects with bone lining cells through a network of canaliculi toward the bone surface (Bonewald, 2011).

According to some studies, canaliculi formation is an active process (Okada et al., 2002, Bonewald, 2006a). Previously, it was believed that the number of canaliculi connecting to an osteocyte did not affect the viability and vitality of the osteocyte, however (Zhao et al., 2000) showed that the lack of dendrite processes increased the chance of apoptosis. Some investigators observed an increase in number of canaliculi between young and adult animals suggesting either that embedded osteocytes can generate new dendrites or that the new bone made in the adult or aging animals generates osteocytes with more canaliculi (Okada et al., 2002, Veno et al., 2005). These investigations also showed that canaliculi are not permanent connections between osteocytes, osteocytes and bone lining cells, but might be dynamic structures, with number of connections at each osteocyte changing in response to stimuli.

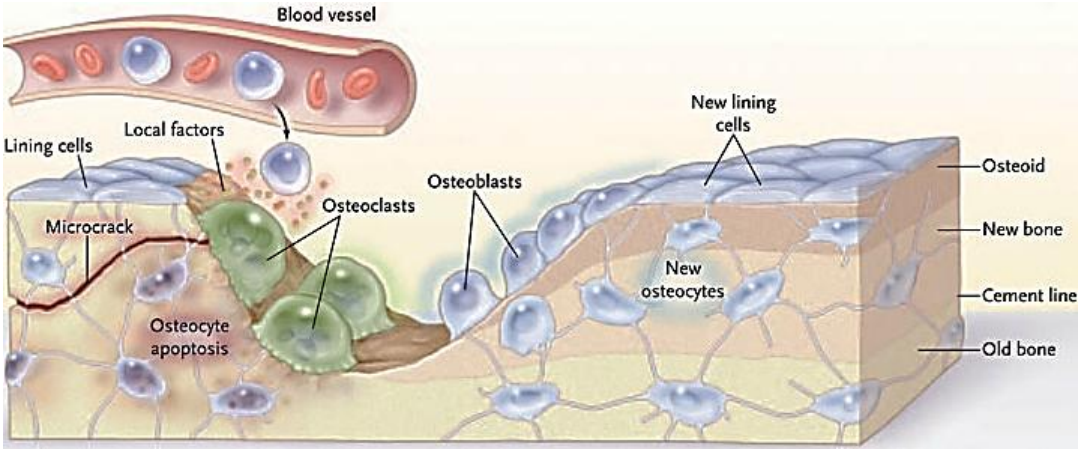

Figure 2-3: The remodelling process. After completion of bone formation, any osteoblasts that remain within the newly formed osteoid become osteocytes. Cytoplasmic processes of the osteocyte extend through the matrix in canaliculi. The osteocytic network detects strain and microfractures, and transmits this information to bone lining cells to initiate a new bone remodelling cycle and repair. Thus, osteocyte processes that are affected by either microcrack or apoptosis induce a cascade of growth factors and cellular migration that produces osteoclast bone resorption followed by osteoblast bone formation (Seeman and Delmas, 2006).

2.3.2 Osteocyte formation

Multipotential mesenchymal stem cells can differentiate into an osteogenic lineage whose base cell is an osteoprogenitor (Aubin et al., 1995, Aubin and Turksen, 1996, Bonewald, 2011), which differentiates into a preosteoblast then an osteoblast (Figure 2-4). An osteoblast has three possible fates: it can undergo an apoptotic process, it can differentiate into a bone lining cell, or it can become trapped in its own osteoid and differentiate into an osteocyte (Manolagas, 2000, Manolagas and Parfitt, 2010). The precise mechanisms of why and how osteoblasts differentiate into osteocytes are unknown, but there is evidence suggesting that other osteocytes stimulate their recruitment and differentiation (Imai et al., 1998). Marotti (1996) originally postulated a theory based on morphological observation, that osteocytes can produce an osteoblast inhibitory signal. Although there is no biochemical evidence available to confirm the existence of this inhibitory factor, Martin (2000) used this theory to develop a mathematical model to predict the bone formation rate in the bone remodelling cycle.

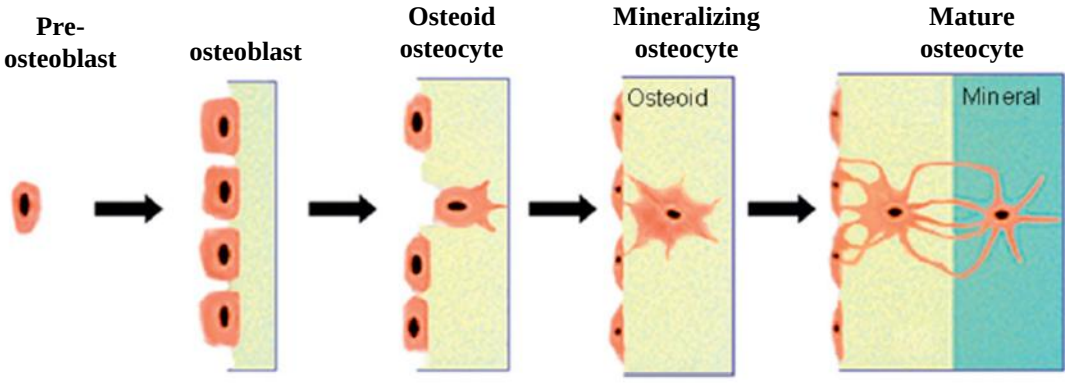

Figure 2-4:The ontogeny of a preosteoblast to a mature osteocyte (Bonewald, 2011).

2.3.3 Osteocyte death and apoptosis

While osteoclasts and osteoblasts exist only transiently on small fractions of the bone surface and are relatively short-lived, osteocytes exist throughout the skeleton and are long-lived. Osteoblasts begin to die by apoptosis as soon as they are created, but the majority of osteocytes remain alive until the bone is replaced. Bone turnover probably determines the life span of most osteocytes, with osteoclasts resorbing the bone and destroying the osteocytes. If the osteocytes reside in bone which has a slow rate of turnover, they may have a half-life of decades. Whether only the osteoclasts determine the fate of living osteocytes is presently unknown, but there is some evidences that osteocytes may be able to undergo a reverse differentiation back into osteoblasts (van der Plas et al., 1994), which may then be re-enclosed again during the formation of new bone (Suzuki et al., 2000). Furthermore, some osteocytes may die by apoptosis, and then be resorbed by osteoclasts (Bronckers et al., 1996, Elmardi et al., 1990).

It has been suggested that when osteocytes die, they release a signal to initiate bone remodelling, thereby resulting in an increase in bone resorption and bone loss (Manolagas, 2006). Osteocyte apoptosis can occur as a result of aging, immobilization, microdamage, estrogen deficiency and glucocortical treatment or in association with pathological conditions such as osteoarthritis, osteoporosis and micropetrosis, which usually leads to an increase in the bone fragility (Frost, 1960, Hattner and Frost, 1963, Dunstan et al., 1990, Weinstein and Manolagas, 2000, Weinstein et al., 2010, Manolagas and Parfitt, 2010). This bone fragility is thought to be due to the inability of apoptotic osteocytes to sense microdamage and so they

fail to signal to the bone surface for repair (Noble, 2008, Noble, 2000, Noble et al., 2003, Manolagas, 2010, Manolagas, 2000). Apoptotic osteocytes also occur in association with the area surrounding a microcrack leading to remodelling and repair of the damaged area (Noble et al., 2003). This is discussed in greater detail in Section 2.3.5.

In contrast to overloading, which induces microdamage and microcracking, a physiological level of load on bone *in vivo* may inhibit apoptosis in the osteocyte network (Noble. et al., 2003). On the other hand, lack of mechanical loading or disuse can lead to apoptosis of osteocytes by oxygen deprivation, especially if associated with immobilization (Aguirre et al., 2006, Basso and Heersche, 2006). It appears that mechanical stimulation provides essential oxygen levels to keep osteocytes viable (Gross et al., 2001, Gross et al., 2005). Again, this is discussed further in Section 2.3.4.

Thus, it appears that apoptotic osteocytes disrupt the integrity of the osteocyte network, this distruption functions as a signalling mechanism for the bone to initiate repair and adaptation to mechanical strain resulting from mechanical stimulation.

2.3.4 Osteocyte function

Blood-calcium/phosphate homeostasis

Osteocytes function as a well-organized and complex network of hemichannels and gap junction coupled cells in each osteon, and play an important role in the

metabolism and maintenance of bone. The bone tissue may exploit two advantages that this unique network offers:

1) An extensive intracellular communication system between osteocytes and bone lining cells by a gap junction based network, and an extracellular communication system between sites within the bone and the bone surface by hemichannels. The details of these two communication systems are discussed in Section 2.7.
2) A remarkable cell-bone surface communication area between osteocytes and bone lining cells, that is about twice as large as the communication area between the osteoblasts and bone lining cells at the bone surface (Johnson, 1966).

These two advantages led to the hypothesis that osteocytes may be in control of local bone remodelling (Bélanger, 1969), and based on this hypothesis, osteocytes must be responsible for blood-calcium homeostasis, later observations supported this theory (Palumbo et al., 1990a, Sissons et al., 1990). Osteoblasts and osteoclasts transport the bulk of calcium into and out of bone (Marotti et al., 1992), however the osteocytes may facilitate the diffusion of calcium into and out of the bone tissue (Bonucci et al., 1990). Thus osteocytes may play a key functional role in the regulation of blood-calcium homeostasis.

Osteocytes may also have a role in phosphate homeostasis, where the osteocyte network can be considered as a gland, that regulates the metabolism of bone phosphates (Nijweide et al., 1981, Westbroek et al., 2002a).

The osteocyte as a mechanosensor

It is well established that bone is very sensitive to the mechanical demands placed upon it, including abnormally low mechanical stress such as bed rest and immobilization which can cause adaptation of its properties such as mass and three dimensional structure. Julius Wolff was one of the first pioneers to propose the functional adaptation theory for bone tissue, known as Wolff's law, which has become widely accepted over the last century (Anderson et al., 1982, Wolff 1892).

In principle, all bone cells may be involved in mechanosensing or generally are sensitive to mechanical stress. The bone cells which could potentially sense mechanical strain and translate this force into a biochemical signal are the osteoblasts, bone lining cells and osteocytes. Of these, osteocytes are thought to be the most likely candidate as a mechanosensor cell in bone tissue. This is because of their many distinctive features such as: (1) their distribution throughout all types of bone matrix; (2) a high degree of interconnectivity with neighbours and bone lining cells; and (3) the existence of gap junctions and hemichannels between cells for the rapid passage of ions and signal molecules.

Furthermore, experimental studies show that osteocytes are the most sensitive of bone cells to mechanical loading and support their proposed role in the mechanotransduction mechanism. Osteocyte activity is seen to increase following a few minutes of loading *in vivo* (Skerry et al., 1989) where tissue strain magnitude ranged from 500 to 2000 μstrain in line with *in vivo* peak strains in bone during dynamic exercise. Many studies have also demonstrated that mechanical loading rapidly changes the metabolic activity of osteocytes and confirmed the

mechanosensory role for osteocytes in bone (El Haj et al., 1990, Dallas and Bonewald, 2010, Lee et al., 2002). Furthermore other computer simulation studies of bone remodelling mechanisms have predicted that the osteocyte is the mechanosensory cell in bone rather than the osteoblast or bone lining cell (Mullender and Huiskes, 1997, Ruimerman et al., 2005). Smit and Burger (2000) postulated a regulation of strain-sensitivity of osteocytes in basic multicellular units (BMU) by using finite element analysis. They also simulated how osteoclasts might attack the areas where osteocytes are unloaded, while osteoblasts are recruited to areas where osteocytes are overloaded.

Thus, osteocytes are believed to be mechanosensors, but the precise mechanotransduction mechanisms in bone, including how osteocytes sense mechanical loading and how these signals transmit to other non sensing cells, and how they eventually induce bone remodelling are unclear. The changes of hydrostatic pressure in the cell, direct cell strain, fluid flow in the lacuna are likely the consequences of the application of force to bone during movement (Pienkowski and Pollack, 1983). However, it appears that the interstitial canalicular fluid flow, driven by extravascular pressure as well as by the applied cyclic mechanical loading, is most likely to inform the osteocytes about the level of bone loading (Cowin, 1999, Cowin et al., 1991, Cowin et al., 1995, Weinbaum et al., 1994, Burger and Klein-Nulend, 1999a).

Canalicular fluid flow and osteocyte mechanosensing

Mechanical strains in bone as a result of normal physiological loading in healthy, adequately adapted bone are relatively small. Several quantitative studies found

that the maximal strain does not exceed 2000-3000 microstrain in bones in humans and animals (Burr et al., 1996). For example, the typical strains in a human tibia measured *in vivo* during vigorous activity are of the order of 1200 microstrain (principal compressive strain) and 1900 microstrain (maximum shear strain) (Burr et al., 1996). This strain was measured using strain gauges covering an area of 1.8 mm by 3.6 mm which would have included thousands of osteocytes. The local strain or cell deformation that may be sensed by an individual cell will also be affected by microstructural features or discontinuities in the bone matrix. The microstructural strains near an osteocyte lacunae were found to be three times larger than the average strain with external strain gauge. Furthermore, the peri-lacunar strain magnification near a microcrack tip can be up to 15 times higher than *in vivo* measured bone strain (Nicolella et al., 2005, Nicolella et al., 2006). However *in vitro* studies of strained bone cells, loaded by stretching or bending, showed that higher deformations (1-10%) were necessary to produce a cellular response (Kleinnulend et al., 1993). For instance, unidirectional cell stretching of 0.7% was required to activate prostaglandin E2 production *in vitro* (Murray and Rushton, 1990), whereas just 0.15% strain from bending of an intact bone can activate adaptive bone formation *in vivo* (Forwood, 1996, Turner et al., 1994). If it is assumed that bone strain is somehow involved in the mechanotransduction mechanism, then the canalicular flow within bone tissue may play a crucial role as a lever system whereby small matrix strains are transduced into a larger signal which an osteocyte can easily sense. Similarly, the theoretical study of Peikarski and Munro (1977) suggested that the extracellular tissue fluid flow through the

lacuno-canalicular system was a result of the strains of bone tissue, with the experimental results of Knothe-Tate et al. (1998 and 2000) supporting this theory. It was also demonstrated that this strain–derived interstitial fluid flow can help keep osteocytes healthy and viable by facilitating the exchange of waste products and nutrients within the osteocyte network of an osteon and the Haversian channels (Kufahl and Saha, 1990).

Experimental studies *in vitro* have suggested that osteocytes are sensitive to fluid shear stress (Kleinnulend et al., 1993, Westbroek et al., 2002a, Westbroek et al., 2002b). The finite element model of Smit et al. (2002) showed that volumetric strain in the bone around a BMU was related to canalicular fluid flow. It also predicted that areas with low canalicular fluid flow might induce local apoptosis of osteocytes. Furthermore this model showed that enhanced shear stress acting on the osteocytes during loading prevented apoptosis in the reversal zone of the BMU and also prevented the detachment of osteoclasts from bone surface. Basso et al. (2006) also reported that the osteocyte apoptosis induced by unloading in a rat bone was highly associated with osteoclastic bone resorption.

It is also proposed that osteocytes can respond as a population to enhanced strain from mechanical loading and the response of each individual osteocyte is related to the magnitude of strain in its local environment (Gluhak-Heinrich et al., 2005, Kotha et al., 2005). However, neither fluid flow nor the resulting osteocyte deformation in bone has been measured directly *in vivo* thus these theoretical predictions have not yet been validated.

2.3.5 Bone remodelling and the role of osteocytes in bone remodelling

Two distinct processes, bone modelling and remodelling, were described in the pioneering work of Frost (1963, 1986). Since then it has become generally accepted that in these two processes, different kinds of bone cells work individually or together to achieve the skeleton's optimum strength. During growth, the mechanism by which osteoblasts form new bone without prior bone resorption is called bone modelling (construction). It can produce alterations in bone shape, size and position in tissue space of typical long bone cross-sections. Bone modelling involves either resorption or formation but not both at any locus. Once the skeleton reaches maturity, modelling decreases and eventually stops.

Bone remodelling (reconstruction) occurs in the mature skeleton in cases where the mechanical loading has been altered considerably and in some disease states. Bone remodeling also occurs to repair of microdamage and replace old bone. Unlike modelling, the bone remodelling process follows a sequence of resorption (by osteoclasts) and formation (by osteoblasts).

There are four main theories as to how bone remodelling occurs. Firstly, it is assumed that there are sensor cells in bone which monitor the mechanical loading (strain) and compare it to a 'normal' range of values, and activate the appropriate biological mechanisms if it is outside that normal range. Based on this idea, computational simulations of how bone adapts to mechanical loading have been developed (Beaupre and Carter, 1990, Carter, 1987, Mullender et al., 1995). In

these investigations, it is simply assumed that when the mechanical loading is very low, bone is removed and when it is too high, new bone is formed.

Secondly, as osteocytes are distributed throughout the bone matrix, many researchers have suggested that osteocytes are the most mechanosensing cells in bone (Cowin et al., 1995, Marotti et al., 1990, Parffit, 1995). The presence of gap junctions and hemichannels in the osteocyte-lacunae network suggests that osteocytes can communicate with osteoblasts and bone lining cells, so producing the necessary signals at the bone surfaces.

Thirdly, in addition to sensing the mechanical stimulus, osteocytes can also sense fatigue damage and transmit signals to activate remodelling to remove any damaged bone (Burr et al., 1992).

Finally, it has been suggested that bone lining cells control the bone remodelling activation in response to signals received from the osteocyte network or hormones (Rodan and Martin, 1981). Although many investigators do not agree with all details of these four key concepts, they generally subscribe to one of these models.

Frost's mechanostat theory (Frost, 1992) distinguished between modelling and remodelling processes. In this theory, disuse initiates remodelling, leading to bone loss, whereas overloading activates leading to bone gain. However, the theory limits itself to the effect of strain on modelling and remodelling, not the effect of microdamage and mechanical damage. Later Martin (2000) developed Frost's idea,

by adding the 'pathologic overload' region to include the effect of fatigue and microdamage on modelling and remodelling.

The important role of osteocyte apoptosis in bone remodelling

The work of Hezenberg et al. (2006) demonstrated that microcracks disconnect communications in the osteocyte lacuna-canalicular system, inducing osteocyte apoptosis (Figure 2-5A). Manologas (2006) suggested that apoptotic osteocyte may also be a form of damage. In addition, he reported that the rate of bone remodelling increased in mid-life women, as a result of osteocyte death.

The distribution of osteocyte apoptosis in the lacuna-canalicular network may provide the required topographical information to target osteoclasts to the microcrack. (Li et al., 2005, Taylor 1997, Vashishth et al., 2000) (Figure 2-5B). A biochemical signal could transmit the size and location of a microcrack to the bone lining cells on the bone surface (via the canaliculi through gap junctions) to initiate bone remodelling and create the bone remodelling compartment (BRC) (Hauge et al., 2001), but the nature of this message is not clear (Figure 2-5C). Bone lining cells are discussed later in this chapter.

Osteocytes transmit a signal to the bone lining cells initiating bone resorption (Nonaka et al., 1995) where, in the resorption phase, a team of osteoclasts resorb the volume of bone containing the microcrack but when the resorption phase ends is unclear (Figure 2-5D).

After the reversal stage osteoblasts form a new volume of bone and refill the void, partly or completely (Han et al., 2004) (Figure 2-5E). Furthermore, osteocytes

can support the differentiation of preosteoblasts into osteoblasts during the formation phase of bone remodelling (Heino et al., 2004). After formation, some of the osteoblasts die, some become bone lining cells and some become trapped in the bone matrix where they differentiate into osteocytes which are connected to each other in the new expanding lacuna-canalicular system where later they will use mechanotransduction to detect the damage and repair of the surrounding bone (Han et al., 2004) (Figure 2-5F).

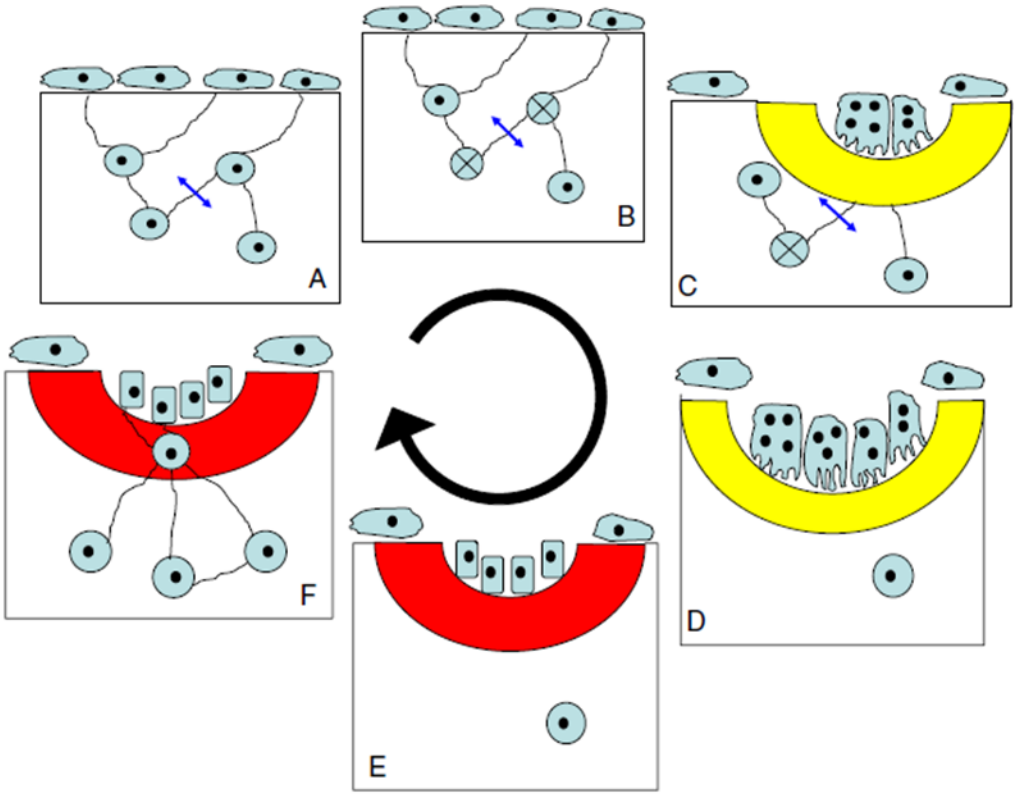

Figure 2-5: The sequence of events after osteocyte death. (A) A microcrack breaks the canaliculi of several osteocytes (B) The microcrack induces osteocyte apoptosis. (C) The number of dead osteocytes provide topographical information to initiate the resorption phase and bone lining cells create the bone remodelling cavity. (D) Osteoclasts resorb the damaged bone. (E) and (F) The reversal stage and osteoblasts form new bone. (F) Some osteoblasts differentiate into osteocytes to reconstruct lacuna-canalicular network (Rochefort et al., 2010).

In summary, osteocytes appear to regulate the formation of osteoclasts and bone resorption during bone remodelling. Thus osteocytes are involved in both the resorption and formation phase of bone remodelling directly or indirectly.

2.3.6 Density of lacunae and osteocyte

Since osteocytes are embedded within the mineralized bone matrix, it is difficult to analyse osteocyte properties and their functions. Sensitive methods, such as the dissector method, with highly advanced microscopes have been developed to reveal their details. Using these methods, investigators have confirmed that cell density plays a crucial role in the growth and size of many bones in the body of animals and humans (Conlon and Raff, 1999 and Nijhout, 2003). It has also been suggested that size, density and distribution of lacunae are important features in bone microstructure which may affect stiffness and other mechanical properties. There have been many studies of the density of lacunae and osteocytes in different regions of long bones, in different species, and in a variety of states of health and disease such as osteoporosis and the menopause (Table 2-1 and 2-2). One of the earliest quantitative studies reported that the number of osteocytes could be up to 10,000 cells per cubic millimetre and 50 canaliculae per cell in a three-dimensional network (Marroti et al., 1990). In the detailed study of Mullender et al. (1996), the number of osteocytes and histomorphometric parameters were quantified in cancellous tissue for a variety of animals. They found a range of osteocyte densities from 294 cells per square millimetre in cows, to 942 cells per square millimetre in rats. In this study, the density of the osteocyte (N.Ocy/BV) and lacunae (N.Lc/BV) per bone volume were calculated by following equations:

$$\text{N.Ocy/BV} = \frac{\text{number of osteocyte per bone area}}{2R+t-2k}$$

$$\text{N.Lc/BV} = \frac{\text{number of lacunae per bone area}}{2R+t-2k}$$

where R, t are an average of "osteocyte radius" and a section thickness respectively and k is the thickness of the smallest part of a cell which must be included in the section for its identification. The number of lacunae in healthy human bone was estimated to be 17,000 cells per cubic millimetre in cancellous bone tissue. The study also revealed that 78% of the lacunae contained osteocytes thus 13,300 cells per cubic millimetre (Mullender et al., 1996).

Reference	Lacuna density	Osteocyte density	Empty lacuna density	Gender	State	Region
Mullender (1996)	17100 /mm^3	13300 /mm^3	-	-	Healthy	Cancellous bone (iliac)
Mullender (1996)	150-210 /mm^2	-	-	F&M	osteoporosis	Cancellous bone (iliac)
Mullender (1996)	12900-17100 /mm^3	10500-13300 /mm^3	-	F&M	osteoporosis	Cancellous bone (iliac)
Vashishth (2000)	450-900 /mm^2	-	-	F&M		cortical bone (femur)
Qiu & Parfitt (2002)	232 ± 28 /mm^2	221 ± 30 /mm^2	11 ± 6 /mm^2	F(W)	Premenopausal	Cancellous bone
Qiu & Parfitt (2006)	257 ± 45 /mm^2	237 ± 43 /mm^2	20 ± 5 /mm^2	F (B)	Premenopausal	Trabecular bone
Qiu & Parfitt (2002)	206 ± 22 /mm^2	188 ± 22 /mm^2	17 ± 7 /mm^2	F(W)	Postmenopausal	Cancellous bone (iliac)
Qiu & Parfitt (2003)	207 ± 22 /mm^2	190± 22 /mm^2	17± 7 /mm^2	F	Postmenopausal	Cancellous bone (iliac)
Qiu& Parfitt (2006)	237 ± 41 /mm^2	213 ± 40 /mm^2	23± 5 /mm^2	F (B)	Postmenopausal	Trabecular bone
Qiu & Parfitt (2003)	128± 39 /mm^2	118 ± 43 /mm^2	10 ± 6 /mm^2	F	Osteoporotic fracture	Cancellous bone (iliac)
Hove (2009)	21800±4000 /mm^3	659 ± 70	-	F	Osteoarthritis	Cortical bone (tibia)
Hove (2009)	8 000± 500 /mm^3	120 ± 30.3	-	F	Osteopenia	Cortical bone (tibia)
Hove (2009)	15600±3400 /mm^3	458 ± 5.8	-	F	Osteopetrosis	Cortical bone (tibia)

Table 2-1: The density of lacunae, osteocyte, and empty lacunae in human bone. F (female), M (male), B (black) and W (white).

Reference	Lacuna density	Osteocyte density	Empty lacuna density	Region
Mullender et al. (1996)	-	295(cow)-943(rat) /mm^2	-	Trabecular bone (femur)
Fritton et al. (2004)	80,600 / mm^3	-	-	Rat (tibia)
Hernandez et al. (2004)	1875-834 /mm^2	-	-	Rat (lamellar bone)
Hedgecock et al. (2007)	694 ± 42 /mm^2	545.6 ± 38 /mm^2	148 ± 19.4 /mm^2	Rabbit (tibia)

Table 2-2: The density of lacunae, osteocytes, and empty lacunae in animal bone.

It is uncertain whether there is a relationship between lacuna density and rate of bone remodelling, but there have been many experiments to investigate the possibility of a connection. One such investigation found that the cortical and cancellous tissue bone remodelling volume can be predicted by osteocyte and lacunae densities (Vashishth et al., 2000). This work also revealed a correlation between increasing osteocyte numbers and an increase in bone volume, and that osteocyte density can predict cancellous and cortical bone volume (Vashishth et al., 2002). In contrast, Qiu et al. (2002b and 2003) found that osteocyte density was inversely associated with the rate of bone remodelling. They also suggested that the age of the bone, not the age of the subject determines the density of osteocytes and that osteocyte density declines with this age in deep bone, so that keeping osteocyte viability may be one of the functions of bone remodelling. Qiu et al. (2002b and 2003) also found that the osteocyte density in fracture patients was less than in healthy controls. They proposed that a deficiency in osteocyte density may cause bone fragility by reducing osteocyte detection of microcracks and microdamage.

Hove et al. (2009) demonstrated that the number of osteocytes in bones with osteopenia is lower than in those with osteopetrosis and osteoarthritis. They also reported that the osteopenic osteocytes were larger than osteopetritic and osteoarthritic osteocytes, and concluded that the differences in osteocyte morphology and their lacunae may indicate differences in the mechanosensitivity of the osteocytes.

Clearly, the exact relationship between the density, connectivity and size of osteocytes, with bone remodelling and bone architecture is complex and deserves further investigation.

2.3.7 Hormone receptors in osteocytes

Parathyroid hormone (PTH) receptors have been found on rat and chicken isolated osteocytes *in situ* (van der Plas et al., 1994, Fermor and Skerry, 1995). This suggested an important role for PTH in the viability of osteocytes and the efficiency of cell-cell communication in osteocytic network (Fermor et al., 1998, Fermor and Skerry, 1995, van der Plas et al., 1994, Bivi et al., 2011, Kimmel et al., 2011, Kimmel et al., 2010, Miyauchi et al., 2000). PTH is also reported to inhibit apoptosis of mature osteoblasts and osteocytes (Jilka et al., 2008, Bellido et al., 2005, Bellido et al., 2003, Rhee et al., 2011).

Oestrogen is another important hormone involved in bone metabolism. Several studies have reported that a decrease in the level of oestrogen in the blood is reflected in a loss of bone mass. If osteocytes are the main mechanosensor cell in

bone, it is possible that osteocytes are the site of set point regulation by oestrogen (Hoyland et al., 1999), because oestrogen regulates the set point for the mechanical responses of bone (Frost, 1992). Furthermore, the higher levels of oestrogen receptors were found in isolated osteocytes rather than in osteoblast or osteoblast precursor cells. The study of Zaman et al. (2006) showed that the oestrogen regulates the content of oestrogen receptors, however osteocytes use them to respond to strain.

2.3.8 Osteocytic-type cells

Only a limited number of primary osteocytes can be isolated *in vivo* (Van der Plas and Nijweide, 1992), which means many researchers have preferred to establish osteocytic cell lines. HOB-01-C1 cells were the first osteocytic cell line to be established from cloned human adult bone *in vitro* (Bodine et al., 1996). These cells are proven to be putative osteocytic markers, but they are temperature-sensitive, and proliferate at 34°C but stop dividing at 39°C.

A post-osteoblast/pre-osteocyte-like cell line (MLO-A5) has been established from the long bone of 14-day-old mice, that can differentiate into osteoid osteocyte-like cells (Kato et al., 2001). Although MLO-A5 cells display all the late osteoblast markers such as PTH type 1 receptor, they begin to express the osteocyte markers as they generate cell processes (Barragan-Adjemian et al., 2006).

Another osteocytic cell line, MLO-Y4 (Kato et al., 1997) expresses complex dendritic processes when seeded at low density (Zhang et al., 2006a). These cells

have been used in many investigations to examine gap junctions, hemichannels, apoptosis and other potential functions of osteocytes (Alford et al., 2003, Bonewald, 2004, Cheng et al., 2001, Gross et al., 2005, Guo et al., 2010, Heino et al., 2002, Heino et al., 2004, Weinstein et al., 2011, You et al., 2008, Zhang et al., 2006a, Zhao et al., 2002). These cells support osteoclast formation and activation (Zhao et al., 2002, Zhao and Grigoriadis, 2002, Heino et al., 2002), osteoblast formation (Heino et al., 2004), and also support the theories that osteocytes are orchestrators of both bone formation and resorption (Heino et al., 2004).

2.3.9 The role of osteocytes in bone disease

Osteocyte viability can play a crucial role in the integrity and maintenance of bone, there is a definite connection between osteocytes and osteoporosis, as described earlier in Section 2.3.3 (Manolagas, 2000 and 2006).

Osteocyte canalicular may also play a role in bone disease. In healthy bone, osteocyte connectivity is high and the orientations of their processes are directed to the blood supply (Knothe et al., 2004). In osteoporotic bone the number of connection decreases as well as the disorientation of cell processes. Conversely, in osteoarthritic bone there is a decrease in connectivity but the orientation is intact (Knothe et al., 2004). Thus, changes in osteocyte connectivity can a have significant effect on osteocyte function, particularly their viability, and also on the mechanical properties of bone (Figure 2-6).

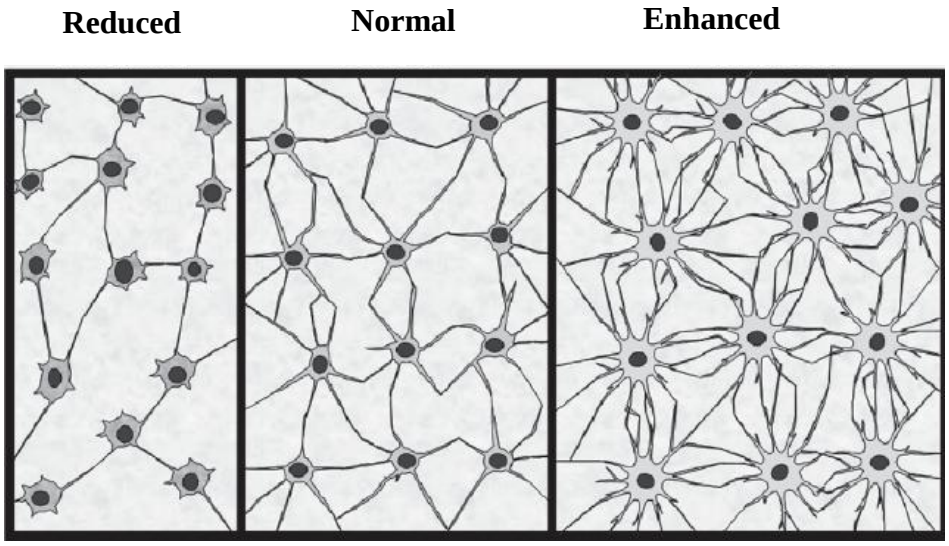

Figure 2-6: The effect of bone disease on the lacuna-canalicular system. Disease may disrupt the lacuna-canalicular system and the change in dendritic will connections dramatically offer osteocyte function and mechanical properties of the bone (Knothe Tate et al., 2004).

Osteonecrosis is "dead" bone that does not remodel, and could be caused by glucocorticoid treatment, lipid disorders, alcohol abuse, radiation or trauma. Osteocyte apoptosis could be involved in this condition, where agents induce the death of the osteocyte cells that results in bone death, where it does not remodel.

2.4 The osteoblast

2.4.1 The phenotype

Osteoblasts are derived from mesenchymal cells (Aubin and Triffitt, 2002) which are located in a single layer adjacent to periosteal or endosteal surfaces of bone (Marks and Odgren, 2002).

Active osteoblasts have the following anatomical structures: a large and round nucleus, cytoplasmic process and gap junctions. In addition they have receptors for the majority of bone agents like PTH, PTHrP, vitamin D metabolites,

etc. It is believed they are responsible for both bone formation through the secretion of unminerellized bone matrix and, the indirect control of resorption level. When the deposition of bone matrix terminates, some osteoblasts undergo apoptosis, while others differentiate into flattened 'bone lining cells' on the bone surface, whereas others become trapped in bone matrix as osteocytes (Marks and Odgren, 2002, Parfitt, 2002). In general, growth factors, steroid hormones and specific genes can modify the differentiation program of preosteoblasts and the degree of osteoblast maturation. Thus osteoblastic cells are observed in four forms *in vivo*: immature osteoblasts (preosteoblasts), mature osteoblasts, osteocytes and bone lining cells (Figures 2-7 and 2-8).

2.4.2 Osteocyte function

Osteoblasts play a vital role in the function and maintenance of the skeleton. Formation occurs in two steps: deposition of the bone matrix and mineralization. The study of Robey in 2002 shows that in addition to the secretion of the bone matrix, osteoblasts also contribute indirectly to the mineralization of the osteoid. The matrix formation process can take about 15 days at the interface between osteoblast and osteoid, with the height of osteoblast nucleus gradually decreasing during the bone formation process. Following production of the new bone matrix, the mineralization process begins which normally takes 10 days in adults (Marie, 1999). Moreover PTH increases the number of osteoblasts and bone formation rates and the density of osteoclasts. Jelika et al. (1999) demonstrated this ability of PTH through inhibiting the apoptosis process in osteoblasts.

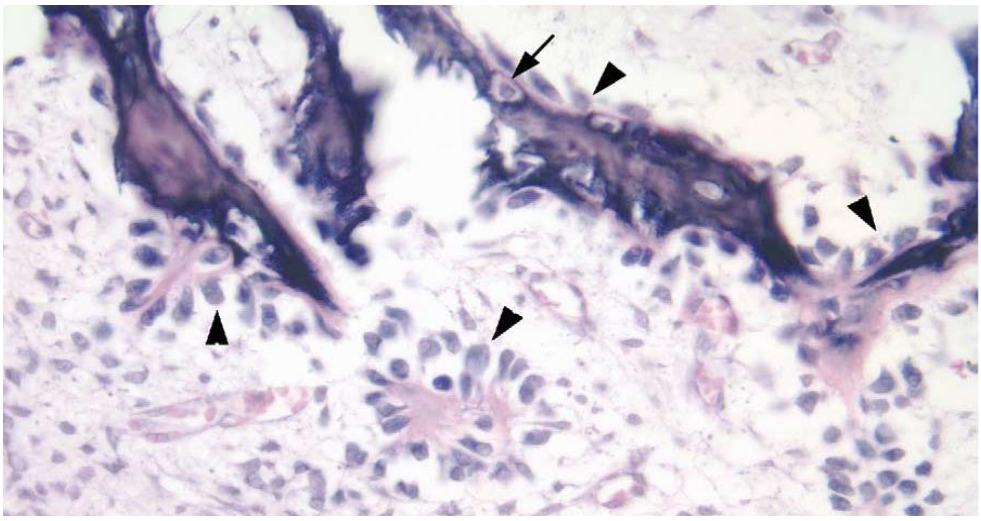

Figure 2-7: Osteocyte maturation. The rows of osteoblasts (arrowheads) are producing osteoid (pink matrix) which is quickly being mineralised (purple matrix) while some osteoblasts are in the process of becoming enclosed in bone matrix as osteocytes (arrow) (Mackie, 2003).

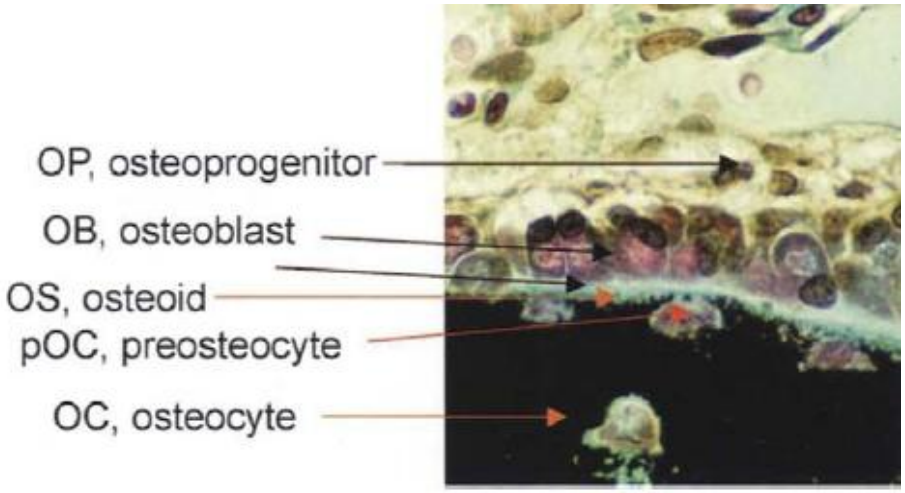

Figure 2-8: The process of osteoblast maturation on the surface of trabecular bone (Lian and Stein, 2008).

2.4.3 The role of osteoblasts in bone diseases

Osteoporosis, Paget's disease and osteoarthritis are bone diseases which are caused by an inadequate number of osteoblasts and reduced bone formation rates. Non-equilibrium between the rate of bone formation and the rate of bone

resorption causes osteoporosis. The most common treatment for osteoporosis is to inhibit osteoclastic resorption in bone remodelling.

2.5 The osteoclast

2.5.1 The phenotype

Osteoclasts are derived from cells in the monocyte-macrophage lineage of the hematopoitetic marrow. Baron et al. (1986) demonstrated how mononuclear cells initially attach to the bone surface, differentiate and eventually form multinucleated osteoclasts, which may contain up to 50 nuclei (Teitelbaum et al., 1996). While the resorption role of osteoclasts in modelling and remodelling is clear, there is no relationship between resorption capacity and the number of nuclei in an osteoclast, although large cells seems to be more "aggressive" (Piper et al., 1992) and they may even be more sensitive to extracellular stimulation factors (Trebec et al., 2007).

2.5.2 The life span of the osteoclast and the resorption cycle

There is a lack of information concerning the osteoclast's life span *in vivo* but according to the experiments of Roodman et al. (1996) it could be up to 7 weeks.

Mononuclear preosteoclasts are proliferated in bone marrow and transported to the bone surfaces by an unknown molecular mechanism (Yagi et al., 2005). *In vitro* experiments have suggested the regulation of bone resorption could be controlled by the cell fusion process (Lee et al., 2006).

It has been demonstrated that viable osteocytes are able to secrete factors which inhibit osteoclast differentiation and activation while dying osteocytes initiate osteoclast activity (Guo et al., 2005, Kurata et al., 2006). This is in agreement with the study of Kurata et al. (2006) who showed that damage of local osteocytes can initiate the differentiation of bone marrow precursors close to the damaged area. In addition it has been observed *in vitro* that osteoclasts do not resorb bone which contains living osteocytes (Guo et al., 2005, Henriksen et al., 2007). At this time evidence suggests osteocytes are the most likely candidates in guiding osteoclasts to the correct resorption site.

Some studies have shown that the withdrawal of bone lining cells on the endosteal surface is the primary indicator of forthcoming resorption (Azari et al., 2011, Hefti et al., 2010). Osteoclasts attach to the bone surface, before uncovering the osteoid and its removal begins. Lakkakorpi and Väänänen (1995) and Väänänen et al. (2000) demonstrated that the single resorption cycle of an individual osteoclast is a complex multistep processes, which induces osteoclast attachment, formation of the sealing zone, plasma membrane polarization, and the resorption itself with final detachment and cell death. According to *in vitro* studies each osteoclast undergoes apoptosis following several resorption cycles (Kanehisa and Heerche, 1988).

2.5.3 The role of osteoclasts in bone diseases

A deficiency of osteoclast activity causes osteopetrosis and other related disorders in humans. In osteopetrosis, the bone becomes thicker, in contrast to more prevalent conditions like osteoporosis, where the bones become thinner and more

brittle. While the rate of bone formation is less than resorption in osteoporosis over a long period of time, the difference in osteoclast number in osteoporotic bone, compared to normal bone has not been proven. Another clinical disease related directly to the activity of osteoclasts is Paget's disease, where an increase in the number of osteoclasts initiates hyper-resorption.

2.6 Bone lining cells

2.6.1 The phenotype

Bone lining cells are quiescent osteoblasts that were not embedded in the bone matrix and remained on the surface after termination of the bone formation process. The morphological characteristics of these cells which cover an inactive bone surface have been regarded as a distinct phenotype. Electron microscopy can be used to investigate these cells (Doty and Nunez, 1985, Miller and Bowman, 1980). Some morphological features of bone lining cells demonstrated through these investigations are as follows; they have a thin, flat nuclear shape and lay directly opposed to the bone surface. Miller et al (1980) examined the density of bone lining cells (number of cells per unit surface perimeter) in beagles, and found their total numbers greatly exceed the number of osteoblasts and osteoclasts found on trabecular bone samples at different ages (Table 2-3). They also reported that the density of bone lining cells is about 19 cells/mm bone surface perimeter, and decreases with age (Miller and Jee, 1987). Bone lining cells are linked to osteocytes through canaliculi while gap junctions exist between neighbouring bone lining cells, and between osteocytes and bone lining cells. Bone lining cells are typically

less than 1μm in thickness and about 12μm in length (Figure 2-9) (Miller and Jee, 1987).

Cells per mm bone surface perimeter				
Age (years)	**Number of each age**	**Bone lining cells (± S.D.)**	**Osteoblasts (± S.D.)**	**Osteoclasts (± S.D.)**
Distal Radius				
1.5-3	7	19.5 ± 3	1.1 ± 1.2	0.9 ± 0.7
7	1	17.4	1.4	0.6
10	1	11.6	0	0.1
13-16	4	20 ± 5.1	0.3 ± 0.5	1.1 ± 0.8
Distal Femur				
1.5-3	4	19 ± 1.5	0.1 ± 0.2	0.8 ± 0.2
8-10	3	16.6 ± 3.1	0.6 ± 3.1	1.9 ± 1.1
12-16	3	12.3 ± 3.3	0.1 ± 0.2	1.7 ± 1.3

Table 2-3: The density of bone lining cells, osteoblasts and osteoclasts found on samples of trabecular bone surface from distal femur of beagles of different ages (Miller et al., 1989).

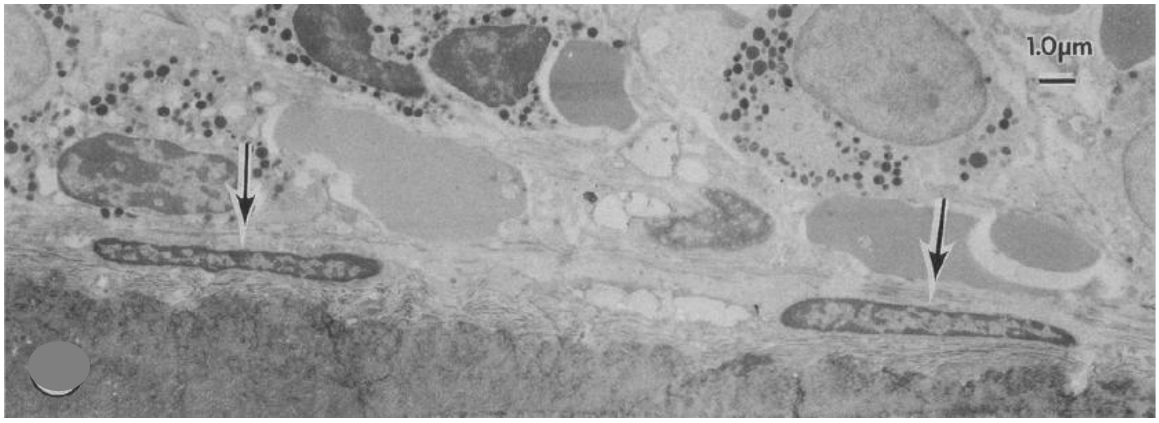

Figure 2-9: A sample adopted from an iliac crest biopsy of 33-year-old female. The bone lining cells in this micrograph are about 1.0 μm in thickness and about 10μm in length. (Miller and Jee, 1987).

2.6.2 Bone lining cell functions

Bone lining cells may be influenced by strain that could instigate adaptive changes, and may play an important role in supporting osteocytes (Baud, 1968). Evidence of this includes the penetration of bone-lining cell processes into canaliculi, and contact with osteocytes via gap junctions. Bone lining cells are also in contact each

other via gap junctions (Miller et al, 1980), suggesting that regions of bone volume might act as a functional osteoblastic network (Doty, 1981). Most investigators in this field confirm the role of bone lining cells as an activator in the bone remodelling process.

2.6.3 Bone lining cells and the activation of the bone remodelling

In vitro studies confirm that the activities of both osteocytes and bone lining cells increase considerably in response to loading and therefore both are involved in bone remodelling regulation.

In order to explain this mechanism, Marotti et al. (1992, 1996) hypothesized that even after osteocytes are completely embedded at a depth in the bone matrix, additional osteocytes are recruited to remain in contact and maintain the connection with the bone surface. Thus, they conclude that these osteocytes send an inhibitory signal to osteoblasts forming bone above them. Alternatively, Martin (2000) suggested that such an inhibitory osteocytic signal is very similar to the mechanism that many investigators believe to be produced by strain or mechanical loading. Based on this premise, he assumed that those mechanical signals would first start when the matrix around a newly formed osteocyte mineralizes and turns bone-like, but this signal may result in different outcomes. Like Marotti and other pioneers (Bonewald, 2011, Eriksen, 2010), Martin (2000) said this signal slows matrix production in neighbouring osteoblasts and allows some of them to become new osteocytes. However, he argued that such a signal fails to stop if the osteocytes remain in the loaded-bone environment. In contrast

he proposed that this signal continues to generate and communicate through the existing network of osteocytes to the bone surface.

In particular, Martin's hypothesis places an emphasis on the genesis and evolution of bone lining cells. These cells start their life cycle as mesenchymal stem cells and go through several preosteoblastic phases before becoming functioning osteoblasts. The morphological evidence confirmed that preosteoblasts communicate with osteoblasts throughout this process (Marotti, 1996). At the same time osteoblasts serve as a bridge between preosteoblasts on one side and osteocytes on the other. With the termination of the bone formation process, the preosteoblasts disappear, however the surface cells still communicate with the network of osteocytes in the bone matrix. Regardless of their differentiation during their life cycle, osteoblasts and bone lining cells never end their connections with their kindred cells. This enduring connection between this family of cells creates a functional osteoblastic network, in which gap junctions play an important role in maintaining constant cell to cell communication.

In summary, bone lining cells activate remodelling unless inhibited by an osteocytic signal. As such, there is a negative correlation between the activation of remodelling and the generation and transmission of the inhibiting signals, where the signal increases as the remodelling decreases. This could happen in several ways consistent with both the general model and the mechanostat theory.

Figure 2-10 shows a small sample of bone tissue where the elliptical objects symbolize osteocytes, the lower bold line a quiescent (not remodelling) bone

surface, and a series of bone lining cells are shown on this surface. The multiple thin lines connecting the osteocytes to one another and to the bone lining cells schematically represent cell processes within canaliculi. The jagged horizontal line indicates microdamage to the calcified matrix, which interferes with generation or transmission of the osteocytic signal. When these inhibitory signals decrease, the bone lining cells initiate activation of remodelling.

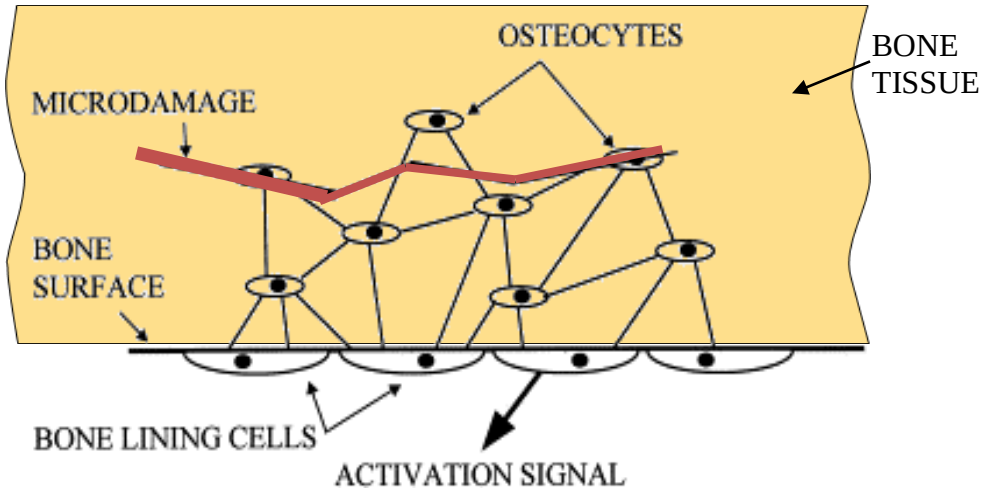

Figure 2-10: The remodelling mechanism in the network of osteocytes-bone lining cells (Adapted from Martin, 2000).

2.7 Gap junctions and hemichannels

2.7.1 Gap junction in bone cells

Gap junctions are intra-cellular channels which play an important role in direct cell to cell communication. They facilitate this mechanism by electrical coupling in which intracellular signalling molecules such as calcium and inositol triphosphate propagate between cells, or by simply serving as connection points which allow the passage of small molecules (<1 kDa), such as small metabolites, from one cell to

another. Gap junctions are composed of proteins called connexin (Eiberger et al, 2001, Saez et al, 2003, Willecke et al, 2002). Three types of connexins have been identified in bone tissues including Cx43, Cx45 and Cx46. Among them Cx43 is of most abundant and can be found in almost all types of bone cells. Several *in vitro* investigations have confirmed the presence of Cx43 in cultured osteoblasts from newborn rat calvaria (Schirrmacher et al, 1992), human bone marrow stromal cells, trabecular bone osteoblasts (Civitelli et al, 1993), murine osteoblasts (Edelson, 1990), primary osteocytes *in vivo* (Mason, 1996), mandibular bone and periodontal ligament cells of rat teeth (Su et al, 1997), osteoblast-like MC3T3-E1 cells (Chiba et al, 1993, Yamaguchi et al, 1994), and osteocyte-like MLO-Y4 cells (Cheng et al, 2001, Thi et al, 2003).

The first morphological verification of the existence of gap junctions between bone cells *in vivo* was provided by Doty (1981). Later on, the complexity and extent of gap junctions between osteocytic processes in bone canaliculi in rat and mouse long bones were demonstrated by transmission electron micrography (Shapiro, 1997).

Yellowley and colleagues (2000) observed the potential role of gap junctions in osteoblast differentiation. Five years later Civitelli et al. (2005) reported the crucial function for gap junctions and Cx43 in osteoblast differentiation and bone development in human and animal models *in vivo*.

Gap junction in osteocyte and Ca^{2+} signalling in bone cells

It has been proven that in *ex-vivo* calvaria organ cultures, gap junctions allow cell–cell communication among the osteocytic network, and that such communication is regulated by parathyroid hormone (PTH) (Jiang et al., 2007).

As discussed previously, it is generally believed that osteocytes communicate the presence of mechanical signals to osteoblasts, bone lining cells, and, perhaps other skeletal cells. Indeed*, in vitro* studies demonstrated that gap junction intercellular communication (GJIC) contributes to hormones, growth factors and Ca^{2+} wave propagation from osteocytes to osteoblasts which is thought to be crucial for bone formation and remodelling (Yellowley et al., 2000) (Figure 2-11).

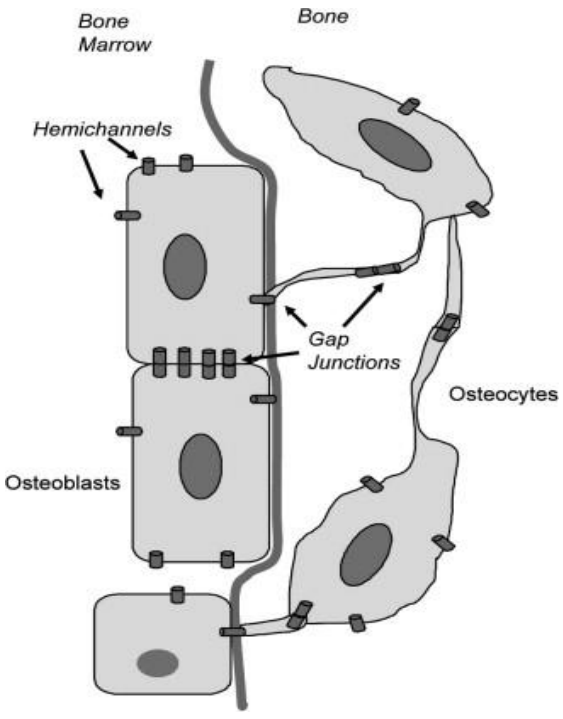

Figure 2-11: Gap junctions and hemichannels in the osteoblast–osteocyte network. Gap junction transcellular channels, formed by the apposition of two connexins, are abundantly present between osteoblasts on the bone surface, as well as at the interface between osteocytic processes and between these processes and osteoblasts on the surface. Connexins also exist as membrane channels, without docking to an opposing connexin, thus representing gap junction "hemichannels". Both gap junctions and hemichannels contribute to connexin's role in bone biology (Civitelli et al., 2008).

2.7.2 Hemichannels

It was indicated in the previous section that connexins constitute the main part of gap junctions. In recent years another function of connexins has been discovered: they form two halves of gap junction channels, called hemichannels (Figure 2-12). Hemichannels exist in osteoblasts and osteocytes, in particular where they appear to function as main transducers of bisphosphonates, which form as a result of antiapoptosis. (Bennett et al., 2003, Ebihara, 2003, Goodenough and Paul, 2003, Romanello, 2001, Plotkin and Bellido, 2001, Plotkin et al., 2002). These channels are located at the cell surface and have no physical contact with neighbouring cells. There are some similarities between hemichannels and gap junction channels, both contribute to the passage of molecules with molecular weights less than 1 kD_a. However, the main function of hemichannels is to create a bridge between cells and their extracellular matrix, while the gap junctions facilitate the communication between neighbouring cells.

There are several factors regulating the function of hemichannels including voltage, protein kinase C, extracellular Ca^{2+}, and retinoic acid (Gomez-Hernandez et al., 2003, Jedamzik et al., 2000, Zhang and McMahon, 2001). One investigation revealed that hemichannels regulate cell volume in response to the change in extracellular physiological calcium (Quist, 2000).

Gap junctions and hemichannels in the mechansensing osteocyte

As discussed earlier, osteocytes may actually respond to mechanically induced fluid flow through the canaliculi surrounding the osteocyte which is probably

responsible for the deformation of the cell membrane. Whitfield (2003) conjectured that the bending of the primary cilia of an osteocyte by extracellular fluid sends signals into the cells through the gap junctions.

Fluid flow shear stress will stimulate a chemical reaction, and the signalling molecules generated would be transmitted between cells by gap junction channels connected through the network of dendritic processes, and through hemichannels between osteocytes and the extracellular matrix. Subsequently, the signalling cascade leads to the expression of the regulatory molecules crucial for modulating bone formation and remodelling cycles (Jiang et al., 2007).

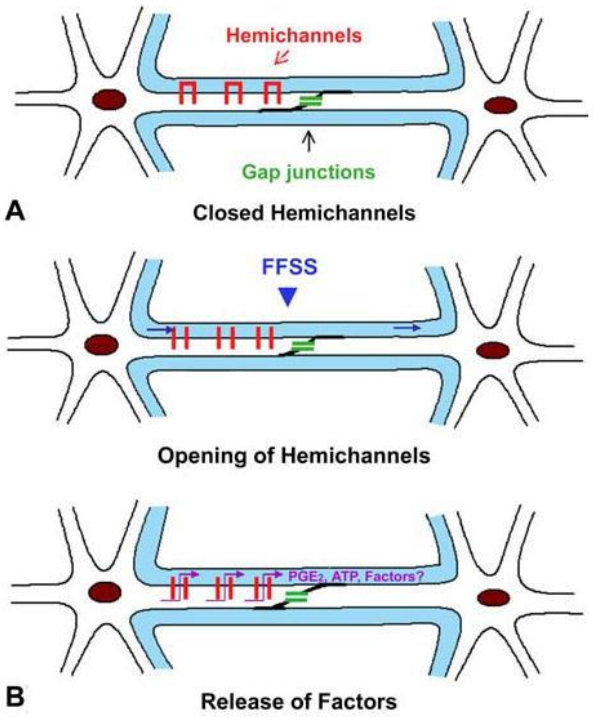

Figure 2-12: The model diagram for the role of hemichannels under fluid flow shear stress in osteocytes. Hemichannels are expressed on the plasma membrane away from cell-cell junction regions. (A) In the absence of mechanical stress, hemichannels remain closed, whereas gap junctions are kept open. (B) Fluid flow shear stress induces the opening of hemichannels (upper panel). PGE2, possibly ATP and other responding physiological factors are released into canaliculi to mediate biological responses elicited by mechanical stress (Jiang et al., 2007).

The osteocytes are connected to each other and the bone lining cells via gap junctions (Doty, 1981, Jones et al., 1993, Knothe Tate et al., 2004), thereby permitting direct cell-to-cell coupling. Gap junction channels mediate the quick intracellular passage of ions and molecular signalling, while the hemichannels mediate extracellular signalling which makes them suitable for sensing mechanical strain and later transmitting these mechanical signals into biochemical reactions (Figure 2-11 and 12).

The signals generated by mechanical stimulation are able to be transmitted between bone cells through gap junction channels, and between cells and the extracellular matrix through hemichannels where hemichannel opening is hypothesized in response to mechanical stress (Jiang et al., 2008) (Figure 2-11 and 12).

2.8 Discussion

The aim of this chapter is to present an overview of the necessary bone biology to understand the contents of this thesis.

Osteocytes are the most abundant cell type in bone comprising of more than 95% of all bone cells, with their normal density between 294 and 942 cells/mm^2. They are osteoblastic cells which were left in the bone matrix following bone modelling and remodelling. Osteocytes are located in a cavity (lacuna) and connected to each other by canals (canaliculi), and are able to communicate with each other and with bone lining cells (BLCs) at the surface of bone through these canaliculi via gap junctions. It is widely believed that the osteocyte-bone lining cell

network controls the adaptive bone remodelling process through the sensing of the mechanical loading on the bone and transmission of a signal to BLCs at the bone surface.

Although the importance of the osteocyte network in the mechanotransduction of bone is now well established, some of the mechanisms involved are still unclear. The mechanotransduction in the osteocyte take place in three steps: 1) stimulation of the osteocyte; 2) detection of the stimulation and 3) initiation of a signalling cascade. The osteocyte senses mechanical strain with functional gap junctions providing the intercellular communication between osteocytes and the transportation of molecules such as calcium (Mullender and Huiskes, 1997).

Aging, loss of ability to sense microdamage signal, loss of mechanical strain and deficiency of sex hormones have all been shown to promote osteocyte death or apoptosis. However apoptotic osteocytes can also occur in association with pathologic conditions such as osteoporosis, osteoarthritis and micropetrosis, usually leading to an increase in bone fragility.

This project aims to develop a simulation of the osteocyte-BLC network and investigate osteocyte signal propagation, the corresponding BLC signals, and the effects of apoptosis and microcrack on that signalling. Firstly, a model of a uniformly distributed osteocyte network will be developed which stimulates the signalling through the network to the BLCs based on strain level. Since Adachi et al. (2009a) identified asymmetric calcium signalling between osteocytes and BLCs, so

bi-directional and asymmetric communication between neighbouring osteocytes and BLCs are then included to the model. More importantly, the sensitivity of the network to increases in osteocyte apoptosis and microcrack length are then examined.

Chapter 3 Previous theoretical and experimental investigations into the role of the osteocyte network

3.1 Introduction

In recent years, a number of investigations have been carried out to examine the osteocyte's function in the mechanotransduction mechanism and bone remodelling process. They have given invaluable insights into the underlying biological responses of the cells. The aim of this research is to apply numerical simulation techniques to understand the effect of those biological processes in a little more detail. The main areas of investigation in this dissertation are:

- mechanotransduction in bone and the osteocyte network,
- the effect of osteocyte apoptosis,
- the effect of microcracks in bone.

3.2 Mechanotransduction in bone and the role of osteocytes

Bones functionally adapt to mechanical usage and activities, such as loading during physical exercises, and unloading, during bed rest and in spaceflight microgravity. The functional adaptation of bone occurs through the remodeling mechanism which is governed by bone metabolism and regulated by the bone cells. The

mechanotransduction mechanism, by which bone cells sense mechanical stimuli and regulate the remodeling process changing the structure of bone to meet the functional demands, is well established. A number of studies have investigated the mechanism of mechanotransduction in bone tissue *in vivo*, *in vitro* and *in situ*.

The model of Duncan and Turner (1995)

Duncan and Turner (1995) developed an *in vitro* model to examine the mechanism of mechanotransduction and the functional response of bone to mechanical strain. They proposed that mechanotransduction can be divided into four phases: (1) mechanocoupling, (2) biochemical coupling, (3) transmission of signal and (4) effector cell response.

Mechanocoupling. Mechanocoupling in mechanosensory tissues refers to the transduction of mechanical forces into local mechanical signal that can be detected by cells. Duncan and Turner (1995) showed *in vivo* that the bone's adaptive response is directly proportional to the rate of strain which determines the local deformation in the bone. It was also demonstrated in the laboratory that applied loading by less than 0.5 Hz frequency does not lead to bone formation, but mechanically induced bone formation is increased at 2 Hz (Duncan and Turner, 1995, Turner and Robling, 2005, Turner et al., 1995). They concluded that bone lining cells and osteocytes are the sensors of local bone strains as they are stretched the same amount as the bone tissue.

The range of peak levels of applied strains are between 400 and 2000 μstrain in humans during varied activities (Martin, 2000, Burr et al., 1995), with a combination of bending and compressive forces established as causing a large

variation of strains on the bone surface (Turner et al., 1994, Turner, 1998, Srinivasan and Gross, 2000, Burr et al., 1998, Hoffler et al., 2006). The osteocyte-bone lining cell network under bending loads in Duncan and Turner's investigation is presented (Figure 3-1). They proposed that a bending force creates tensile stress on one side of the bone and compressive stress on the other. This creates a pressure gradient in the interstitial fluids that drives extracellular fluid flow from regions of compression to region of tension. Fluid flows through the canalicular system and across the osteocytes pumping nutrients into the cells and creating fluid shear stresses on osteocytes cell membranes.

The results of Duncan and Turner's (1995) study show how an adaptive response in bone could be directly proportional to the rate of applied strain *in vivo* (Wang, 2008, Srinivasan and Gross, 2000, Bonewald, 2006b, Burger and Klein-Nulend, 1999a, Cowin, 2002, Nicolella et al., 2008, Charras and Horton, 2002).

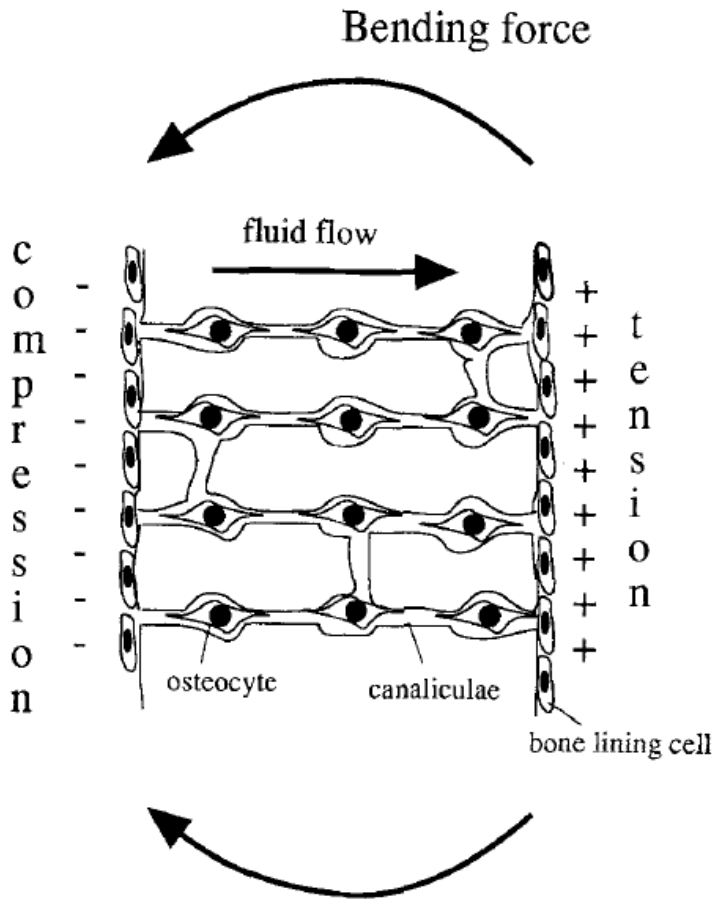

Figure 3-1: Schematic representation of a trabecula under bending loads (Duncan and Turner, 1995).

Other experimental investigations suggest that the rate of stress-produced fluid flow within the bone matrix shows a positive correlation with the rate of strain (Alford et al., 2003, Burger and Klein-Nulend, 1999a, Cowin, 2002, Han et al., 2004, Knothe Tate et al., 2004, Srinivasan and Gross, 2000, You et al., 2008, Turner et al., 1994). They also suggest the possibility that fluid flow within bone converts mechanical load into cellular signal. Similarly, microdamage due to the repetitive loading in bone over time was reported as another form of mechanical coupling (Ducher et al., 2009, Yingling et al., 2001, Duncan and Turner, 1995).

Biochemical coupling and transmission of biochemical signal. According to the experiment of Duncan and Turner (1995), the second phase of mechanotransduction is 'biochemical coupling''. In this stage of mechanotransduction, there is a proposed mechanism for the coupling of a cellular-level mechanical signal into an intracellular biochemical signal. Ion channels can be gated by mechanical strain, making them the best candidate as the initial biochemical coupling mechanism since no second messenger is required to activate the channels. Duncan and Turner (1995) presented two possible pathways by which a biochemical signal in the sensor cell is transmitted to the effector cells increasing osteogenic activity following mechanical loading: either through the activation of osteoblasts at the bone surface, or activation with the osteocyte and bone lining cell network. They suggested the latter was the most probable pathway due to the abundance of osteocytes and their extensive network of connectivity (Figure 3-2).

Effector response. The last step of Duncan and Turner's mechanotransduction mechanism is 'effector response' which plays a critical role in initiating the bone remodelling process, which is dependent upon the magnitude, duration and rate of the applied mechanical load. It was revealed that cyclic loading is the most potent stimulator of new bone formation, however longer duration lower amplitude loadings have the same effect on bone formation as loads with higher amplitude and shorter duration. They also added that the sensitivity of the sensor or effector cells to mechanical loading may be changed by hormones interacting with local mechanical signals.

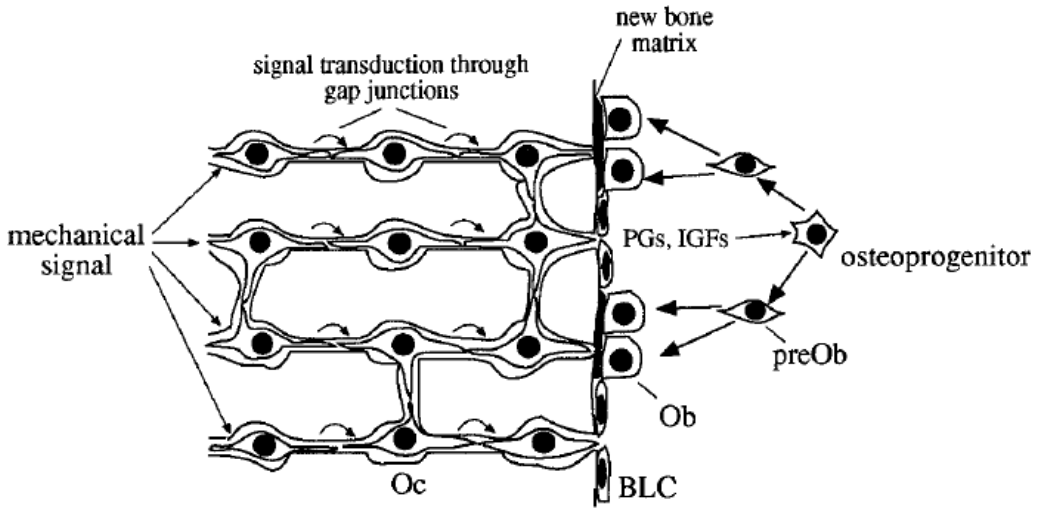

Figure 3-2: Schematic illustration of the suggested signal transduction pathways after a mechanical stimulus (Duncan and Turner, 1995). The mechanical signal is transmitted through the osteocytic network (Oc), via gap junctions, to the bone lining cells (BLCs). The BLCs stimulate osteoprogenitor cells to divide and differentiate into preosteoblasts (preObs). The preosteoblasts continue to differentiate into osteoblasts (Obs) which attach to the bone surface and produce new bone matrix.

The model of Burger and Klein-Nulend (1999)

Burger and Klein-Nulend (1999) presented a theoretical model for mechanotransduction in bone, emphasising the role of osteocytes as the most proficient mechanosensory cells in bone regulating bone remodelling. They assumed the mechanical stimulation activates osteocytes to produce the anabolic paracrine factors, which are transported via gap junctions through the osteocytic network to the bone surface recruiting new osteoblasts at the surface. Based on these assumptions, they presented a schematic model showing how the osteocyte network could regulate bone remodelling (Figure 3-3). Local bone gain and bone loss were explained as a result of local overuse and disuse. In the steady state, normal mechanical use keeps osteocytes viable and ensures a basal level of fluid flow through the lacuna-canalicular system, suppressing osteoblastic activity as well as osteoclast attack (Figure 3-3.A).

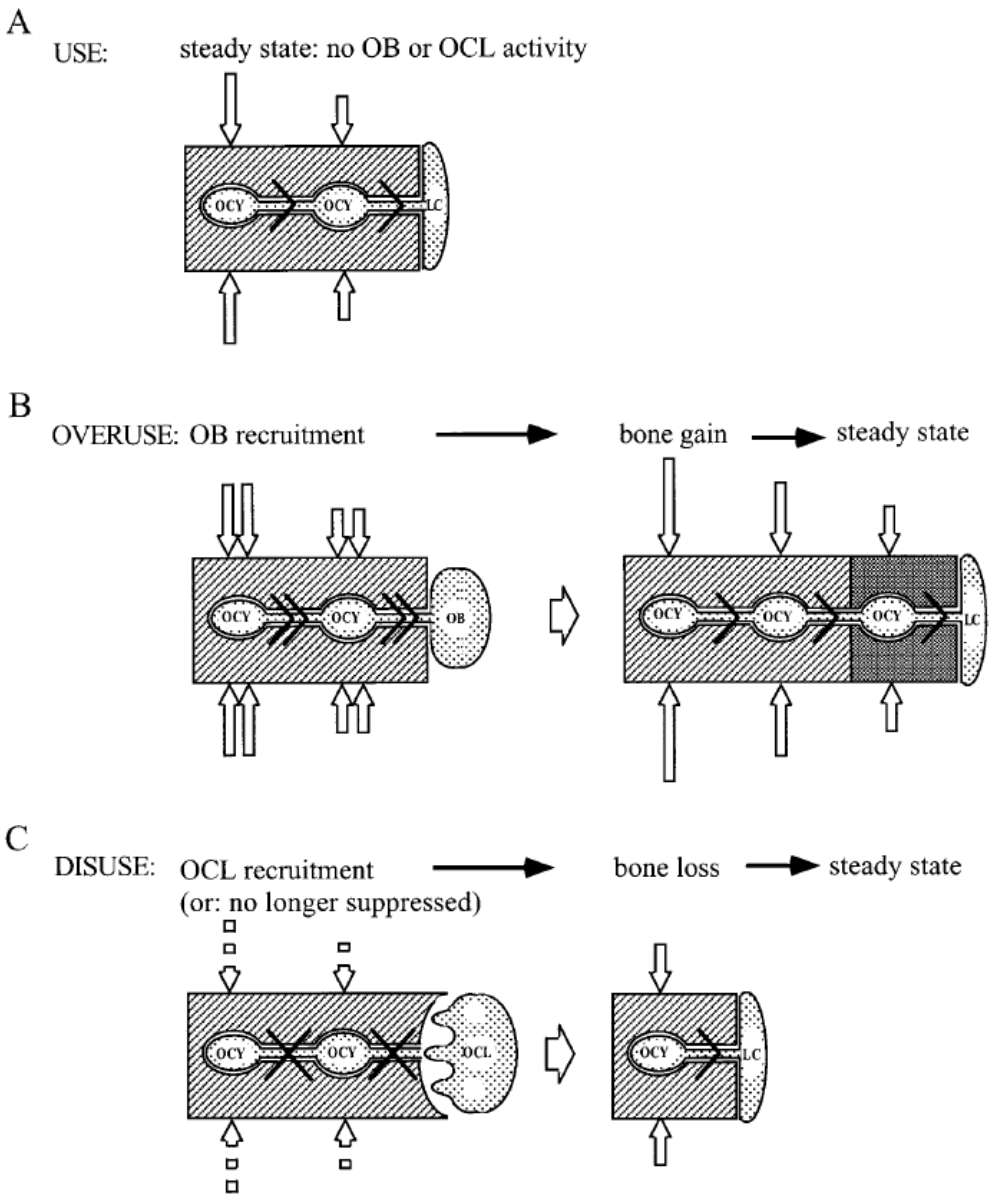

Figure 3-3: Schematic representation of how bone remodelling may be regulated by the osteocytic network (Burger and Klein-Nulend, 1999a). In the steady state, an arrowhead indicates the basal level of fluid flow through the lacuna-canalicular porosity. In the overuse state, double arrowheads represent an increase of fluid flow. Finally the lack of fluid flow in disuse state is represented by crosses through canaliculi. OCY, osteocyte; LC, Bone lining cell; OB, osteoblast; OCL, osteoclast; hatched area, mineralized bone matrix; dark-grey area, newly formed bone matrix; white arrows symbolize direction and magnitude of loading.

In the overuse state, overstimulation of osteocytes by abnormally high fluid shear stress leads to the release of a recruitment osteoblast signal (Figure 3-3.B). It is also noted that activated bone lining cells may re-differentiate as osteoblasts to

build new bone. Subsequently, the new formed bone re-establishes the normal state of basal fluid flow. In comparison, disuse means under-stimulation of osteocytes by a lack of fluid shear stress, resulting in a reduction of osteocyte viability or even osteocyte death which releases an osteoclast-recruiting signal or the absence of osteoclast-suppressing signal or both (Figure 3-3.C).

Based on the theory of osteocytic inhibition of osteoclasts, Burger and Klein-Nulend (1999) also presented a hypothetical model explaining how bone remodelling may be initiated by fatigue damage (Figure 3-4). They assume that repetitive loading in the normal physiological range causes fatigue micro-damage which affects the integrity of the osteocytic and lacuna calanalicular network by disrupting canaliculi and severing osteocyte processes. Disruption of the communication between damaged osteocytes and bone lining cells would then activate osteoclast recruitment, thereby initiating bone resorption (Figure 3-4.A). Resorption of the damaged bone then results in overuse and initiation of bone formation by osteoblasts (Figure 3-4.B), which would stop when the normal state of mechanical loading was reached (Figure 3-4.C). They also assume that the activity level of bone cells is regulated by hormones, such as sex hormones or parathyroid hormones, at each level of the mechanotransduction, including osteoblast/osteoclast recruitment and activity.

The role of osteocytes as mechanosensors in the inhibition of bone resorption due to mechanical loading, was validated *in vitro* by You et al. (2008). Part of the Turner and Klein-Nulend (1999)'s model relating to the activation of resorption by fatigue loading, and the regulation of osteoblasts and osteoclasts by

mechanosensitivity of osteocytes to shear stress, have also been experimentally tested and validated (Turner, 1998, Turner et al., 1994). However the assumption of modulation of the level of the cell activity by hormones in a systemic manners seems to be very unlikely *in vivo* (Harter et al., 1995).

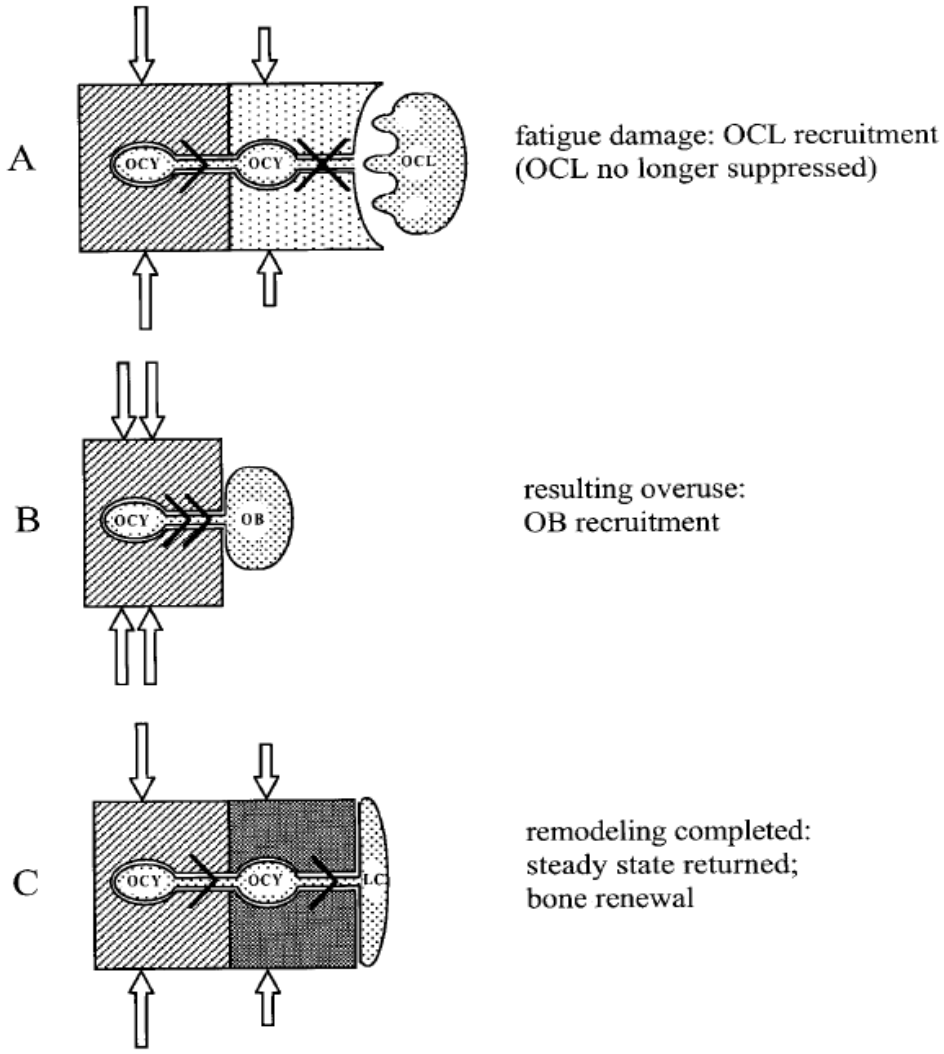

Figure 3-4: Schematic representation of how bone remodelling may initiated by fatigue damage (Burger and Klein-Nulend, 1999a). Matrix with fatigue is indicated by stippled matrix and other symbols are same as Figure 3.

Mullender and Huiskes (1997) employed an idealised trabecular bone model to investigate whether osteocytes or bone lining cells play the

mechanosensory role in bone. They developed two theoretical models to determine the best candidate for the mechanosensor (Figure 3-5). In the first, osteocytes are activated by mechanical loading to stimulate basic multicellular units (BMUs) and bone remodelling can be controlled by local feedback as shown in Figure 3-5. In the second, bone lining cells or osteoblastic cells on the bone surface sense the mechanical signal and stimulate BMUs without mechanosensory stimuli from osteocytes. Their results suggest that osteocytes are more efficient sensors of strain than bone surface cell, as osteoblastic cells are less sensitive than osteocytes to external loads because the architectures produced by osteocytes was more appropriate with mass distribution relative to the applied mechanical stimuli.

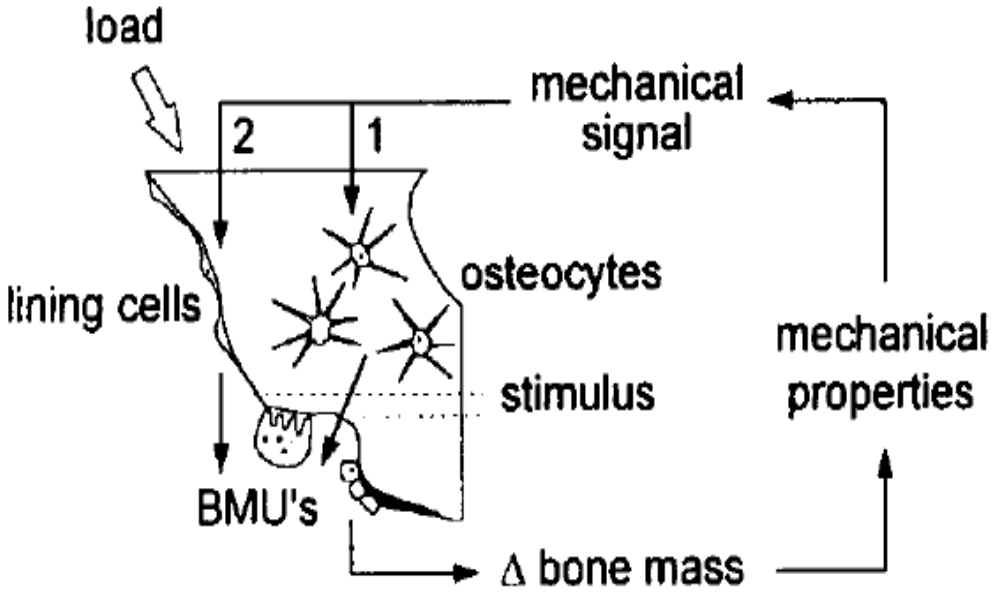

Figure 3-5: Schematic representation of two alternative theoretical regulatory schemes (Mullender and Huiskes, 1997).

Based upon the sensitivity of osteocytes to mechanical stimuli, Ausk et al. (2006) proposed a simulation of calcium signalling in a network of 81 osteocytes during application of mechanical loading to predict the global activity in the

network. The simulation was based on a small section of bone, with a 2-dimensional uniformly distributed osteocyte network which was subject to bending. It was assumed that each osteocyte was connected to its neighbours. Strain values experienced by the osteocytes varied throughout the network to replicate the effect of a bending type load. The range of cell activity at each time step ranged from 0% (inactive) to 100% (maximally activated cell). Each simulation assumed the following: (1) cell activity was calculated for each osteocyte based on the level of strain it experienced, according to specified activity thresholds; (2) there was symmetrical communication between neighbouring osteocytes, (3) the activity signals were modulated by calcium stores. Ausk et al. (2006) examined the effect of heterogeneity in the model for all parameters related to cellular function and the governing of cell activity. Their results show that the application of heterogeneity significantly affected the network response. However the model was limited in that it assumed symmetrical intercellular communication between osteocytes and ignored bone lining cells.

Later, experiments performed by Adachi et al. (2009) indicated that the intercellular communications between osteocyte cells and osteoblast cells are not symmetrical. They applied a direct mechanical stimulus to a single osteocyte then measured the calcium wave propagation between that cell and its neighbouring osteocytes and osteoblasts on the bone surface (Figure 3-6). The measurement of the calcium wave propagations between the osteocytic and osteoblastic cells indicated that the efficiency of calcium response propagation between bone cells depends on the type of 'receiver' cell but is independent of the transmitter cell

type. For example, they found that while 34.7% of the calcium signal level is transmitted from an osteocyte to a bone surface cell (BSC), only 9.4% is transmitted in the opposite direction, these signals are illustrated in Figure 3-6. They also suggest that because of this asymmetric communication between osteocyte and osteoblast cells, the mechanosensing by osteocytes near to the bone surface and connecting osteoblast cells, may be responsible for the mechanoregulation of the bone remodelling process. Several more experimental investigations have demonstrated that the application of a mechanical stimulus to an osteoblast cell induces an intercellular calcium signalling response which propagates to neighbouring cells (Guo et al., 2006, Huo et al., 2011, Huo et al., 2010, Hoffler et al., 2006, Charras and Horton, 2002).

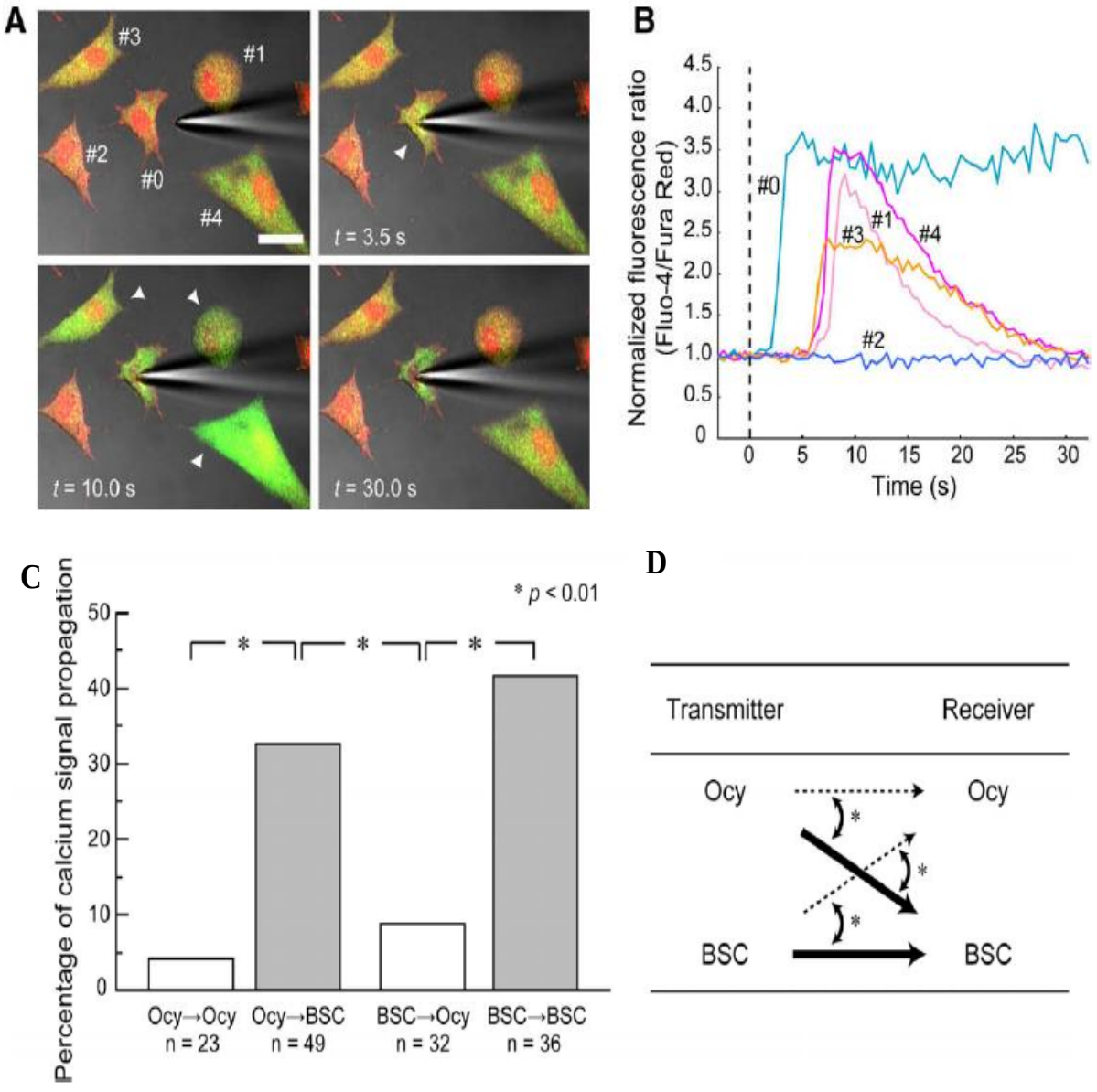

Figure 3-6: Time course change in [Ca2+], in bone surface cells (BSCs) and osteocytes (Ocy) in response to applied mechanical stimulus. (A) Cells #0 (Ocy) was stimulated to initiate a calcium signalling response (t=3.5s, arrowhead) and it transmitted to Cells #1, 3, 4 (BSCs) (t=10s, arrowhead). (B) The calcium propagation signal over time has been shown for each cell. (C) Percentage of intercellular for each pair of four possible combinations in cell types. (D) Four possible combination of communication based on the transmitter and receiver type cell (Adachi et al., 2009a).

In addition to the examination of mechanotransduction in a single osteoblastic cell, Charras and Horton (2002) provided an estimation of the threshold cellular strain level which is required to initiate an intracellular calcium reaction in primary osteoblasts. They examined mechanotransduction and its modulation in a single cell using atomic microscope indentation. The results demonstrate that osteoblastic cells respond to mechanical stimuli following a sigmoidal dose-response relationship (Figure 3-7). They also observed that intercellular calcium rises in a stimulated cell and can be propagated to neighbouring cells through the gap junctions but they did not determine the transmission levels as Adachi et al. (2009) did.

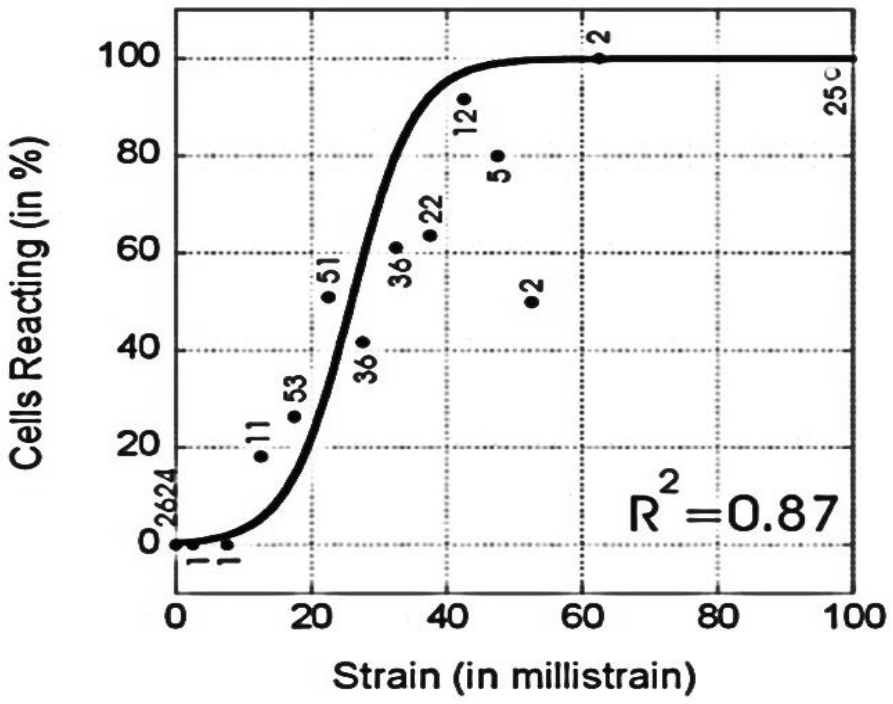

Figure 3-7: Reaction of osteoblastic cells to applied strain. The numbers refer to the number of cells in each strain group (Charras and Horton, 2002).

Guo et al. (2006) successfully cultured bone cells into a micropatterned MC3T3-E1 (osteoblast-like cells) network with dimensions similar to those of an *in vivo* osteocyte network. They did this using micro contact printing and self-assembled monolayers, a technique previously used in a study conducted by Guo et al. (1995). The bone cells in these networks were able to form gap junctions between each other, shown by immunofluorescent staining for the gap junction protein connexin 43. It was also demonstrated that the intracellular calcium response of an indented bone cell in this network could be transmitted to neighbouring bone cells through multiple calcium waves. Furthermore, the propagation of these calcium waves were found to diminish with increase in cell separation distance. This study provided experimental data in support of the fact that the osteocyte network 'memory' of mechanical loading is similar to the 'memory' in neural networks. For example, referring to Figure 3-8, intracellular calcium signals were observed to propagate from a single stimulated bone cell (cell #1) to neighbouring cells in the network. The calcium transmission in cell #1 increases rapidly after a short delay followed by a decrease, to less than the initial baseline level. Comparison of these experiments with those of Adachi et al. (2009) confirms two different patterns of signal propagation for osteoblasts and osteocytes (Figure 3-7), while propagation for all cells in this network followed the same pattern. However note that Adachi et al. (2009) investigated the calcium wave propagation between MLO-Y4 osteocyte-like cells and MC3T3-E1 osteoblast-like cells, while Guo et al. (2006) only studied MC3T3-E1 osteoblast-like cells within the osteocyte network.

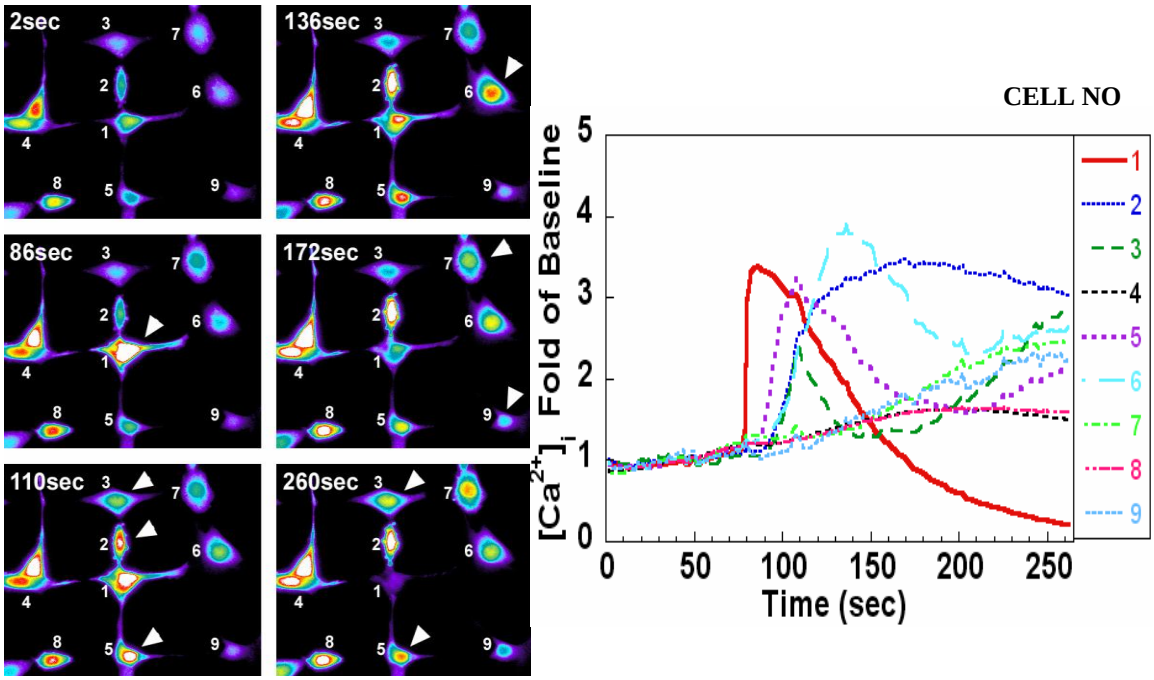

Figure 3-8: Demonstration of calcium signal propagation from a single indented bone cell (#1) to adjacent cells in the cultured network pattern (Guo et al., 2006).

3.3 The effect of apoptosis in bone

It is widely believed that aging, loss of ability to sense microdamage, loss of mechanical strain, and deficiency of sex hormones all promote osteocyte death or apoptosis as described in Chapter 2 (Dodd et al., 1999, Weinstein and Manolagas, 2000, Jilka et al., 2007). Apoptosis in osteocytes can also occur in association with pathological conditions such as osteoporosis (Qiu et al., 2003, Almeida et al., 2007). Dead osteocytes can remain in the bone for many months, but are eventually removed, leaving empty lacunae. A number of researchers have investigated osteocyte density and apoptosis in bone tissue *in vivo*, *in vitro* and *in situ* by using advanced microscopy. Frost (1963) undertook a study to consider whether the number of osteocytes changes with age. The results revealed a significant decline

in occupied lacuna density in human cortical bone from 95% at age 10 to 70% at age 40, then after 40 the density of lacunae remains constant. However since osteocytes still stain after their death, Frost's results may not be completely accurate. Later, Qiu et al. (2002) observed that viable osteocyte density in the human iliac cancellous bone fell considerably, between 20 to 70 years, but they also found an increase in empty lacunae or apoptosis density. In 92 cases, they measured different densities of osteocytes and empty lacunae in superficial bone (<25 μm from the surface) and in deep bone (>45 μm from the surface). The number of osteocytes in deep bone was significantly less than superficial bone at all ages in both genders. They also reported the decline in osteocyte density increased in deep bone rather than in superficial bone. This occurs with age in women as it does in men however, the pattern of osteocyte distribution within and between trabeculae was not affected by either menopause or age. Based on this observation, Qiu et al. (2002) concluded that the age-related osteocyte deficit was accompanied by an increase in empty lacunae and a decrease in the percentage of osteocyte-occupied lacunae, suggesting that bone remodelling may maintain osteocyte viability in iliac cancellous bone.

Qiu et al. (2003) examined iliac bone biopsies from 56 healthy women and 44 women with clinical vertebral fractures, and found that the osteocyte density declined in the patients with the fractures by 34% compared with healthy subjects of the same age. Many more empty lacunae were observed in the fracture group in both superficial and deep bone. They also found that the osteocyte deficit in fracture patients was accompanied by a decrease in lacunae and no change in the

percentage of osteocyte-occupied lacunae. They suggested that the reduction in both lacunae and osteocyte density in the osteoporotic bone may therefore be related to a decrease in the number of osteoblasts available for embedding in the matrix. Similarly, Mullender et al. (2005) reported a reduction in the number of osteocytes in the osteoporotic iliac crest in men and women compared to healthy subjects. The findings demonstrated that the osteocyte density is dependent on gender as well as age and disease. They also suggested that a reduction in osteocyte density in osteoporotic patients relates to imperfect bone remodelling which ultimately leads to bone loss. Conversely, the work of Busse et al. (2010) concluded that aging not only decreases the total number of osteocyte lacunae in cortical bone, but also changes the osteocyte distribution and contents (Figure 3-9). Based on the observation of micropetrosis by Frost (1960), they presented the parameter of the mineralized osteocyte lacunae per bone area, which reflects the number of osteocyte lacunae that were filled with mineralized tissue. The results in aged bone showed that the amount of hypermineralized calcium phosphate in apoptotic osteocyte lacunae was increased compared to younger cases. They suggested a pathway for the effect of aging on bone fragility (Figure 3-10), and revealed that increasing age was correlated with a decrease in osteocyte lacunar density and an increase in osteocyte apoptosis, both of which affect the bone repair processes. They (Busse et al., 2010a) also suggested that osteocyte death was a major contributor to lacunar hypermineralization (micropetrosis) and an impaired bone remodelling process as described in Section 2.3.3. They concluded that a failed or delayed bone repair mechanism in aging bone could account for this

increase in hypermineralized lacunae, and the decrease in osteocyte lacunar density which ultimately affects the mechanical properties of the whole tissue.

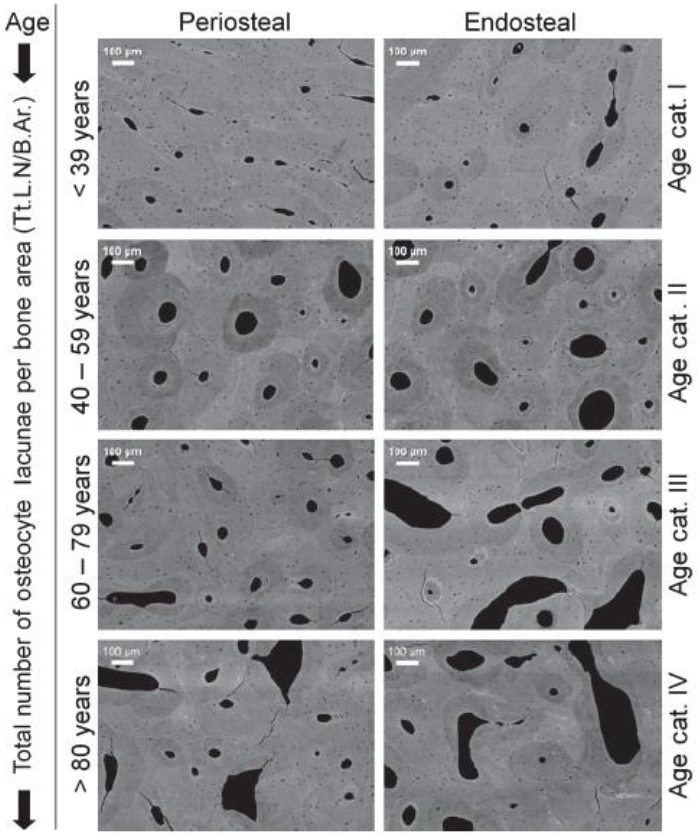

Figure 3-9: Distribution of osteocyte lacunae in different age cases. The number and distribution of osteocyte lacunae decrease with age (Busse et al., 2010).

Clark et al. (2005) examined osteocyte apoptosis in osteotomiesed chicken radii. They demonstrated that the incidence of osteocyte apoptosis increased within 12 hours of osteotomy, followed by an increase in osteoclast presence, but a numerical relationship between osteocyte apoptosis and number of osteoclasts was not established due to sample complexity. The results suggest the possibility of direct involvement of osteocytes in bone fracture repair. Similarly, an increase in osteoclast numbers with increasing osteocyte apoptosis was reported in both cortical and trabecular mouse bone within 3 days from when loading of the bone

ended (Aguirre et al., 2006). In addition, a reduction in trabecular and cortical bone width, spinal bone mineral density and vertebral strength followed unloading with increasing cortical porosity observed within 4 weeks. Despite increased remodelling by an increased numbers of osteoclasts, mechanical unloading resulted in increasing osteocyte apoptosis and a decreasing bone formation rate, which could not compensate for the resorption rate. This impaired bone remodelling process leads to loss of bone mineral and also strength

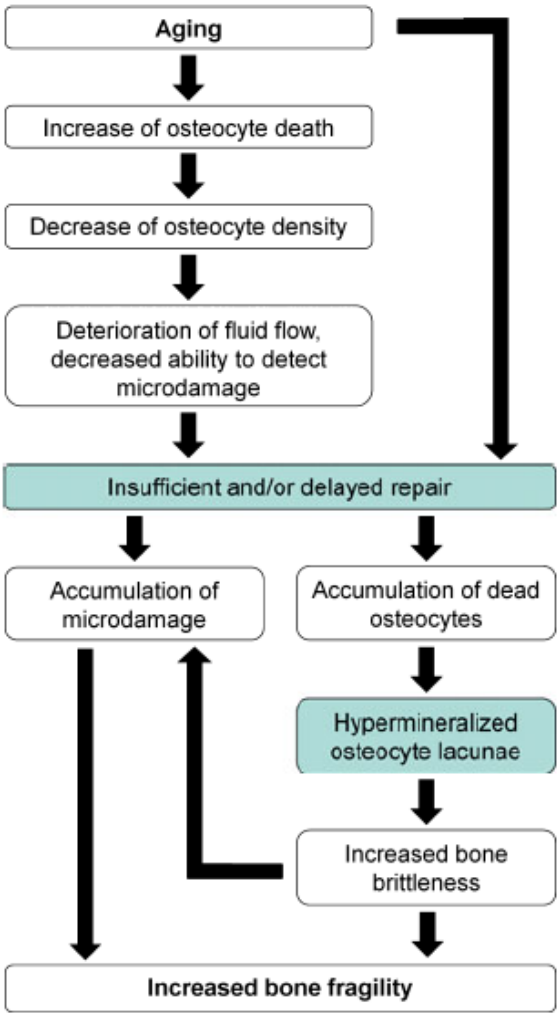

Figure 3-10: A suggested pathway of the effect of aging on bone fragility (Busse et al., 2010).

The development of a transgenic mouse model by Ikeda (2008) with specific ablation of osteocytes also revealed same results as those observed by Aguirre et al. (2006) and Clark et al. (2005). In another investigation, Tutsumi et al. (2007) used a single injection to ablate 70% of the osteocytes in transgenic mouse model, so the effects of osteocyte apoptosis could be classified into short and long term categories. Microfractures, impaired mineralization and resorption in cortical bone were the short term effects of osteocyte ablation within 8 days. However, no short term effects were observed in trabecular bone. They also reported a decrease in trabecular connectivity and thickness, an increased cortical porosity followed by a decrease in the cortical area of the femur, and ultimately osteoporosis in the bone were the long term consequences of osteocyte deficiency.

The numerical correlation between osteocyte apoptosis and rate of bone remodelling in rabbit tibial midshafts was examined by Hedgecock et al. (2007). The number of viable osteocytes, osteocyte lacunae, empty lacunae and apoptotic osteocyte density were quantified (Table 3-1). The data also demonstrated a linear correlation between the density of apoptotic osteocytes and remodelling.

	Osteocyte lacunae density (#/mm^2)	**Empty lacunae density (#/mm^2)**	**Osteocyte nuclei density (#/mm^2)**	**Apoptotic osteocyte density (#/mm^2)**	**Apoptotic osteocyte percentage (#/mm^2)**
Overall	694.5 ± 42.1	148.9 ± 19.4	545.6 ± 38.0	48.0 ± 40.3	9.1 ± 8.3

Table 3-1: The density of osteocyte and its viability in tibial rabbit (Hedgecock et al., 2007).

They suggested that the density of osteocyte apoptosis required to activate bone remodelling is 45 apoptotic osteocytes/mm^2. Below this critical value, the rate of

bone remodelling was constant whereas above the threshold, this remodelling rate increased in a linear fashion. These observations support the theory of initiation of bone remodelling by signalling of osteocytes undergoing apoptosis.

3.4 The effect of microcracks in bone

One of the physiological events in bone is the formation of microcracks, which may be a consequence of fatigue loading *in vivo*. Frost (1985) originally proposed that the potential stimulus initiating bone remodelling was microcrack formation which leads to a disruption of the canalicular connections in the osteocyte network. However more recent studies have suggested that osteocyte processes are ruptured when microcracks traverse them (Figure 3-11), and may directly secrete passive or active components into the extracellular matrix which induce bone remodelling to repair the area (Hazenberg et al., 2006) .

It has also been observed that microcracks are able to grow during constant stress in cortical bone leading to increased microdamage by a time dependent build up of local strain (Hazenberg et al., 2006). In contrast, other researchers (Civitelli, 2008; Eriksen, 2010b; Guo et al., 2005; Hazenberg et al., 2006; Hazenberg et al., 2007; Marotti, 2010; Nijweide et al., 1998; Rubinacci et al., 2002) believe that active gap junctions provide the intracellular communication in osteocyte-canalicular systems and inhibit the activation of osteoclastic resorption, and it is this which is interrupted by the microcrack. However there is mounting evidence for the view that the apoptotic response is localised in regions containing microcracks. Thus osteocytes are the key factor in interrupting the transmission

system and triggering bone remodelling (Martin, 2000, Emerton et al., 2010, Hazenberg et al., 2006, McNamara and Prendergast, 2007).

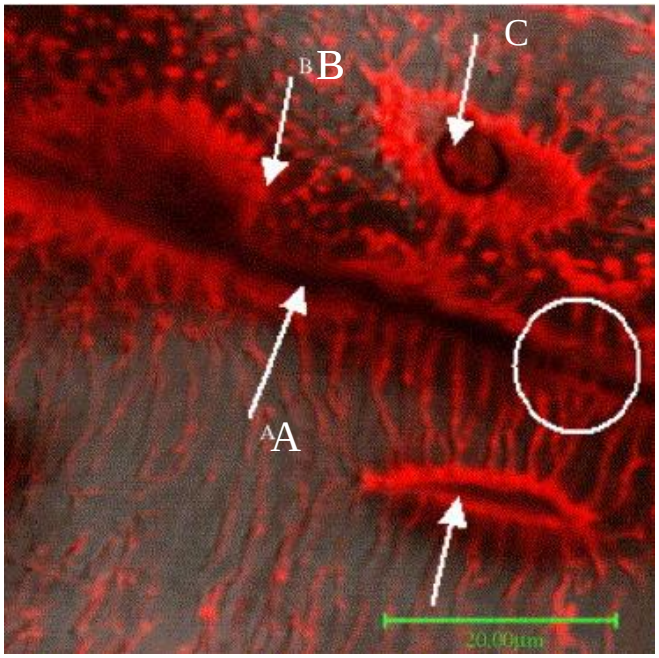

Figure 3-11: A confocal microscopy image of a microcrack and three effected osteocytes (solid arrows) by microcrack. Many of the cell processes are broken, but some processes seem to cross the crack faces (circle) (Hazenberg et al., 2006).

Many investigators have observed that microcracks are distributed through the local micro structure in human and animal cortical and trabecular bone (Tables 3-2 and 3-3). Only linear microcracks are observed in cortical bone, but linear and cross-hatched cracks appear in trabecular bone. In the latter, the density of trabeculae appears to be a function of the density of microcracks, where a decrease in trabeculae is observed with an increasing density of microcracks (Mori et al, 1997).

The lengths of microcracks reported in the literature vary greatly, with most studies examining microcracks in the interstitial tissue and only a small number in osteons. Wasserman et al. (2008) reported that the length of 1,141 microcracks

ranged between 54.4 and 2,285 μm (Figure 3-12). They also suggest that linear microcracks of the femoral mid–shaft grow in planes parallel to osteons and that their lengths do not change with age.

It was generally believed that the density of microcracks relates to gender, age, porosity and osteocyte density. Schaffer et al. (1997) found that microcrack density increases remarkably in human femoral cortical bone with age and are larger in females than in males at a comparable age, however they do suggest that crack length is independent of age. Conversely, Vashishth et al. (2000) found that there were no gender–related differences in osteocyte lacunar density and microcracks and porosity, but they described an exponential relationship between osteocyte density and microcrack density.

Three-dimensional images of single microcracks in trabecular bone (Fazzalari et al., 1998) and cortical bone (O'Brien et al., 2000) obtained by reconstructing serial sections of two-dimensional confocal microscopy images is one of the techniques used to examine individual microcracks and damaged regions *in vivo*. However the depth of these observed microcracks were limited to approximately 200 μm from the surface (Fazzalari et al., 1998, O'Brien et al., 2000, Wang et al., 2007, Zarrinkalam et al., 2005) and the field of view is small. In later studies, some microcracks were found within 500 μm of the bone surface in compact bone by using epifluorescence microscopy (O'Brien et al., 2003). Furthermore, the computational study of Gefen and Neulander (2007) proposed a critical size of microcrack which would initiate the bone remodelling process in a trabecular bone. They suggested that a microcrack with a minimal length of 48 μm and

minimal depth of 13% of the trabecula's thickness from the bone surface, or longer microcracks closer to the surface (7% of the trabecula's thickness) for trabeculae with a length of 900 μm and thickness of 80-800 μm were required to activate bone remodelling.

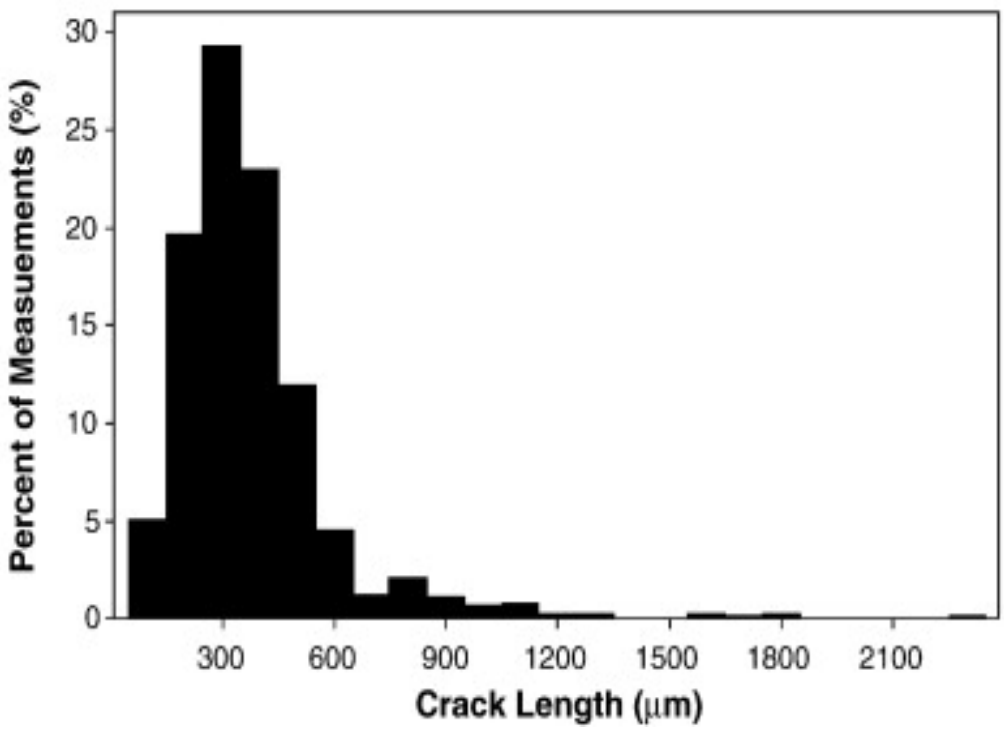

Figure 3-12: The lengths of 1,141 observed cracks in bone (Wesserman et al., 2008).

Reference	Density of microcrack (#/mm²)	Length of microcrack (μm)	Crack surface density (μm/ mm²)	Species	Section	Region
Schaffler et al. (1989)	-	80	-	Bovine	longitudinal	femur
Burr and Martin (1993)	-	88 ± 54	-	Equine	longitudinal	metacarpal
Mori and Burr (1993)	-	58	-	Canine	longitudinal	radius
Lee et al. (1995)	-	55 ± 18	-	Ovine	longitudinal	Radius
Gomez et al. (2005)	0.022 ± 0.008	41 ± 10	0.84 ± 0.27	Racing Thoroughbreds	transverse	Metacarpal
Gomez et al. (2005)	0.013 ± 0.006	37 ± 15	0.50 ± 0.29	Non-athletic horses	transverse	Metacarpal

Table 3-2: Microcrack density and length in different animals.

Reference	Density of microcrack (#/mm²)	Length of microcrack (μm)	Crack surface density (μm/ mm²)	Section	Region
Burr and Stafford (1990)	-	88 ± 38	-	longitudinal	rib
Burr and Martin (1993)	-	296 ± 257	-	Transverse	rib
Lee et al. (1998)	-	82 ± 29	-	longitudinal	rib
Donahue et al. (2000)	0.35 ± 0.30	75.04 ± 24.21	25.91± 21.22	longitudinal	Metatarsal
Donahue et al. (2000)	0.28 ± 0.27	81.67 ± 23.54	22.53 ± 23.02	longitudinal	Metatarsal
(Zioupos, 2001)	1.2 ± 0.8	10-2250	-	Transverse and longitudinal	Femur
Qiu et al. (2005)	1.32 ± 0.63	63.5 ± 26.9	-	longitudinal	Rib (interstitial bone)
Qiu et al. (2005)	0.25 ± 0.26	61.9 ± 22.3	-	longitudinal	Rib (Osteon)
Wasserman et al. (2008)	-	54.4 - 2285	-	longitudinal	Femur

Table 3-3: Microcrack density and length in humans.

3.5 Discussion

It is widely agreed that in the bone remodelling cycle the load experienced by the bone is sensed by the osteocyte and bone lining cell network, which leads to the removal of old bone and subsequent formation of new bone. Inevitably, there will be some osteocytes and their canalicular connections which function incorrectly through apoptosis and microcracks, but there is evidence in some diseases such as osteoporosis, that the number of apoptotic osteocytes is higher than normal. Experimental evidence shows that this will affect the functioning of the osteocyte network, and potentially lead to higher rates of remodelling observed with osteoporosis. The aim of this research is to develop a simple osteocyte and bone lining cell network model to investigate cell signalling and communication in the network under loading, and examine the sensitivity of the network to changes in osteocyte apoptosis and the effect of microcrack length. The next chapter describes the basic model used in these simulations.

Chapter 4 A basic simulation of the osteocyte and bone lining cell network

4.1 Introduction

Osteocytes are the most abundant cell type in bone and are located in lacunae, connected to each other by canals, and are able to communicate with each other and with bone lining cells (BLCs) at the surface of bone through these canaliculi via gap junctions. It is widely believed that this osteocyte-bone lining cell network controls the adaptive bone remodelling process through the sensing of the mechanical loading on the bone and transmission of a signal to BLCs at the bone surface, as discussed in detail in Chapter 2. The mechanotransduction in the osteocytes takes place in three steps: 1) stimulation of the osteocyte; 2) detection of the stimulation and 3) initiation of a signalling cascade (Rochefort et al., 2010). The osteocyte senses mechanical strain with functional gap junctions providing the intercellular communication between osteocytes and transportation of molecules such as calcium (Ishihara et al., 2008, Yellowley et al., 2000).

In this chapter, a simulation of cellular communication in the osteocyte and bone lining cell network is developed. The work proceeds in two steps. First, a simple model of just the osteocyte network is developed, which is then activated by the application of the strain, and the signals then propagated through the canalicular system in order to apply communication between cells. Once the basic algorithms of this simple osteocyte network are established, it is extended by

including bone lining cells on the surface.

4.2 A basic simulation of just the osteocyte network

4.2.1 Methods

Model Development

The model developed here is based on an idea proposed by Ausk et al. (2006) who described a simulation of calcium signalling in a small abstract network of just 81 osteocytes during loading in order to predict the global network activity. In the current research, a section of bone was considered, with a 2-dimensional uniformly distributed osteocyte network. It was assumed that each osteocyte was connected to its neighbours by canaliculi as illustrated in Figure 4-1. The sample size was 4×4mm with an assumed network of 100×100 osteocytes (Vashishth et al., 2000). Thus, the horizontal and vertical canaliculi have a length of 42μm, with an effective osteocyte density of 625/mm^2 (Wang et al., 2005b, Schneider et al., 2010). Strain values experienced by the osteocytes were assumed to be varied between ε_{min} at the lower (internal) edge of the sample and ε_{max} at the upper (external) edge to simulate the effect of a bending type load. The cell activity simulated at each time step range from 0% (inactive) to 100% (maximally activated). In a simulation, an activity signal is calculated for each osteocyte based on the level of strain it experiences according to specified activity thresholds. Then a cycle of communication between neighbouring osteocytes takes place through the canalicular network via gap junctions, again this is dictated by predefined amounts.

The specific details of the model are as follows:

Calculation of activity signal

Firstly, the strain $\varepsilon\ i,j$ experienced by each cell is calculated based on its location and tissue strains using the following equation:

$$\varepsilon\ i,j\ = \begin{matrix} \varepsilon_{max} & i = 100 \\ \varepsilon_{min} + \ n_i \times \frac{\varepsilon_{max} - \varepsilon_{min}}{n-1} & i < 100 \end{matrix} \quad (1)$$

where $\varepsilon\ (i,j)$ is the strain at location (i,j), $\varepsilon_{min}$and ε_{max} and are the minimum and maximum strains on the lower (internal) edge and upper bone surface respectively, with a linear variation in between, simply calculated by row number, n_i with n being the total number of rows (n=100).

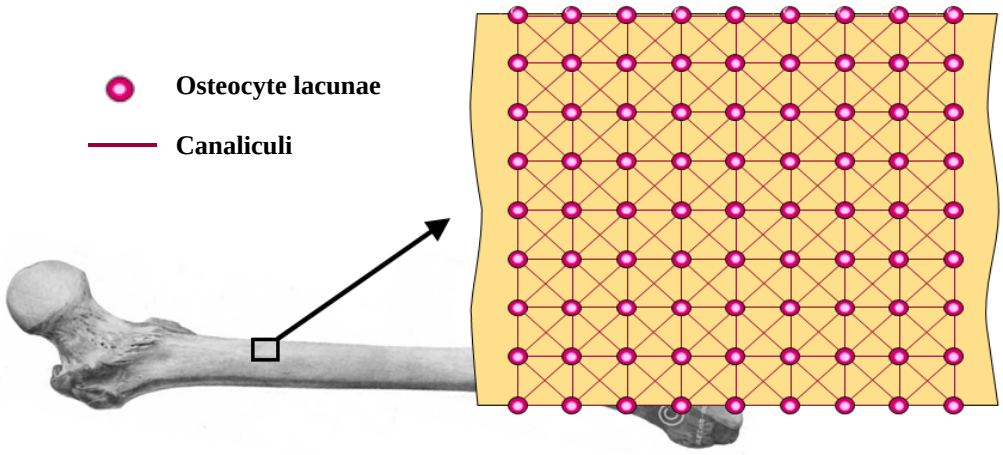

Figure 4-4-1: Small section of the idealized osteocytic network. The vertical and horizontal distance between osteocytes is 42μm.

A sigmoidal dose-response curve was assumed for the relationship between the applied strain magnitude and intracellular calcium signal activity, as reported by Charras and Horton (2002). Here, it was simplified to a piece-wise linear variation, so that the activity signal for each cell was defined as follows:

$$S^{\varepsilon}(i,j) = \begin{cases} 0\% & \varepsilon(i,j) \le T^{\varepsilon}_{min} \\ 100 \times \frac{\varepsilon(i,j) - T^{\varepsilon}_{min}}{T^{\varepsilon}_{max} - T^{\varepsilon}_{min}} \% & T^{\varepsilon}_{min} \le \varepsilon(i,j) \le T^{\varepsilon}_{max} \\ 100\% & \varepsilon(i,j) \ge T^{\varepsilon}_{max} \end{cases} \quad (2)$$

where $S^{\varepsilon}(i,j)$ is the activity signal for the cell located at coordinates (i,j) in response to the strain, and T^{ε}_{min} and T^{ε}_{max} are the threshold strain magnitudes to initiate and maximise cell activity respectively.

Calcium wave propagation between osteocytic cells was modelled whereby activated osteocytes could propagate signal to adjacent cells (Yellowley et al., 2000). In order to apply this communication in the network simulation, it was assumed that each cell could receive a signal from its neighbours ($S_c(i,j,t)$). Thus the basic network communication equations were as follows:

$$S_C(i,j,t) = \frac{\sum_{n=1}^{N} S_n(i,j,t-1)}{N} \quad (3)$$

$$S_0(i,j,t) = \begin{cases} S^{\varepsilon}(i,j), & t = 1 \\ max\left(S_c(i,j,t),\ S_0(i,j,t)\right), & t \neq 1 \end{cases} \quad (4)$$

where $S_0(i,j,t)$ is the activity signal induced in the cell located at (i,j) at time '*t*' by transmission of signals from neighbours in addition to its own signal activity response to the strain at that point; $S_c(i,j,t)$ is the average activity signal induced in the cell by transmission of signals from neighbours dependent on its previous activity level; N is the number of neighbours of the cell at coordinate (i,j).

Simulation

Network simulations defined by equations (1) to (4) were solved using Matlab (v7.7.0, Mathworks, Natick, USA) with typically over 250 iterations with initial

parameter values as defined in Table 4-1. All parameters such as the location, the strain, the number of neighbours and received signal from neighbours at each iteration were defined individually for each osteocyte as its properties in this model. These parameters could also vary. In the first simulation, one reporter was used to characterise the status of the network at each iteration where each iteration corresponds to one second in time. “Mean network activity” was calculated by averaging the instantaneous net signal at each osteocyte. It was also assumed that the numerical values of cellular functions ($T^{\varepsilon}_{min}, T^{\varepsilon}_{max}$) were homogenous for all of the cells in the network. Then variations of threshold strain values were examined ($T^{\varepsilon}_{min}, T^{\varepsilon}_{max}$) on the mean network activity signals. The effect of heterogeneity (H) was also included as suggested by Ausk et al. (2006). In this case numerical values of the cellular functions ($T^{\varepsilon}_{min}, T^{\varepsilon}_{max}$) were altered by parametrically varying their values of the standard deviation assuming a normal distribution. In total, the code to implement this simulation consisted of 140 lines, with each iteration Matlab code taking approximately 2 seconds on a Windows XP PC. The part of code related to calculation of cell activity based on strain is available in Appendix A.

Parameter	Symbol	Value	Units	References
Number of cells	m×n	100×100	-	-
Row number	i	1 to 100	-	-
Column number	j	1 to 100	-	-
Applied min strain	ε_{min}	-1000, 600	μstrain	-
Applied max strain	ε_{max}	1000	μstrain	-
Threshold strain to initiate cell activity	T^{ε}_{min}	50, 500, 1000	μstrain	(Martin, 2000)
Threshold strain to maximize cell activity	T^{ε}_{max}	1000, 1500, 2000	μstrain	(Martin, 2000)
Cycle duration	t	1 to 1000	second	-
Heterogeneity	H	0, 5%, 10%, 15%, 25%, 50%	-	-

Table 4-1: The numerical values of parameters were utilised in the osteocyte network.

4.2.2 Results

Variation of T^{ε}_{min} and T^{ε}_{max}

In the model when the osteocyte network was subject to a range of applied strain magnitude ($\varepsilon_{\min}$ and $\varepsilon_{\max}$), the mean network activity signal established a maximum invariant baseline responses of 90% (Figure 4-2, line o). When strain magnitude thresholds ($T^{\varepsilon}_{\min}$ and $T^{\varepsilon}_{\max}$) were incorporated into the model, the mean network activity signal decreased with increasing either $T^{\varepsilon}_{\min}$ or $T^{\varepsilon}_{\max}$ (Figure 4-2, lines a and d); for instance when the applied strain range was between -1000 and 1000με ($\varepsilon_{\min} = -1000$ and $\varepsilon_{\max} = 1000\mu\varepsilon$) and the strain thresholds values were 500 and 2000 με ($T^{\varepsilon}_{\min} = 500$ and $T^{\varepsilon}_{\max} = 2000\ \mu\varepsilon$), the mean activity signal had an

invariant activity of 11.11% (Figure 4-2, line a). However, it increased by 21% when the maximum strain threshold decreased by 50% (i.e. $T^{\varepsilon}_{max} = 1000$ με) (Figure 4-2, line d). It also increased by 40% when minimum and maximum strain thresholds decreased by 90% and 25% ($T^{\varepsilon}_{min} = 50$ and $T^{\varepsilon}_{max} = 1500$ με) respectively with the applied strain range of 600 to 1000 με ($\varepsilon_{min} = 600$ and $\varepsilon_{max} = 1000$με) (Figure 4-3).

Then, when osteocytes were enabled to communicate through the network, the mean network activity signal dramatically increased (Figure 4-2, lines b and e); for instance when the applied strain range was between -1000 and 1000με ($\varepsilon_{min} = -1000$ and $\varepsilon_{max} = 1000$με) and the strain thresholds values were 500 and 2000 με ($T^{\varepsilon}_{min} = 500$ and $T^{\varepsilon}_{max} = 2000$ με) and osteocytes communicated with each other, the mean activity signal increased from 11.11% to 32% in 100 seconds after load application (Figure 4-2, line b). The mean network activity signal also increased significantly by 69% when the maximum strain threshold decreased by 50% (i.e. $T^{\varepsilon}_{max} = 1000$ με) (Figure 4-2, line e).

When heterogeneity was included in the strain thresholds, the mean network activity level increased at low stimulus magnitude (Figures 4-2 and 4-3); for instance when the applied strain range was between -1000 and 1000με ($\varepsilon_{min} = -1000$ and $\varepsilon_{max} = 1000$με) and the strain thresholds values were 500 and 2000 με ($T^{\varepsilon}_{min} = 500$ and $T^{\varepsilon}_{max} = 2000$ με) and osteocytes communicated with each other and the heterogeneity of 25% was included in strain thresholds (H (T^{ε}_{min}) =H (T^{ε}_{max}) =25%) , the mean activity signal increased significantly by 69%, from 32%

to 100%, in 250 seconds after load application (Figure 4-2, line c). The mean network activity signal also reached the maximum quicker than before when the maximum strain threshold decreased by 50% (i. e. $T^{\varepsilon}_{max} = 1000\ \mu\varepsilon$) (Figure 4-2, line f).

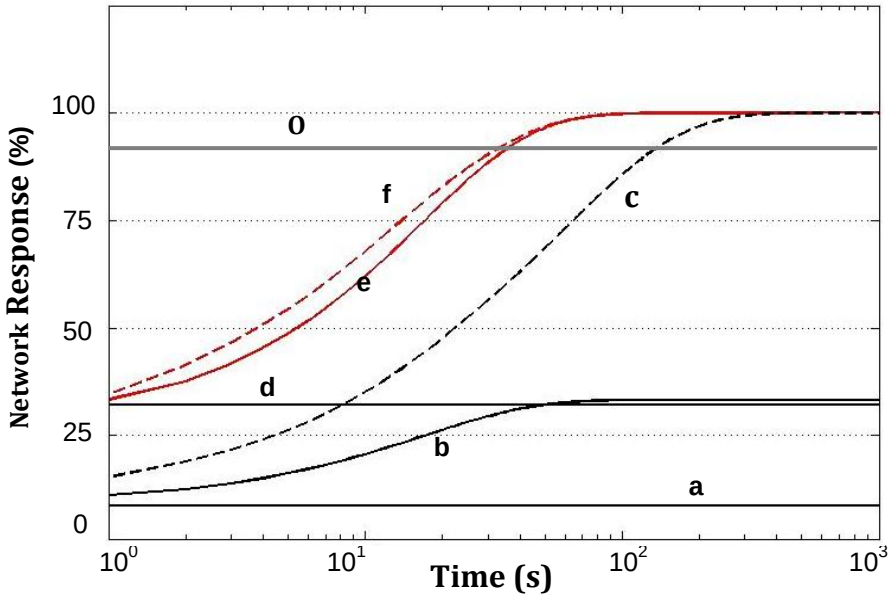

Figure 4-2: Mean network response with time (increasing number of iterations) and variation of $T^{\varepsilon}_{min}, T^{\varepsilon}_{max}$. When the strain applied the osteocytic network establish baseline response (a: $T^{\varepsilon}_{min} = 500\ \mu\varepsilon$, $T^{\varepsilon}_{max} = 2000\ \mu\varepsilon$ and d: $T^{\varepsilon}_{min} = 500\mu\varepsilon$, $T^{\varepsilon}_{max} = 1000\ \mu\varepsilon$). Communication between cells take place (b and e). Then include the heterogeneity in strain thresholds (H (T^{ε}_{min}) =H (T^{ε}_{max}) =25%), network response increase rapidly (c and f).

Homogenous thresholds parameters

In a model where all cellular functions and parameters are homogeneous in all cells (with $\varepsilon_{min} = 600$, $\varepsilon_{max} = 1000$, $T^{\varepsilon}_{min} = 50$, $T^{\varepsilon}_{max} = 1500\ \mu\varepsilon$), network activity is minimal at the (lower) internal surface and increases towards the (upper) outer surface (Figure 4-4). The signal experienced by the cells on the surface is high and relatively uniform. The variation of the mean network activity signal with time for this case is shown in Figure 4-3. The solid black line shows the mean osteocytic

network signal, with no heterogeneity which follows an invariant baseline response of 51.97%.

Heterogeneous threshold parameters

Even with a small percentage of heterogeneity in the model, the signalling is increased significantly. The sample contour plots of activity in Figure 4-4 at t = 1 and t = 100 seconds show an increase in activity level as the degree of heterogeneity increases. Due to the random distribution of the heterogeneity for each cellular function, each osteocyte in each simulation gains individual cell activity at each second, as illustrated in Figure 4-4. Short *movies* of the variation of the signals with different heterogeneities are available on the CD in the Appendix C (Movies 4-1, 4-2, 4-3, 4-4 and 4-5).

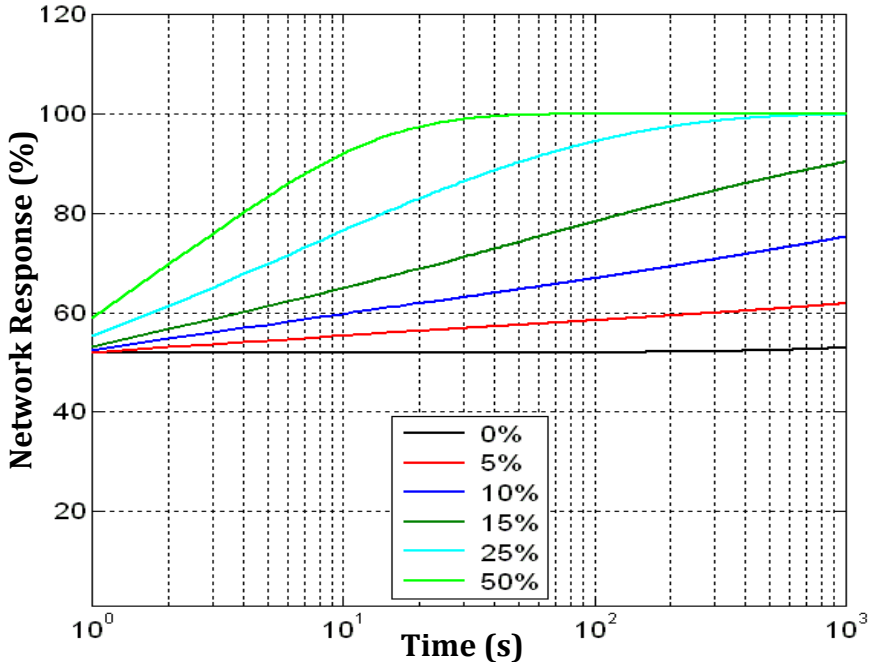

Figure 4-3: Mean network response with time.

The variation of the mean network signal over time for the different

heterogeneity scenarios is shown in Figure 4-3. When the levels of heterogeneity were increased, steady state mean network activity also increased. Beyond a certain level (20% heterogeneity) mean network activity reached maximum values of 100% activity within a certain period of time. With just 5%, 10%, 15%, 25% heterogeneity, the network response levels are increased by 7%, 16%, 27% and 43% respectively at 100 seconds following strain application (Figure 4-3). Where 50% heterogeneity occurs maximal signal levels are reached just 40 seconds after strain application.

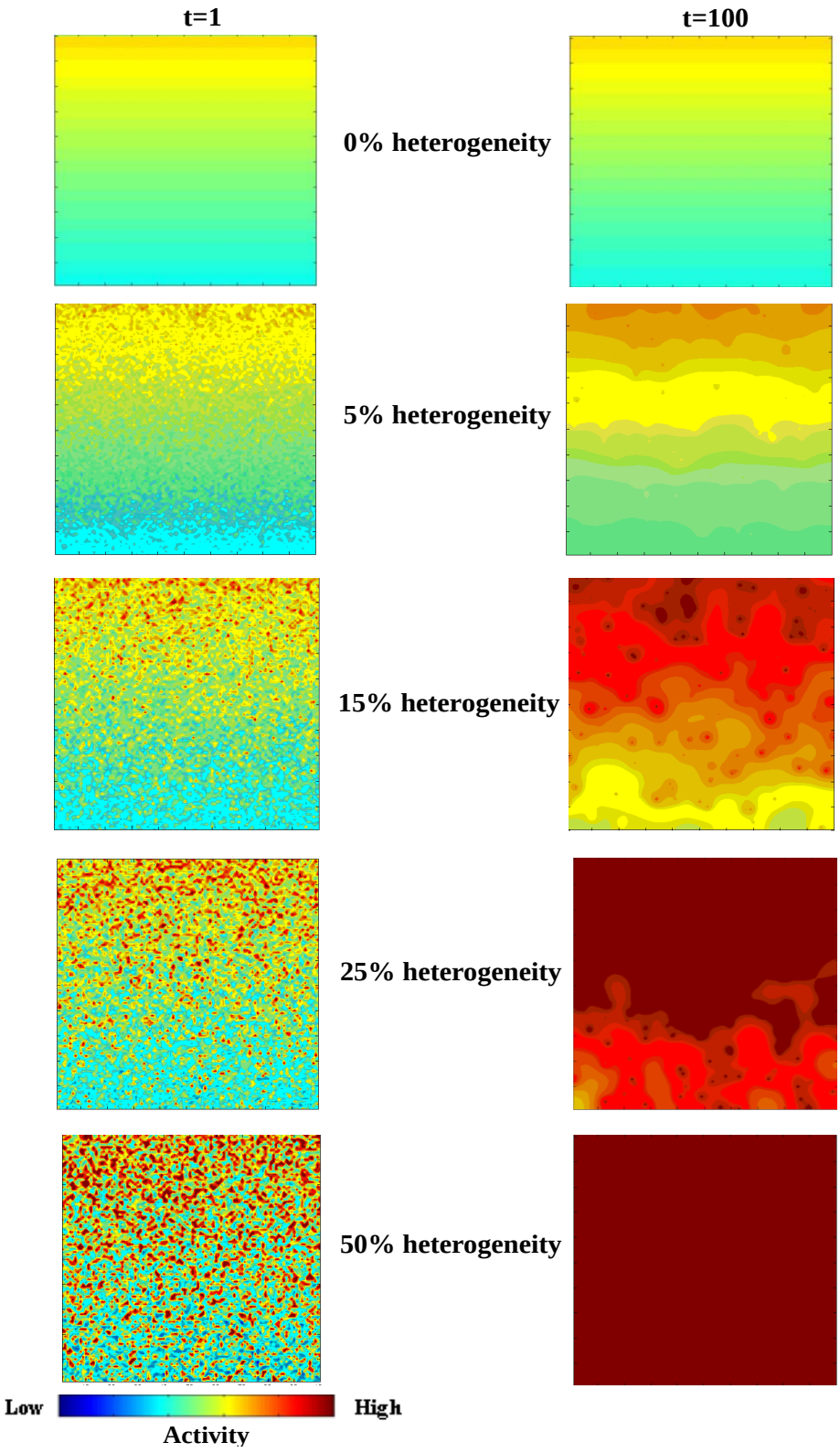

Figure 4-4: Contour plots of network activity after 1 and 100 seconds for sample models with increasing levels of heterogeneity.

4.2.3 Discussion

In these first simple simulations, each osteocyte was activated based on the mechanical strain it experienced, assuming a simple bending type load. The activity signal was dependent on a cell's location and according to specified activity thresholds. Then intercellular communications through interconnecting canalicular via gap junctions took place.

Using the basic model parameters defined previously, without heterogeneity, the network activity is found to be relatively uniform (Figures 4-4), as is the mean network response (Figure 4-3). With heterogeneity, the mean network response is increased significantly, with just 15% heterogeneity leading to an increase in mean network response signal of 27% at 100 seconds (Figure 4-3). The variations in the predicted mean network signals as illustrated in Figure 4-2 compare well with the model of osteocytic signalling network published by Ausk et al. (2006) (Figure 4-5). Apart from strain thresholds, secondary cell-cell communication thresholds were predefined in Ausk's model which indicated that activity signal from neighbours ($S_c(i,j,t)$) needed to surpass to initiate and maximally influence activity in the recipient cells. There is no evidence to support such a constraint on secondary cell-to-cell communication. Thus it appears that a powerful positive feedback is provided by adding cell heterogeneity to the network, allowing extremely low magnitude stimuli to maximally activate the entire network (Figure 4-3). Threshold strain values also provide the negative feedback to the network activity (Figure 4-2).

A number of simplifications and assumptions have been made during parameterisation of the cellular functions, which could affect the results. As discussed in Chapters 2 and 3, a certain strain magnitude is required to initiate cell activity in bone (Martin, 2000, Frost, 1992, Charras and Horton, 2002) and here this cellular function is represented by T^{ε}_{min} and T^{ε}_{max}. It was also assumed that cell communication occurs between each osteocyte and all its immediate neighbours however the concept of averaging cell activity within neighbourhoods is just a hypothesis. This is discussed further in the model of the next chapter.

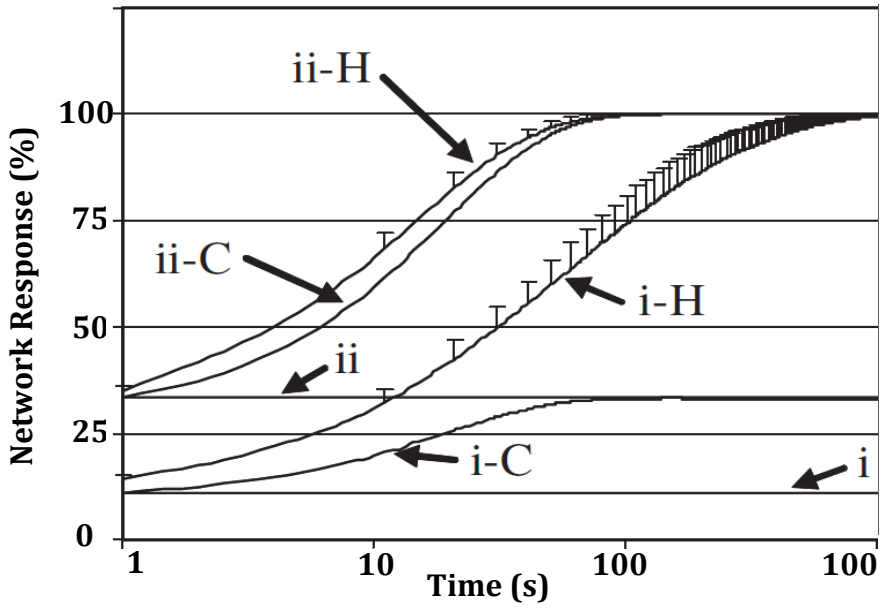

Figure 4-5: Network response with time reported by Ausk et al. (2006). i and ii show mean network responses when the strain applied with the strain thresholds. i-C and ii-C show mean network responses when osteocytes are able to communicate. i-H and ii-H show the mean network response with heterogeneity. This figure can be compared to Figure 4-2 (For full details see (Ausk et al., 2006)).

Despite the idealisation and all of the assumptions and simplifications, the results clearly show that inclusion of cell heterogeneity has a marked effect on the signal both at the osteocyte and the network. However this network is too

simplistic since it does not consider the bone lining cells on the bone surface, which are also key elements of the mechanotransduction mechanism in bone.

4.3 A simulation of the osteocyte and bone lining cell network

4.3.1 Methods

Model development

The simple osteocytic network modelled in the previous section is based on the idea proposed by Ausk et al. (2006). In this section, a layer of bone lining cells BLCs is also included in the model, assuming the same 2 dimensional uniformly distributed osteocyte network. Again, it was assumed that each osteocyte was connected to its neighbours and, at the surface, adjacent BLCs, as illustrated in Figure 4-6. In total it was assumed that 100 BLCs lay along the surface of the bone sample. Thus the typical size of each BLC was 40 μm which is similar to the size reported in the literature (Miller et al., 1989). Again, strain values experienced by the osteocytes varied from ε_{min} at the lower edge of the sample to ε_{max} at the upper edge to simulate the effect of a bending type load. The range of BLC activity simulated at each iteration (second) could range from 0% (inactive) to 100% (maximally activated). The simulation proceeded in the same way as before, except the simulation also included the BLCs. In a simulation, an activity signal is calculated for each osteocyte based on the level of strain it experiences according to specified activity thresholds. Then a cycle of communication between

neighbouring osteocytes and bone lining cells takes place through the canalicular network via gap junctions, again this is dictated by predefined amounts. The activity signal for each bone lining cell is also calculated based on the signals which they received from neighbouring osteocytes. The specific details of the model are as follows:

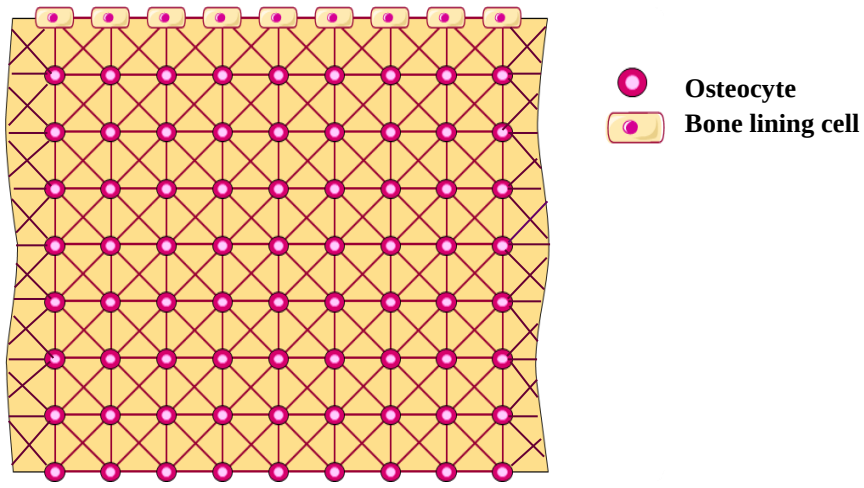

Figure 4-6: Small section of the idealized osteocyte and bone lining cell (BLC) network.

Calculation of activity signal

The strain $\varepsilon\ i,j$ experienced by each cell followed Equation (1) except for the BLCs where:

$$\varepsilon\ i,j\ = \begin{cases} 0 & i = 101 \\ \varepsilon_{max} & i = 100 \\ \varepsilon_{min} + \ n_i \times \frac{\varepsilon_{max} - \varepsilon_{min}}{n-1} & i < 100 \end{cases} \quad (5)$$

where $\varepsilon\ (i,j)$ is the strain at location(i,j), ε_{min} and ε_{max} and are the minimum and maximum strains on the lower (internal) edge and upper bone surface respectively,

with a linear variation in between, simply calculated by row number, n_i with n being the total number of rows (n=101).

In this first simulation, it was assumed that only the osteocytes could sense the mechanical strain and hence the BLC strain was assumed to be zero. Then the activity signal for each cell was calculated following equation (2). The remaining parts of the simulation followed in the same way as before.

Simulation

Network simulations defined by equations (2) to (5) were solved using Matlab (v7.7.0, Mathworks, Natick, USA) with typically over 1000 seconds (as Section 4.2.1) with initial parameter values defined in Table 4.1 except the number of cells is in this instance was 100×101. In addition to the "Mean network activity" reporter, another reporter was used to characterise the status of the BLCs at each second. "Mean BLC activity" was calculated by averaging the signal activity at the BLCs. It was also assumed that numerical values of cellular functions ($T^{\varepsilon}_{min}, T^{\varepsilon}_{max}$) were homogenous for all cells in the network. Then the effect of heterogeneity (H) was included as described earlier in Section 4.2.1, and the effect on the BLC activity reported with 5%, 10%, 15%, 25% and 50% heterogeneity. In total, the code to implement this simulation consisted of 165 Matlab lines, with each iteration taking approximately 3 seconds on a Windows XP PC. It also took more than 5 seconds for each iteration when an output of the model was set to produce a movie from the behaviour of network over time.

4.3.2 Results

Variation of osteocyte heterogeneity on BLC response

The variation of the mean surface (BLC) signals with time for the different heterogeneity scenarios is shown in Figure 4-7. The solid black line shows the mean BLC signal, with no heterogeneity. It reaches its peak at 10 seconds after application of the load and follows a low-magnitude steady state response of 65.52%. With 5%, 10%, 15% and 25% heterogeneity, the BLC levels are increased by 6.97%, 16.51%, 27.19% and 34.48% respectively, at 100 seconds after strain application (Figure 4-7). Mean BLC signal with 50% heterogeneity reaches at maximum peak at 85 seconds after strain applications while it reaches 100% signal level with 25% heterogeneity 25 seconds afterwards.

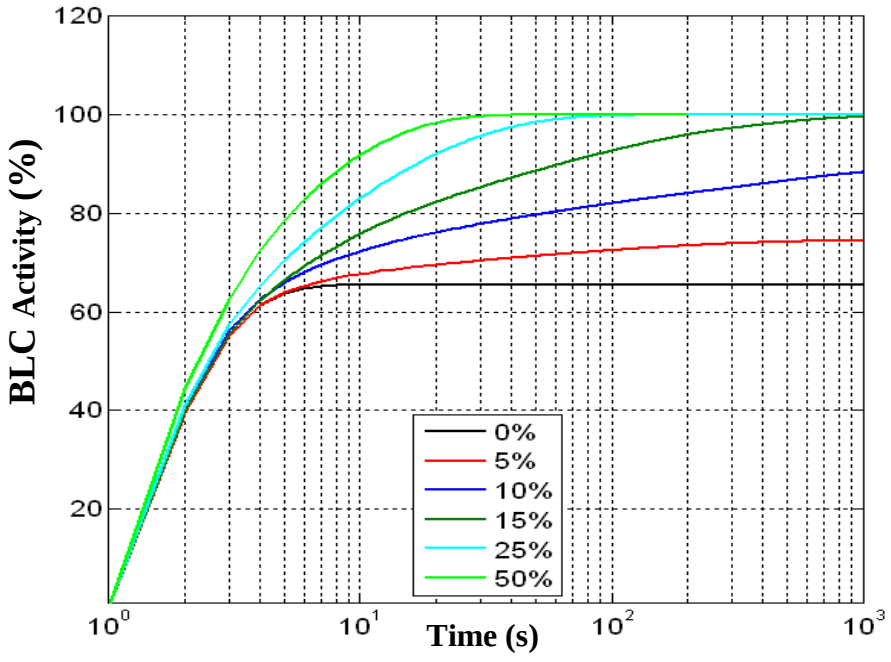

Figure 4-7: Mean bone lining cells activity with time and different heterogeneity.

4.3.3 Discussion

In this model, each osteocyte is activated based on the mechanical strain it experiences, and provides symmetrical intercellular communications through interconnecting canaliculi via gap junctions. The aim of this model is to examine the sensitivity of the BLC signal to increases in heterogeneity of cellular functions using the simple network model.

Using the basic model parameters defined previously, without heterogeneity, the mean BLC response increase for 10 seconds to an invariant baseline of 65.5% (Figure 4-7). In the heterogeneous simulations, the mean BLC signal rapidly increased to maximal level, with just 25% heterogeneity leading to an increase in mean BLC response of 34% (Figure 4-7). Note if $H = 0$ the maximal activity signal levels reached its peak quicker than if $H \neq 0$. Furthermore the trend of the predicted mean BLC signal, i.e. rapid increase after stimulation, compares well with the experiments (Guo et al., 2006, Huo et al., 2010, Adachi et al., 2009a, Charras and Horton, 2002, Hung et al., 1996) . In these experiments, it was observed that osteoblasts respond to a mechanical stimulus with a dramatic increase in intracellular calcium signals. However in these experiments single osteoblastic cells were stimulated not the entire osteocyte-BLC network. It appears that heterogeneity provides a powerful positive feedback to the BLC, as does the osteocytic network, that permits BLC to reach maximal level of response.

As with Section 4.2.3, a number of simplifications and assumptions were made in this simulation. It was assumed that only osteocytes can sense the

mechanical loading and generate the activity signal, however there is some evidence that BLCs may also respond directly to strain (Cowin, 2002, Duncan and Turner, 1995). It was also assumed that communication in this network is bidirectional and symmetrical, although the experiments of Adachi et al. (2009a) suggest asymmetrical communication. This effect is examined in the next model.

Chapter 5 The osteocyte and bone lining cell network with propagation factors and calcium decay

5.1 Introduction

In Chapter 4, the simulation of the osteocyte and bone lining cell (BLC) network was modelled. The communication between osteocytes and BLCs was assumed to be symmetrical. However, Adachi et al. (2009a) identified asymmetric calcium signalling between osteocytes and BLCs. As discussed in Chapter 3, they applied direct mechanical stimuli to an osteocyte *in vitro* to investigate the intercellular communication between osteocytes and bone surface cells (which included osteoblasts). In their experiment the percentage of calcium signal propagation from a stimulated osteocyte to a bone lining cell was measured and analysed. It was also observed that intercellular calcium signal of bone cells decline by removing the stimulus from the cell (Adachi et al., 2009a, Charras and Horton, 2002, Guo et al., 2006, Hung et al., 1996, Huo et al., 2010).

In this chapter, a simulation of asymmetric cellular communication in the osteocyte and BLC network with "calcium decay" is developed. The work proceeds in two steps; first, the basic model of the osteocyte-BLC network with asymmetric communication is developed, which is activated by the application of strain, then the signal is propagated and transmitted through the canalicular system in order to apply asymmetrical communication between cells. Once the basic algorithms of

this simple osteocyte network are established, it is extended to include "calcium decay".

5.2 Osteocyte and bone lining cell with propagation factors

5.2.1 Methods

Model development

The basic osteocyte-BLC network was modelled in Chapter 4. It was assumed that each osteocyte was connected to its neighbours and, at the surface, adjacent BLCs, as illustrated in Figure 5-1. The sample size and the number of cells were assumed as Chapter 4. The cell activity simulated at each time step ranges from 0% (inactive) to 100% (maximally activated). In a simulation, an activity signal is calculated for each osteocyte based on the level of strain it experiences according to specified activity thresholds. The activity signal for each bone lining cell is also calculated based on the signals received from neighbouring osteocytes. Then a cycle of asymmetrical communication between neighbouring osteocytes and bone lining cells takes place through the canalicular network via gap junctions, again this is dictated by predefined amounts, based on the values measured by Adachi et al. (2009a). The specific details of the model are as follows:

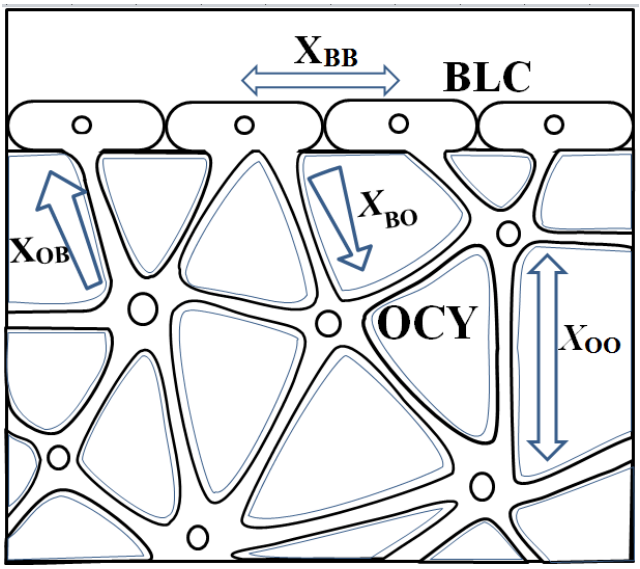

Figure 5-1: A close up view of the asymmetric signal propagation between the osteocyte (OCY) and bone lining cell (BLC) with variation of propagation factors (adapted from Adachi *et al.* 2009).

Calculation of activity signal

Firstly, the strain $\varepsilon\ i,j$ experienced by each cell follows equation (5) in Chapter 4, then, the activity signal for each cell is calculated using equation (2) in Chapter 4.

Calcium wave propagations between osteocytic and osteoblastic cells have been examined in detail by Adachi et al. (2009a) who measured the osteocyte-to-osteocyte (X_{OO}), osteocyte-to-BLC (X_{OB}), BLC-to-osteocyte (X_{BO}) and BLC-to-BLC (X_{BB}) propagation factors. These signals are illustrated in Figure 5-1 with their values summarized in Table 5-1. Note that the signalling is not symmetric. For example, Adachi et al. (2009a) found that while 34.7% of the signal level is transmitted from an osteocyte to a BLC, only 9.4% is transmitted in the opposite direction. In order to apply this bidirectional and asymmetrical communication in the network simulation, it was assumed that each cell could receive a signal from its neighbours ($S_g(i,j,t)$) while also simultaneously transmitting a signal

($S_l(i,j,t)$) to them. Thus the basic network communication equations were as follows:

$$S_g\ i,j,t\ = \ {}^{N}_{n_n=1} x_n \times S_n\ i,j,t-1 \tag{6}$$

$$S_l(i,j,t) = \ {}^{N}_{n_n=1} x_n \times S_n(i,j,t-1) \tag{7}$$

$$S_c(i,j,t) = (S_0\ i,j,t-1\ +\ S_g\ i,j,t\ -S_l\ i,j,t\ ) \tag{8}$$

$$S_0(i,j,t) = \begin{matrix} S^{\varepsilon}\ i,j & t=1 \\ S_c\ i,j,t-1 & t\neq 1 \end{matrix} \tag{9}$$

where $S_0(i,j,t)$ is the activity signal induced in the cell located at i,j at time '*t*' by propagation and transmission of signals from neighbours in addition to its own signal activity response to the strain at that point; $S_c(i,j,t)$ is the activity signal induced in the cell by propagation and transmission of signals from neighbours dependent on its previous activity level; N is the number of neighbours of the cell at coordinate i,j ; and x_n is the corresponding propagation factors depending on the type of cell-cell communication (i.e. X_{OO}, $X_{OB,}$ X_{BO} or X_{BB}).

Parameter	Symbol	Value	Units
Number of cells	m×n	100×101	-
Row number	i	1 to 101	-
Column number	j	1 to 100	-
Applied min strain	ε_{min}	600	μstrain
Applied max strain	ε_{max}	1000	μstrain
Threshold strain to initiate cell activity	T_{min}^{ε}	50	μstrain
Threshold strain to maximize cell activity	T_{max}^{ε}	1500	μstrain
Propagation factor BLC-BLC	X_{BB}	22.2, 44.4, 48.4, 48.8, 57.7, 88.8	%
Propagation factor OCY-BLC	X_{OB}	17.35, 34.7, 37.8, 38.1, 45.1, 69.4	%
Propagation factor BLC-OCY	X_{BO}	4.7, 9.4, 10.2, 10.3, 12.2, 18.8	%
Propagation factor OCY-OCY	X_{OO}	2.15, 4.3, 4.6, 4.7, 5.6, 8.6	%
Cycle duration	t	1 to 300	seconds

Table 5-1: The numerical values of parameters were applied in the simulations.

Simulation

Network simulations defined by equations (2), (5) and (6) to (9) were carried out using Matlab (v7.7.0, Mathworks, Natick, USA) with typically over 100 seconds with initial parameter values as defined in Table 5-1. The simulations returned the activity at each osteocyte and BLC throughout the network. Two reporters were used to characterise the status of the network at each time. “Mean network activity” was calculated by averaging the instantaneous net signal at each osteocyte, while “mean BLC activity” was determined by averaging the signal

activity at each BLC. It should be noted that numerical values of cellular functions ($T^{\varepsilon}_{min}, T^{\varepsilon}_{max}$) were assumed to be homogenous for all cells in the network. In the first simulation the applied propagation factors were assumed to be same values as measured in Adachi's experiment when the propagation factors of osteocyte-to-osteocyte, osteocyte-to-BLC, BLC-to-osteocyte and BLC-to-BLC were 4.3%, 34.7%, 9.4% and 44.4% respectively. Then investigate the variation of propagation factors in the signalling of network (Ocys) and BLC. In this case, the propagation factors values were altered by scaling of Adachi's propagation factors; for instance halving and doubling and scaling Adachi's propagation factors by 1.09 and 1.1 and 1.3.

5.2.2 Results

In the first simulation, when the propagation factors were assumed be exactly as they measured by Adachi et al. (2009a) the mean BLC activity reaches its peak 35 seconds after strain application and follows a low-magnitude steady response of 100%, however the mean network activity signal had an invariant of 51.16% (Figure 5-2).

Variation of propagation factors in the network

The variation of the mean surface (BLC) signals and osteocyte network (Ocys) with time for the different propagation factors are shown in Figures 5-2 and 5-3.

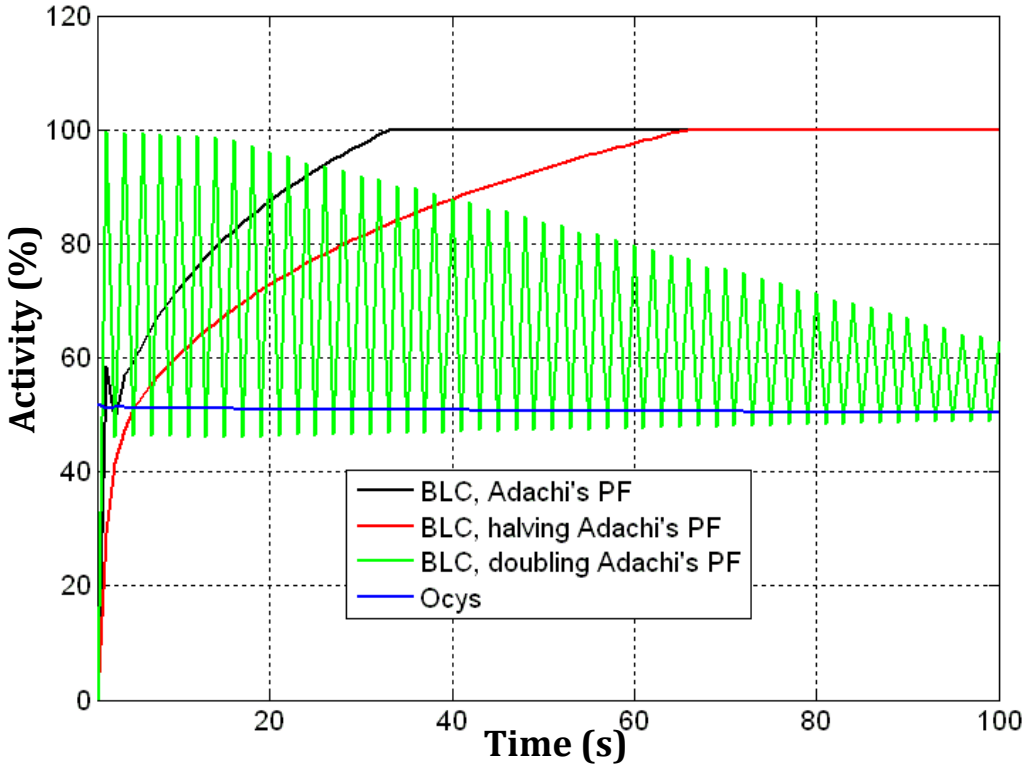

Figure 5-2: Mean BLCs and network (Ocys) activity with time and variation of propagation factors. Solid black and red and green lines show the mean BLC activities when the applied propagation factors (PF) were same as Adachi's, halves of Adachi's and doubles of Adachi's in model. The solid blue line shows the mean network activity signals when different PF were applied in model.

When the propagation factors were less than Adachi's, the BLC activity signal reaches its peak longer to reach its peak value than the simulation with Adachi's propagation factors; for instance by halving the Adachi's propagation factors, the time for the mean BLC signal to reach a maximum is double that (i.e. 70 seconds) than that for Adachi's propagation factors (Figure 5-2).

In the simulation when the propagation factors were assumed to be greater than Adachi's, the mean BLC reached the maximum and followed a decline to activity level of the mean network activity signal. When the levels of Adachi's propagation factors were increased, the peaks and the time when the mean BLC

signals reached the maximum, decreased; for instance in the models with Adachi's propagation factor scaled by 1.1 and 1.3, the mean BLC peak signals were reduced by 4% and 12% at 32 and 20 seconds after strain applications respectively. Steady state mean BLC activity signal also decreased by increasing the level of Adachi's propagation factors. However, high frequency fluctuations were observed in the model when the Adachi's propagation factors were doubled (Figure 5-2).

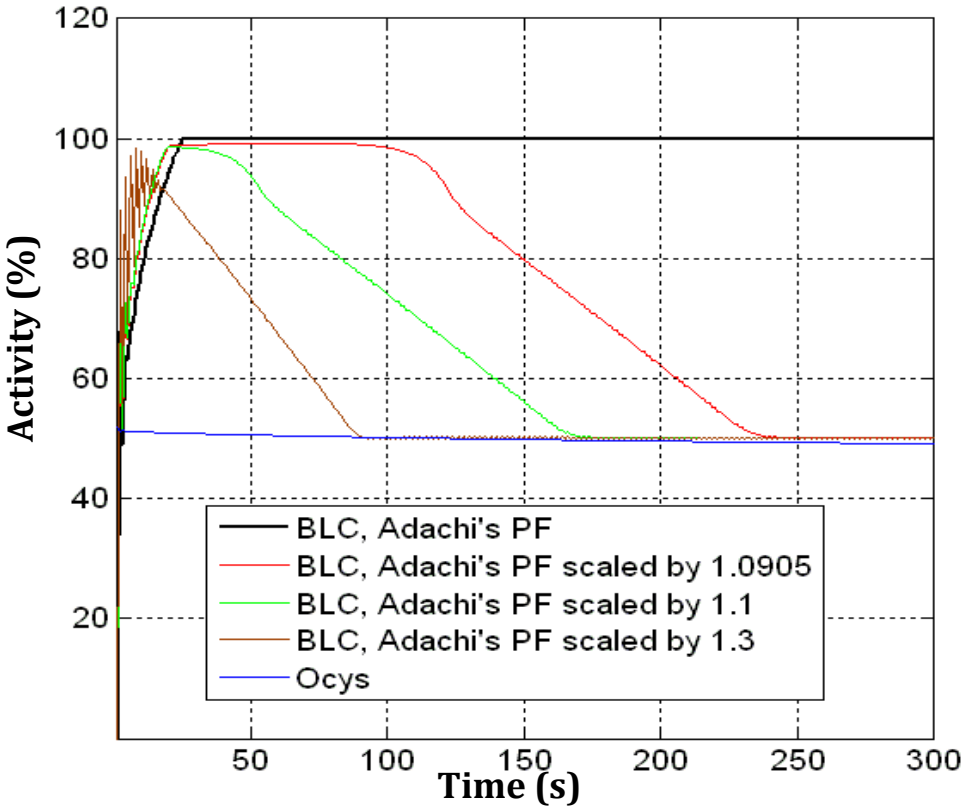

Figure 5-3: Mean BLCs and network (Ocys) activity with time and variation of propagation factors. Solid black, red, green and brown lines show the mean BLC activities when the applied propagation factors (PF) were same as Adachi's PF values, Adachi's PF scaled by 1.0905, 1.1 and 1.3 in model. The solid blue line shows the mean network activity signals when different PF were applied in model.

Despite the significant difference in the mean BLC signals which resulted from various propagation factors, the mean network response is nearly invariant (Figures 5-2 and 5-3).

5.3 Osteocyte and bone lining cell with propagation factors and calcium decay

5.3.1. Methods

Model development

In this simulation, the osteocyte-bone lining cell network with bidirectional and asymmetrical communication was modelled in the same way as before, except when the mechanical stimulus is removed a calcium decay factor (CD) was applied in the network. The specific details of the model are as follows:

Calculation of activity signal

All parts of the simulations were followed as before, except when the CD factor is applied in the network:

$$S_0(i,j,t) = \begin{cases} S^{\varepsilon}\ i,j & t = 1 \\ S_c\ i,j,t-1 & t < T \\ CD \times S_c\ i,j,t-1 & t \geq T \end{cases} \quad (10)$$

where $S_0\ i,j,t$ is the activity signal induced in the cell located at i,j at time 't' by propagation and transmission of signals from neighbours in addition to its own signal activity in response to the strain at that point; $S_c(i,j,t)$ is the activity signal induced in the cell by propagation and transmission of signals from neighbours, dependent on its previous activity level; n_n is the number of neighbours the cell has at coordinate i,j ; and x_n is the corresponding propagation factors depending on the type of cell-cell communication. The experiment of Charras and Horton

(2002) observed that when the stimuli was removed from the cell, intracellular calcium levels in each cell decreased after a while, back to the baseline. Thus, this model assumed that over time the different signals propagate through the osteocyte network to the bone lining cells, but gradually these signals decrease by a specified "calcium decay" (CD) at time 'T' where the CD was applied in the model for all osteocytes.

Simulation

Network simulations defined by equations (2), (5), (6) to (8) and (10) were solved using Matlab (v7.7.0, Mathworks, Natick, USA) with typically over 100 iterations with initial parameter values as defined in Table 5-1 including the CD factor . The simulations returned the activity at each osteocyte and BLC throughout the network. Two reporters, as before, were used to characterise the status of the network at each second. "Mean network activity" was calculated by averaging the instantaneous net signal at each osteocyte, while "mean BLC activity" was determined by averaging the signal activity at each BLC. It should be noted that numerical values of cellular functions ($T^{\varepsilon}_{min}, T^{\varepsilon}_{max}$) are homogenous for all cells in the network. Then the variation of CD (0.1%, 1% and 10%) at various time 20 and 26 seconds after strain application (T=20s and T =26s) in the signalling of the network and the BLCs on the surface was investigated.

5.3.2 Results

Variation of calcium decay factor in the network

The variation of the mean surface (BLC) signals and mean network over time for

the different calcium decay factors is shown in Figure 5-4. The effect of the CD factor add this throughout was assessed by running simulations with calcium decay factors of 0.1%, 1% and 10% at 20 iterations after load application where all propagation factors are assumed to be exactly as they were measured by Adachi *et al* (2009).

The solid blue line shows the mean BLC signal where the CD factor is 10% (Figure 5-4). It reaches its peak of 88.68% activity, at 1 second after the application of the CD and follows a significant decline to baseline activity at 28 seconds after strain application, while the mean network response decreases dramatically 8 seconds following CD application (Figure 5-4). With a CD of 1% and 0.1%, the peak mean BLC signals are increased by 4% and 10% at 24 and 39 seconds after strain application respectively and subsequently decrease to baseline, 57 and 280 seconds after CD application, however the mean network immediately after CD application follows a significant decrease (Figure 5-4).

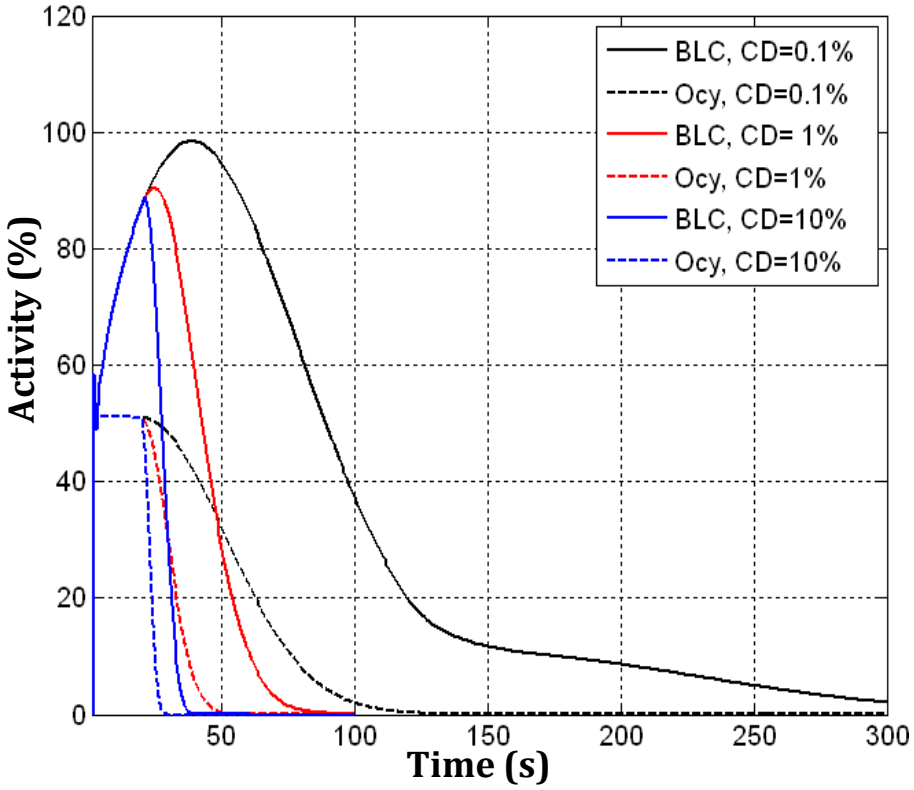

Figure 5-4: Mean BLCs and network (Ocys) activity with time and different CD factors. Black solid and dashed lines show the mean BLC and network activities when the CD factor of 0.1% is applied at 20 seconds after load application. Red lines show the mean BLC and network activities when the CD factor of 1% is applied. The Blue lines show the mean BLC and network activities when the CD factor of 10% is applied.

The results are as expected, with an increase in CD resulting in a decrease in the peak level of mean BLC signal.

5.4 Discussion

The simulation of the osteocyte lacunar network with asymmetrical communication in response to mechanical stimulus was modelled. The effects of the variation of propagation factors and CD in the signalling of the osteocyte-BLC network were examined.

Using the basic model parameters defined previously, and normal

propagation factors but without CD, the activity signals of the mean BLC are found to be sensitive to values of propagation factors, however the mean network response is invariant with a baseline activity of 51.17% (Figure 5-2 and 5-3). Adachi's propagation factors scaled by 1.0905% were found to produce critical values in this model (Figure 5-3). When less than these values, the mean BLC signal reach a steady state maximum value (Figure 5-2), but when greater than critical value the mean BLCs activity decline after they reach their different peaks (Figure 5-3). It appears that when the CD factor is included, the mean BLC activity reaches a peak then follows a significant decline (Figure 5-4).

The variation in the predicted mean BLC signal is illustrated in Figure 5-5a and compares well with the observed intercellular calcium signal variation a BLC when an adjacent osteocyte is stimulated, as measured by Adachi *et al* (2009) (Figure 5-5b). The variation in the predicted mean BLC signal with different CD factors (Figure 5-5a) also compares well, i.e. rapid increase after strain application , loading cycle duration (over 100 seconds) and a decrease after the CD application, with the some experiments *in vitro* and *in situ* (Charras and Horton, 2002, Guo et al., 2006, Hung et al., 1996, Huo et al., 2010). It seems that just by changing the value of the CD factor, the simulation can produce the mean BLC signal of different experiments. The results may also explain why the region closest to the bone surface is mechanically sensitive to osteocytic mechanosensation and cellular communication.

Apart from the asymmetrical communication, all simplifications and

assumptions in the parameterisation of the cellular functions in this model were similar those in Chapter 4. In conclusion, a simulation of the osteocyte-BLC network has been developed to investigate osteocyte signal propagation and the corresponding BLC signals, with different propagation and calcium decay factors. The results clearly show that inclusion of asymmetrical communication and CD factor have noticeable effects on the signal at the BLCs.

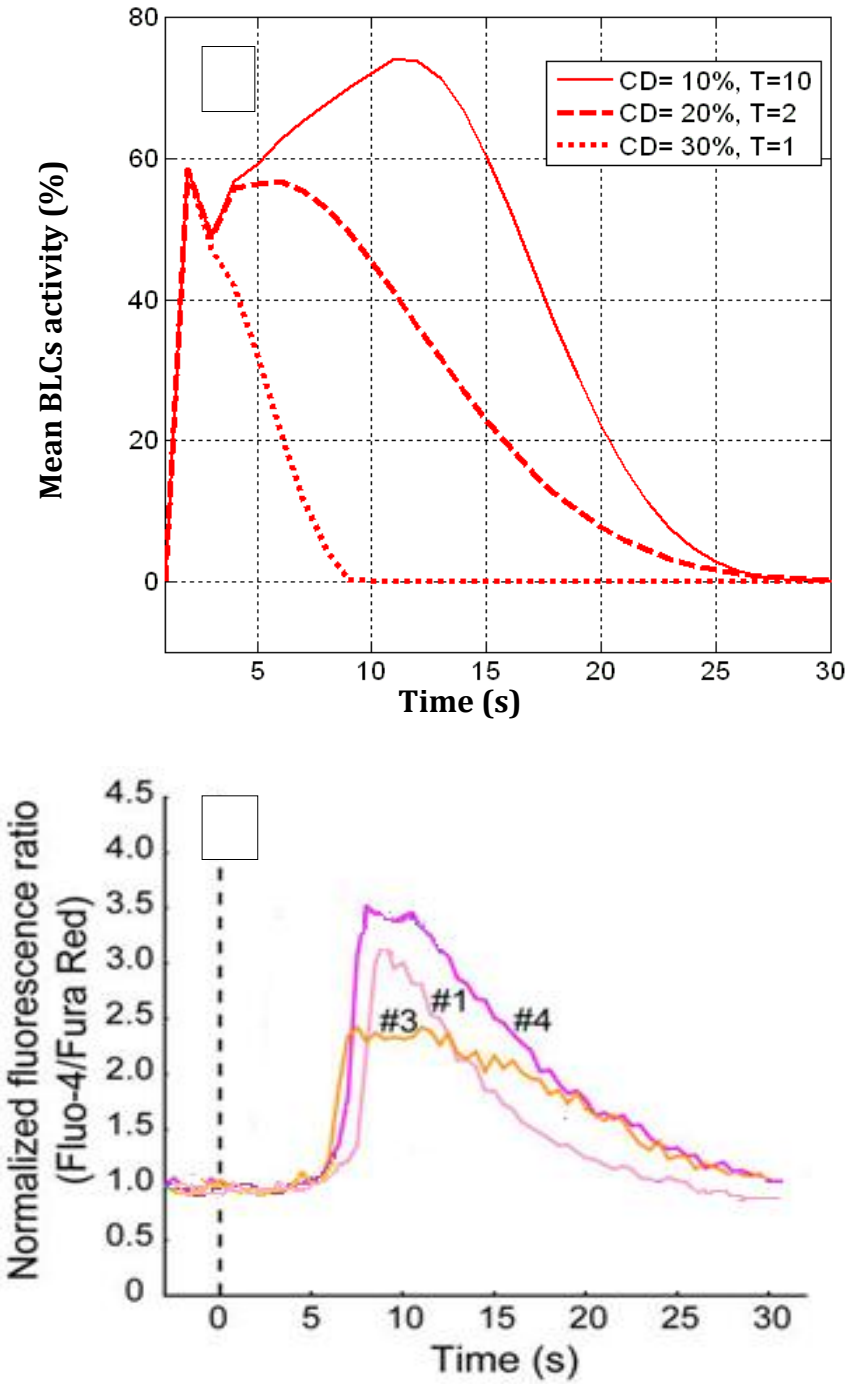

Figure 5-5: BLCs activity. a) BLCs response reported by Adachi et al. (2009) and b) Mean BLC response of current model using same propagation factors as Adachi et al. (2009) measured, where the CD of 10%, 20% and 30% applied at 1 (T=1), 2 (T=2) and 10 (T=10) seconds after load application respectively.

Chapter 6 The effect of apoptosis and microcracks in the signalling in the osteocyte and bone lining cell network

6.1 Introduction

Microcrack formation followed by disruption of the canalicular connections in the osteocytic network is a potential stimulus which initiates bone remodelling as discussed in Chapter 3. The rupture of cell processes by the microcrack also induces apoptosis in osteocytes (Hazenberg et al., 2006, Taylor et al., 2007). Aging, loss of ability to sense microdamage signal, loss of mechanical strain and a deficiency of sex hormones have all been shown to promote osteocyte death or apoptosis. Apoptotic osteocytes can also occur in association with pathological conditions such as osteoporosis with 6% to 10% apoptosis (Qiu et al., 2003, Almeida et al., 2007).Furthermore, iliac cancellous bone osteocyte density is reported to decline in patients with a vertebral fractures (Qiu et al., 2003, Almeida et al., 2007).

In this chapter, the effects of osteocyte apoptosis and microcracks on the signalling of the osteocyte and BLC network are investigated by using the network model, developed in Chapter 5.

6.2 The effect of apoptosis in signalling of in the osteocyte and bone lining cell network

6.2.1 Methods

Model Development

The osteocyte-bone lining cell network with asymmetrical communication and calcium decay was developed in Chapter 5. The simulation in this chapter proceeded in the same way as before, but included a viability factor for each osteocyte. The specific details of the model are as follows.

Calculation of activity signal

Firstly, the strain $\varepsilon\ i,j$ experienced by each cell follows equation (5) in Chapter 4, then, the activity signal for each cell is calculated using equation (2) in Chapter4.

The asymmetrical network communication follows equations (6) and (7) in Chapter 5. A "Life Coefficient" (LC) is defined for each osteocyte in the network, value 0 to 1, to characterise the viability of the osteocyte; (LC=0 means it is dead, LC = 1 means it is healthy, with an intermediate value signifying an osteocyte that is not functioning to its maximum capability, possibly due to disease, damage or age-related decline). Then the equations to calculate $S_c(i,j,t)$ is as follow:

$$S_c(i,j,t) = LC\ i,j\ \times (S_0\ i,j,t-1\ +\ S_g\ i,j,t\ -S_l\ i,j,t\ ) \quad (11)$$

where $S_c(i,j,t)$ is the activity signal induced in the cell by propagation and transmission of signals from neighbours dependent on the state of the osteocytes

(LC) and its previous activity level. Then the activity signal $S_0(i,j,t)$ for each cell is calculated using equation (9) or equation (10) when the effect of calcium decay is added to the model.

Simulation

Network simulations defined by equations (2), (5), (6), (7), (9) or (10) and (11) were solved using Matlab (v7.7.0, Mathworks, Natick, USA) with typically over 100 seconds with initial parameter values as defined in Table 5-1. In the first simulation, all osteocytes were assumed to be healthy (LC = 1) and capable of communication. The simulations returned the activity level at each osteocyte and BLC throughout the network. Two reporters, the same as before, were used to characterise the status of the network at each time. "Mean network activity" was calculated by averaging the instantaneous net signal at each osteocyte, while "mean BLC activity" was determined by averaging the signal activity at each BLC. Based on the results in Chapter 5, the effect of the CD factor was also assessed by running simulations with the calcium decay factor of 1% at 20 iterations (seconds) after strain application where all propagation factors are assumed to be exactly as they were measured by Adachi et al (2009) because the corresponding results compared very well with the discussed experiments in Chapter 5. The effect of 1% CD factor was also examined at 26 seconds after strain application because in this case, the mean BLC activity could reach the maximum peak of 100% activity follow a great decline to baseline activity level.

Then the effect of osteocyte apoptosis was included by preventing signalling

at and through the affected osteocytes as suggested by Tatsumi et al. (2007). In these cases, the unviable cells were distributed randomly throughout the model, with 3, 5 and 9% of the total number of osteocytes affected, with their LC values set to zero.

6.2.2 Results

Variation of apoptosis in the signalling on the network and BLC

In the model where all cells are alive and healthy, network activity is minimal at the (lower) internal surface and increases towards the (upper) outer surface (Figure 6-1a). However, the signal drops rapidly at the edge and as the BLC layer is approached, before increasing again to the maximum value on the surface. Along the surface, the BLC activity is nearly constant (Figure 6-2a), except towards the sides of the model where it decreases slightly.

Even with a small number of apoptotic cells in the model, the signalling is interrupted significantly. The location of the dead osteocytes is obvious in Figure 6-1, since they have zero activity signals and appear as blue islands. They also affect other osteocytes up to a radius of 3 cells (126μm) from the dead osteocyte. These sample contour plots of activity at t = 20 seconds show an increasing decline in activity level as the degree of apoptosis increases. At the surfaces themselves the BLC signals fluctuate significantly (Figure 6-2), with the level of fluctuation increasing as the degree of apoptosis increases. Short movies of the variation of the signals with different rate of apoptosis are available on the CD in the Appendix C (Movies 6-1, 6-2 and 6-3).

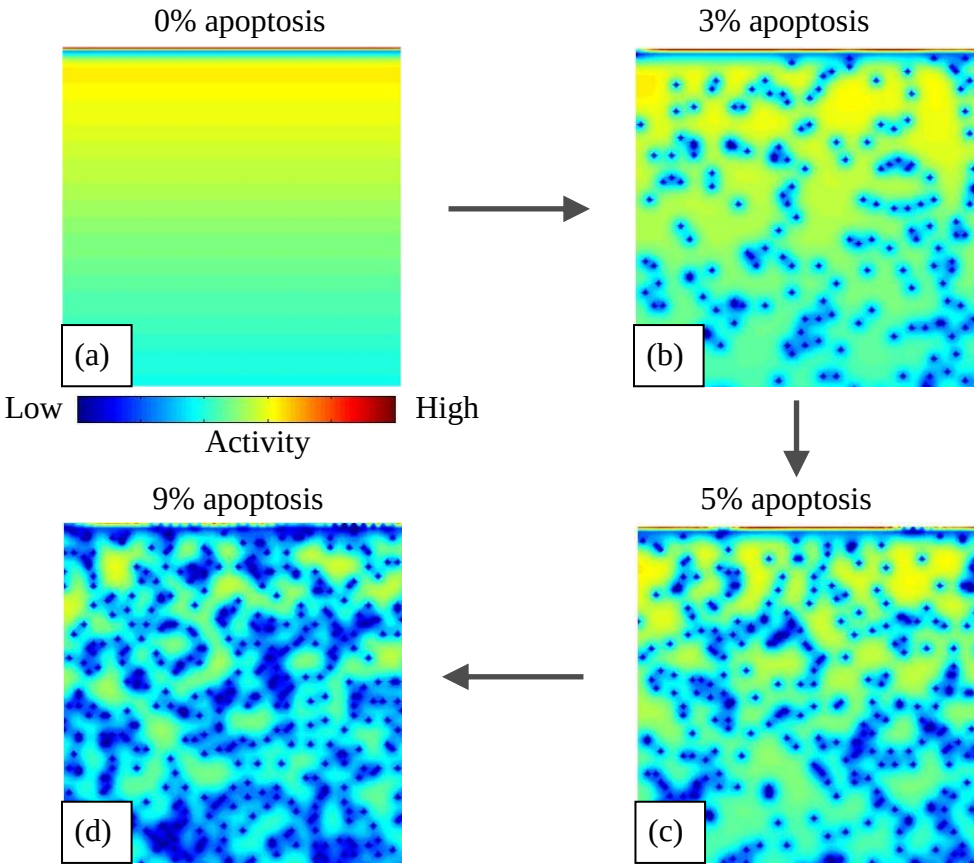

Figure 6-1: Contour plots of network activity after 20 seconds for sample models with increasing levels of osteocyte apoptosis.

Due to the random distribution of the apoptotic osteocytes, each simulation will produce slightly different results, as illustrated in Figure 6-3, which shows the top 840μm of bone in 5 runs with 5% apoptosis after 20 seconds. Overlaid on the plots is the variation of the BLC activity along the surface. The results of 10 such simulations without calcium decay (CD) finds that the maximum mean peak BLC activity varies between 68.42% and 82.56%, with a mean of 75.41% (standard deviation 4.81) (Table 6-2). However the results of 10 such simulations with calcium decay (CD) at 20 and 26 seconds finds that the maximum mean peak BLC

activity varies between 63.54% and 74.69%, 67.14% and 87.85% with means of 69.19% and 77.78% respectively (standard deviation 5.02 and 5.65) (Tables 6-3 and 6-4).

Apoptosis (%)	3%	5%	9%
Average maximum BLC activity	94.23	82.56	68.62
Overall average BLC activity	85.61	75.41	64.13
Average minimum BLC activity	70.62	68.42	58.63
Standard deviation	8.40	4.81	3.54

Table 6-1: Variation of peak BLC activities (and standard deviations) for different levels of apoptosis over 10 simulations of each without calcium decay.

Apoptosis (%)	3%	5%	9%
Average maximum BLC activity	94.05	87.85	72.23
Overall average BLC activity	87.469	77.778	61.747
Average minimum BLC activity	78.49	67.14	55.4
Standard deviation	4.64	5.65	5.02

Table 6-2: Variation of peak BLC activities (and standard deviations) for different levels of apoptosis over 10 simulations of each with calcium decay at 26 seconds.

Apoptosis (%)	3%	5%	9%
Average maximum BLC activity at B	86.93	74.69	64.02
Overall average BLC activity	83.92	69.19	58.91
Average minimum BLC activity at A	79.1	63.54	54.03
Standard deviation	4.33	5.02	5.24

Table 6-3: Variation of peak BLC activities (and standard deviations) for different levels of apoptosis over 10 simulations of each with calcium decay at 20 seconds.

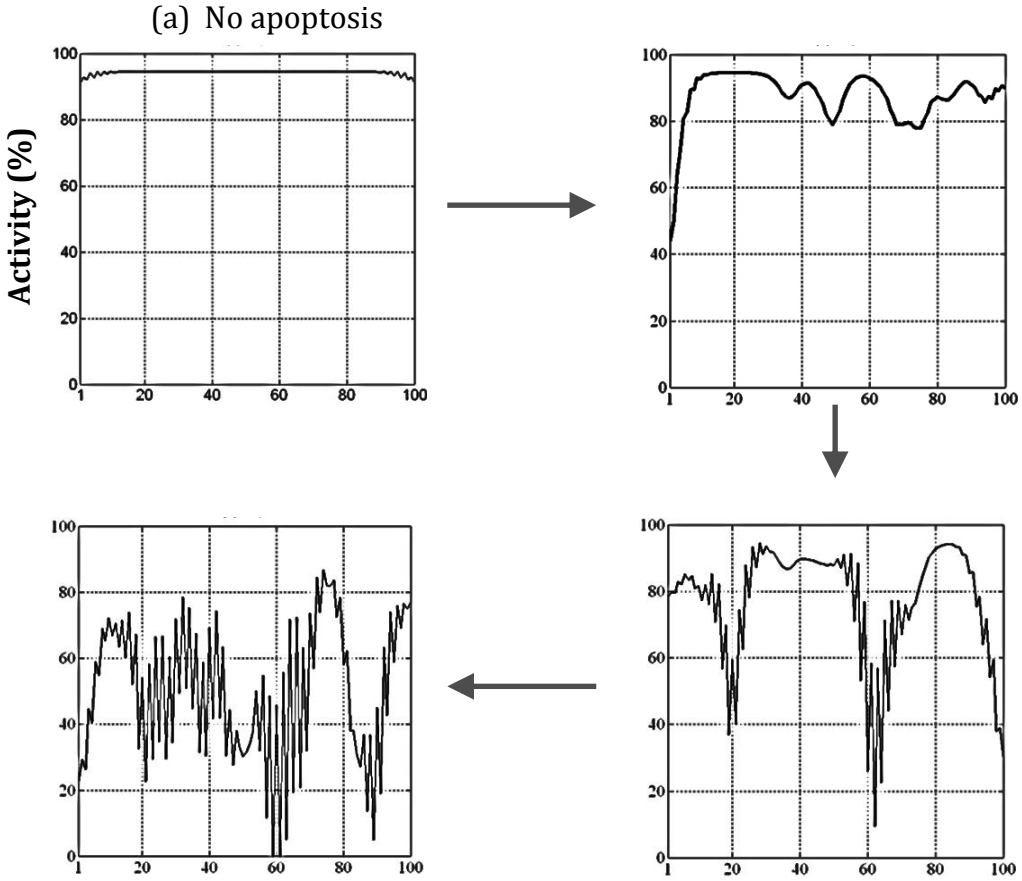

Figure 6-2: BLC activity across the top of the model, after 20 iterations for sample models with increasing levels of osteocyte apoptosis.

The variation of the mean network and surface (BLC) signals with time for the different apoptosis scenarios are shown in Figure 6-4, 6-5, 6-6. The solid red line shows the mean BLC signal, with no apoptosis. Mean BLC signal without calcium decay (CD) reaches 100% activity at 26 seconds after strain application, while the network activity follows a low-magnitude steady state response of 51% (Figure 6-4). With just 3%, 5% and 9% osteocyte apoptosis, the peak BLC levels are reduced by 14%, 25% and 37% respectively and subsequently decrease to approximately 51%, 50% and 48% activity levels, at 180, 111 and 97 seconds following strain application (Figure 6-4). Also, the mean network signal is significantly affected, as shown by the black dashed lines in Figure 6-4, which

continues to decline after loading, rather than reaching a steady state as observed with no apoptosis.

Where the calcium decay is included at 26 seconds after strain application, the mean BLC signal with no apoptosis reaches a peak of 100%, same as the model without the calcium decay, however it follows the great decline to baseline activity afterwards (Figure 6-5). The peak BLC levels are reduced by increasing the percentage of the apoptosis (Figure 6-5).

If the calcium decay factor is included at 20 seconds after strain application, the mean BLC signal with no apoptosis reaches a peak of 90.42%, at 5 seconds after application of calcium decay. With calcium decay and 3%, 5% and 9% osteocyte apoptosis, the peak BLC levels are reduced by 7.92%, 22.09% and 36.39% respectively. At 23, 21 and 14 seconds following strain application signals decrease to approximately 8.03%, 8.09% and 7.96% activity levels, at 42, 40 and 39 seconds after calcium decay application (Figure 6-6).

The mean network signal is affected significantly, as shown by the black dashed lines in Figure 6-5 and 6-6, which continue to decline after loading, rather than reaching a steady state as observed with no apoptosis before the CD application. The mean network signal with no apoptosis is 50.88, where the CD is applied 26 seconds after strain application, while with 3% and 5% and 9% apoptosis, signals dropped by 10%, 16% and 26.26% (Figure 6-5).

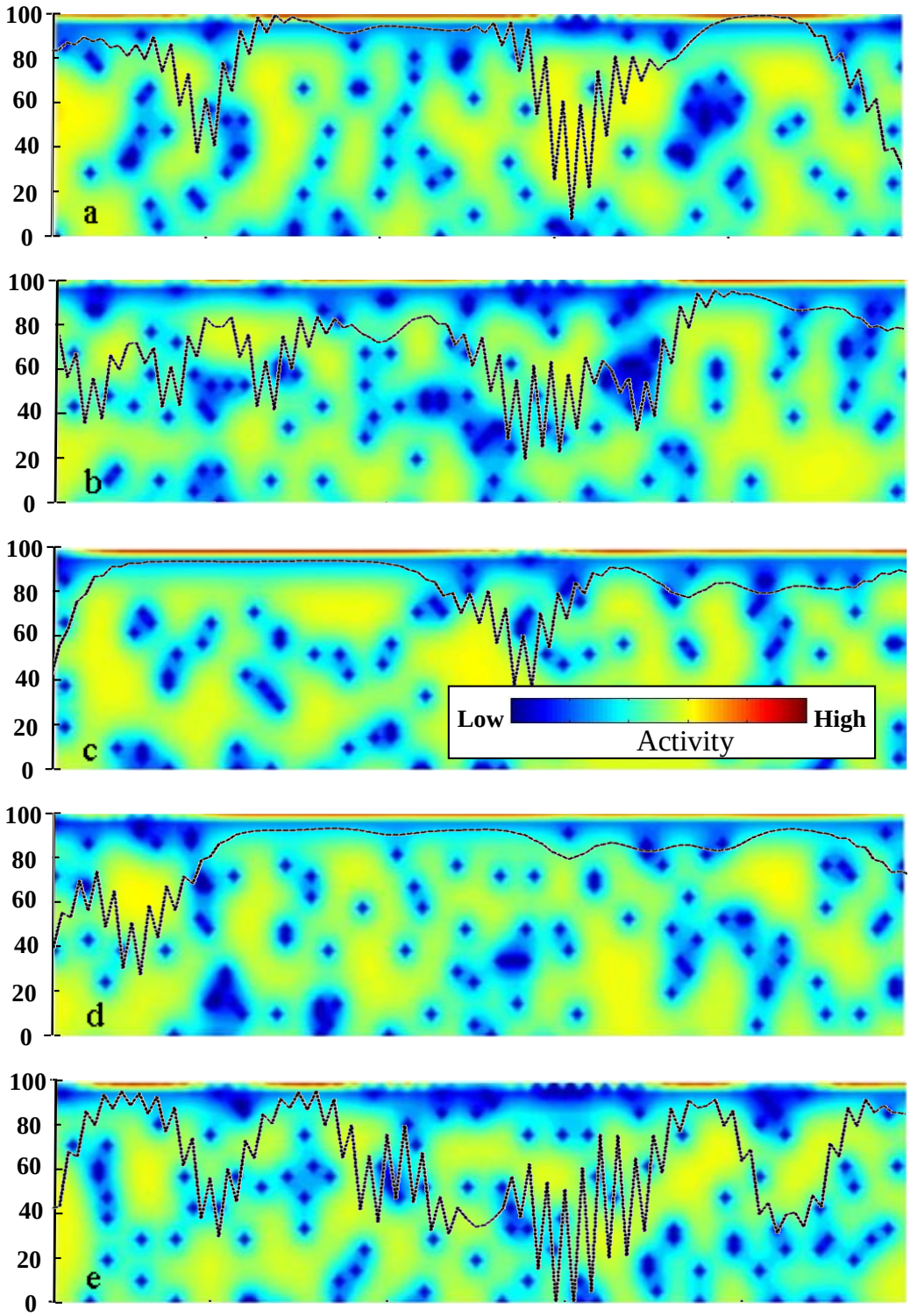

Figure 6-3: Contour plots of osteocyte activity in the top 840μm of bone (20 rows of osteocytes) after 20 seconds for five sample models with 5% osteocyte apoptosis. The overlaid dashed black lines show the variation in BLC activity along the surface of the bone.

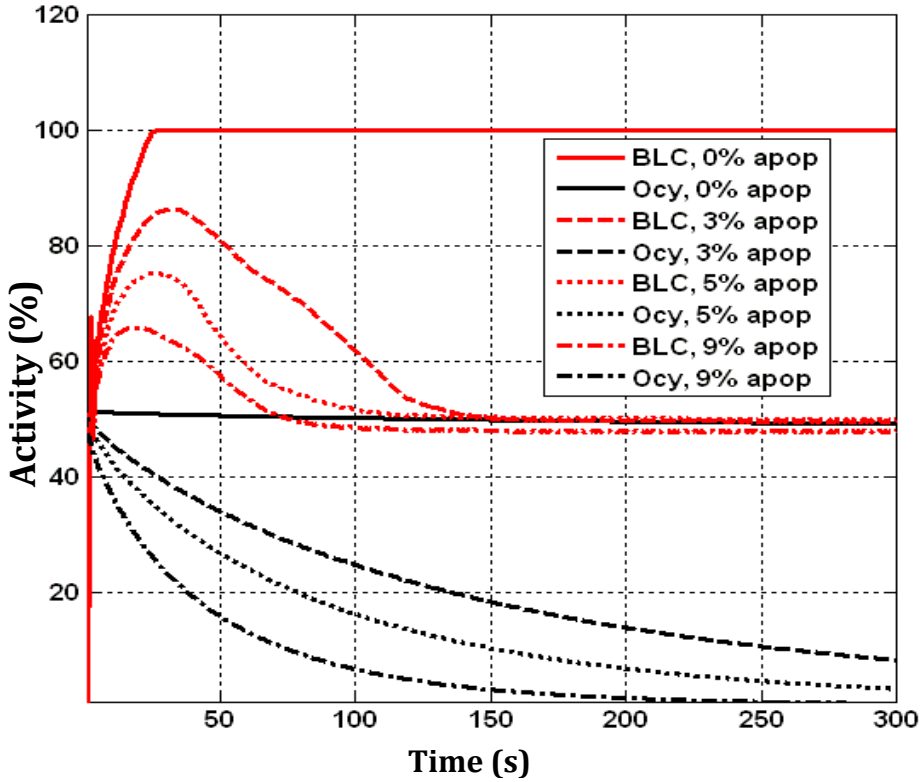

Figure 6-4: Mean network and BLC response without calcium decay.

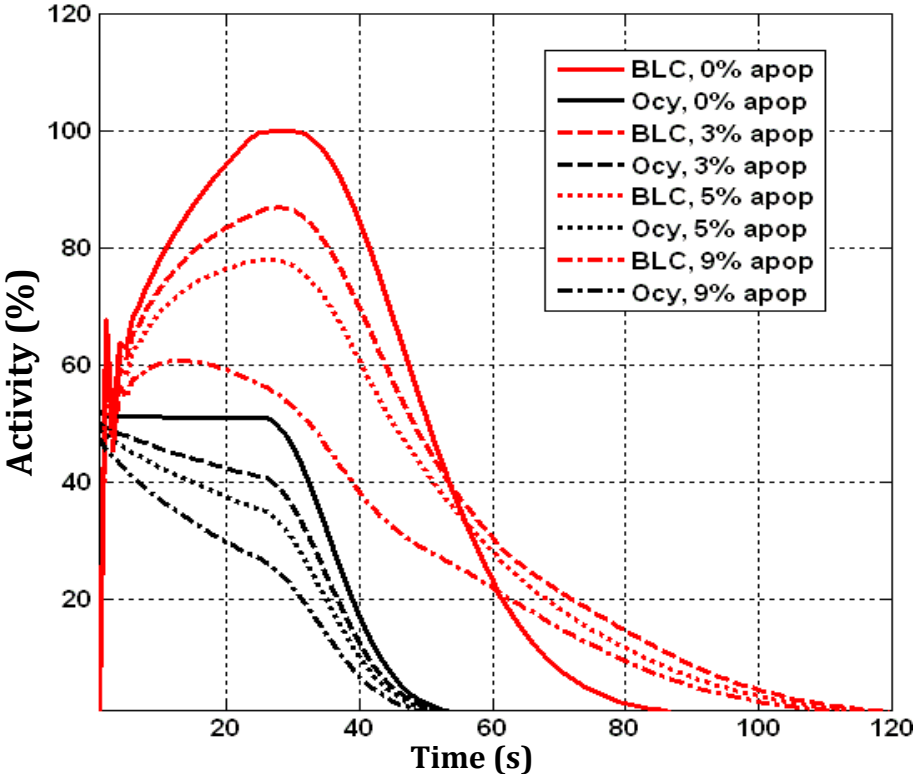

Figure 6-5: Mean network and BLC response with calcium decay at 26 seconds.

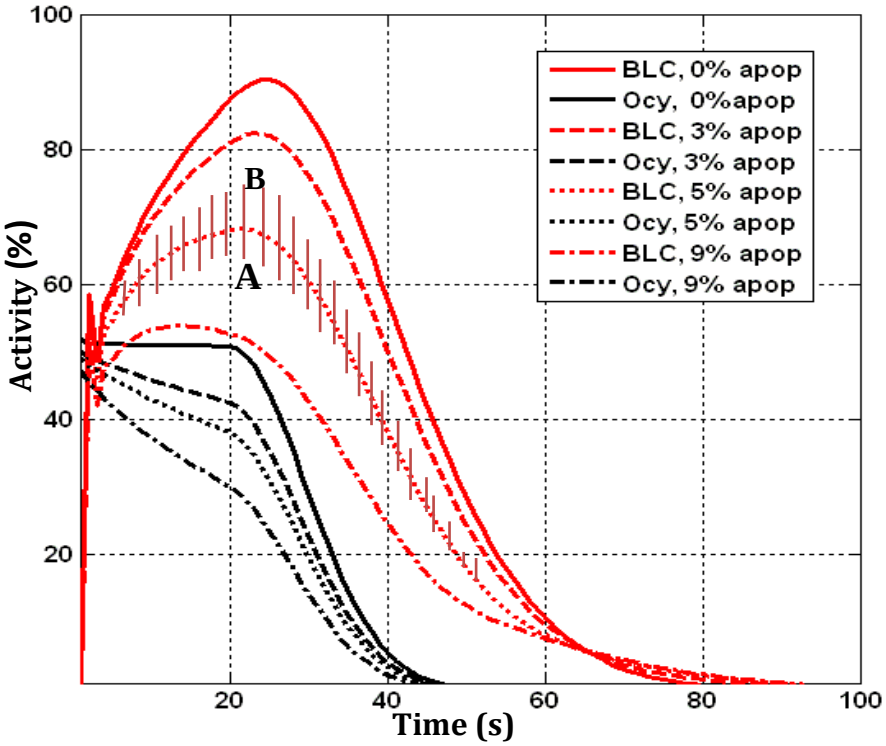

Figure 6-6: Mean network and BLC response with calcium decay at 20 seconds.

6.2.3 Discussion

The simulation of the osteocyte and bone lining cell network in response to mechanical stimulus is modelled including and the examination of the sensitivity of the network to changes in osteocyte apoptosis.

When cells are viable, the BLC response is found to be relatively high and uniform (Figures 6-1a and 6-2a, at 20 seconds), reaching 100% activity after 26 seconds (Figure 6-4). In apoptotic simulations, however, BLC activity is reduced significantly. The simulations with 3% apoptosis led to a decline in peak BLC signal of 14% in the model without calcium decay factor and also with the CD factor at 26 seconds after strain application, but nearly a half of that decline was observed in the model with calcium decay, when it applied 20 seconds after strain application

(Figures 6-4, 6-5 and 6-6). The variation in the BLC signal across the surface of the bone varies enormously (Figure 6-3), with mean surface signals varying by a standard deviation of 8% and 4.64% including CD factor in the model. The variations in the predicted mean BLC signals (Figures 6-4, 6-5 and 6-6) compare well with the general behaviour observed experimentally by Adachi et al. (2009a) (Figure 5-5b) and others (Charras and Horton, 2002, Guo et al., 2006, Hung et al., 1996, Huo et al., 2010). As expected, the greatest declines in BLC signal are observed when the apoptotic osteocytes occur nearest to the surface (Figures 6-3a and 6-3e). This also suggests that regions close to the surface are the most mechanically sensitive (Adachi et al., 2009a), and the location of the apoptotic osteocytes are more important than their density (Hedgecock et al., 2007, Qiu et al., 2003). It may be that remodelling is initiated at these locations, when the BLC signal drops below a certain critical level, which would remove and replace some of the most superficial osteocytes, but not those deeper in the bone matrix, possibly making it vulnerable for further remodelling (Martin, 2000). The mean BLC activity signal decreased at peak by increasing the level of osteocyte apoptosis. It may refer to an increase the rate of bone remodelling in the study by Hedgecock et al. (2007) which showed that there was a direct relationship between the density of osteocyte apoptosis and the rate of remodelling if the density of apoptosis was greater than 7% per square millimeter .

All simplifications and assumptions in the parameterisation of the cellular functions in this model were similar those in Chapter4. A simulation of the osteocyte-BLC network has been developed to investigate osteocyte signal

propagation, the corresponding BLC signals, and the effect of osteocyte apoptosis on those signals. The results clearly show that the inclusion of apoptosis has a marked effect on the signal at the BLCs on the bone surface. Since below the outer surface layers, most of the apoptotic osteocytes are in the bulk of the bone material, any resultant surface remodelling and replacement of affected osteocytes will then have a minimal effect on the level of signalling at the surface. This may explain the mechanism which leads to increased remodelling and the eventual bone loss observed in osteoporosis (Tatsumi et al, 2007).

6.3 The effect of microcrack in signalling of the osteocyte and bone lining cell network

6.3.1 Methods

Model Development

The model of the osteocyte-bone lining cell network with asymmetric communication and calcium decay developed in Section 6.2.1, is now used to investigate the effect of microcracks on network signalling and BLC activity.

Simulation

Since it has been observed that a microcrack breaks the canaliculi of the lacunar network and induces osteocyte apoptotic death (Rochefort et al., 2010, Noble and Reeve, 2000, Seeman, 2006), the effect of microcracks was included by preventing signalling at and through the affected osteocytes (as illustrated in Figure 6-7 and 6-8). In these cases, the cells affected by the microcrack had their LC

values set to zero. For instance to simulate microcrack A (Figure 6-7) with 42 μm length at one layer (42 μm) below the BLC, it was simply assumed that the two osteocytes located on this microcrack were affected and unviable. Thus, their LC values were set to zero, similar to the apoptotic model. The other crack positions and lengths of cracks were treated in the same way. Figure 6-8 also shows microcracks with different length at A and B.

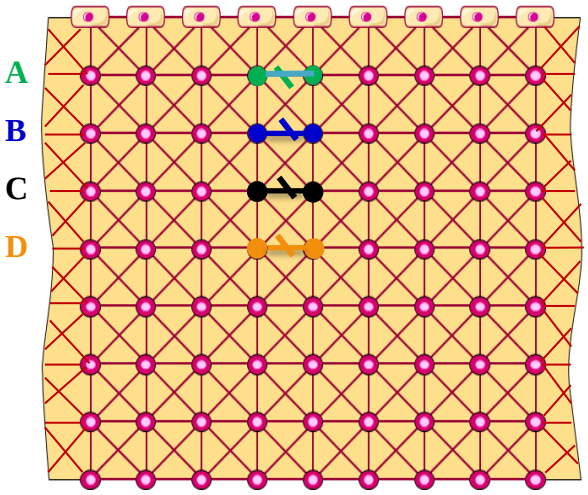

Figure 6-7: The idealized osteocyte (OCY) and bone lining cell (BLC) network with microcrack. A, B, C and D show 4 different microcracks, that break the canaliculi, at 42 (one layer below the BLC), 84 (two layers below the BLC), 126 and 168 μm below the surface with similar length of 42 μm.

In the simulation, the propagation factors were assumed to be exactly as they were measured by Adachi et al. (2009). The effect of the CD factor also was assessed by running simulations with the calcium decay factor of 1% at either 20 or 26 iterations (seconds) after strain application as the corresponding results compared very well with the experiments discussed in Chapter 5. Then the effects of variety of microcracks with different length of 42μm, 168μm, 252μm and 1mm at different positions of 42μm, 84μm, 126μm and 168μm below the surface (Figures 6-7 and 6-8) were examined on the signalling of BLCs and network.

It should be noted that the simulation proceeded in exactly the same way as in Section 6.2.1.

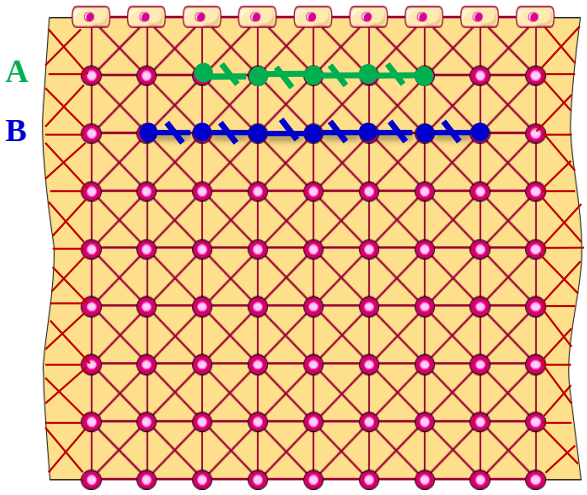

Figure 6-8: The idealized osteocyte (OCY) and bone lining cell (BLC) network with 2 microcracks at A and B. A shows a microcrack with length 168 µm, that breaks canaliculi and affects the viability of 5 osteocytes, at 42 µm (one layer below the BLC). B shows a microcrack with length 252 µm, that breaks canaliculi and affects the viability of 7 osteocytes, at 84 µm (two layers below the BLC).

6.3.2 Results

Variation of microcrack location

With no microcrack, the BLC activity is nearly constant (Figure 6-9a and 6-9b), except towards the sides of the model where it shows a slight decrease because of edge effects. As before the mean BLC activity reaches a peak after 26 seconds after strain application and follows a constant 100% baseline activity (Figure 6-9c) however it declines if calcium decay is applied into the model (Figure 6-9d).

Even with a tiny microcrack of 42 µm in the model, the signalling of the BLCs is interrupted significantly. The BLC activity at t = 26 seconds decreases the microcrack gets closer to the surface (Figure 6-9a and b). With microcracks at A, B,

C and D, the BLC activities are reduced by 67%, 23%, 14.32% and 7.1% respectively (at 26 seconds after strain application Figure 6-9a). When calcium decay is included, the activities decreased by typically just 1% (Figure 6-9b). The microcracks also affect the signal at other osteocytes located near the microcracks with microcracks at A, B, C and D. Thus, the radius of affected BLCs signal are 420 μm (11 cells), 336 μm (9 cells), 294 μm (8 cells) and 252 μm (7cells) at 26 seconds after strain application (Figure 6-9a and b). The mean BLC activities are reduced by 5.18%, 1.77%, 1.18% and 0.49% at 26 seconds with microcracks at A, B, C and D (Figure 6-9c and d). Also, while there is a slight effect on the mean network signal in the model with microcracks and CD (Figure 6-9d), the mean network signal is not effected by microcracks in the model without CD (Figure 6-9c).

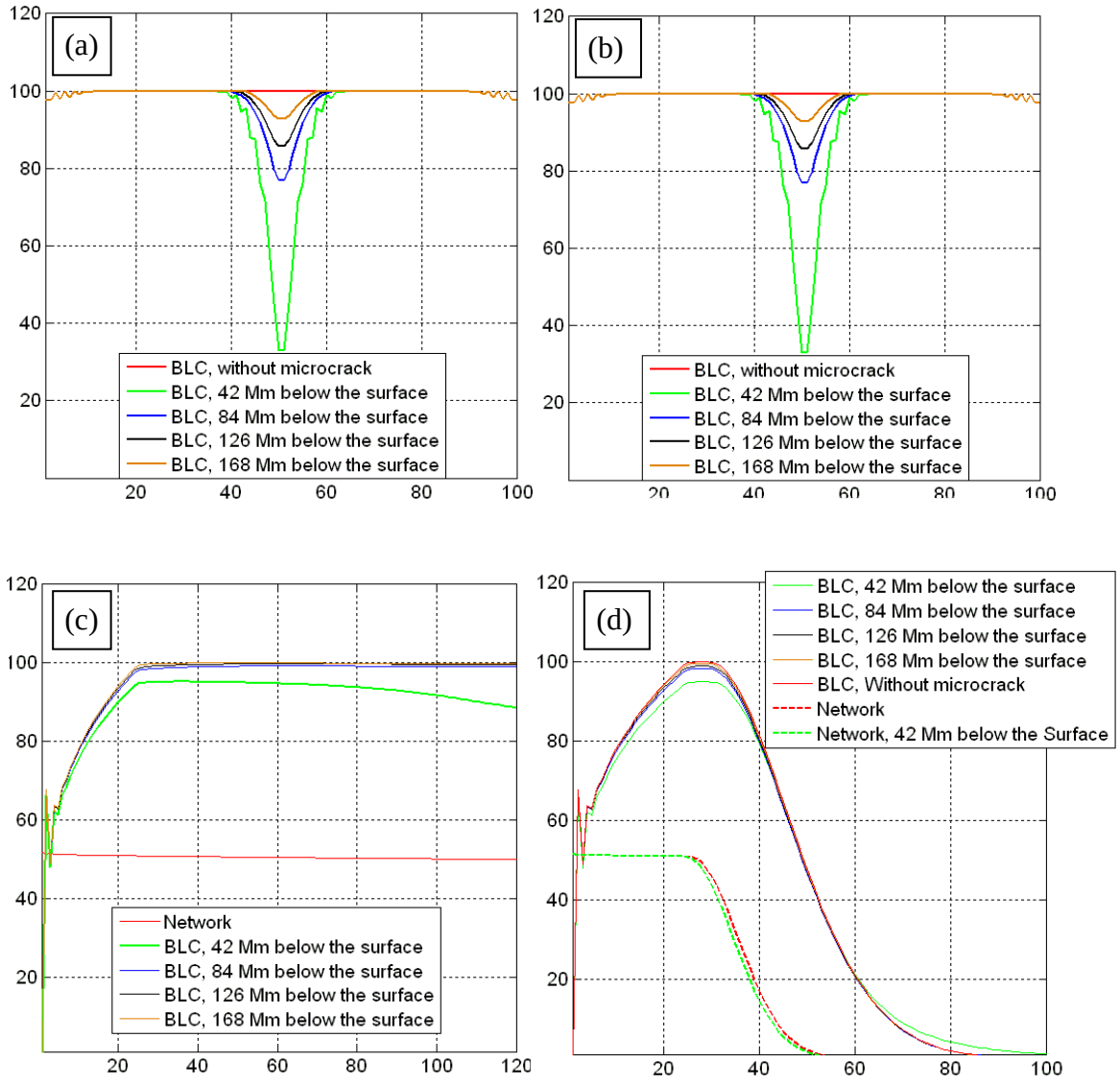

Figure 6-9: BLC activity across the top of the model, after 26 iterations for sample models without CD (a) and with CD (b) and mean BLC and network response without CD (c) and with CD (d).

Variation of microcrack length

The variations in the mean network and surface (BLC) signals over time for microcracks at different lengths at different depths are in Figures 6-10, 6-11, 6-12 and 6-13. Figure 6-10a shows the mean BLC with microcrack of length 42μm,

168µm and 252µm positioned 42µm below the bone surface. The peak levels (at 26 seconds) are reduced by 5.18%, 8.56% and 10.56% respectively and subsequently decrease, however, the mean network activity is not visibly affected by the increasing length of the microcracks (Figure 6-10a).

The maximum BLC activity levels are reduced by 67%, 98.6% and 100% with microcracks of 42µm, 168µm and 252µm respectively (Figure 6-10b) at A. With the microcrack of 252 µm, the BLC are reduced by 100%, 51.3%, 33.4% and 23.86% respectively at levels A, B, C and D (Figure 6-10b, 6-11b, 6-12b and 6-13c) and also the mean BLC activity are reduced by 10.56%, 3.94%, 3.37% and 1.68% at time where calcium decay is applied (Figure 6-10a, 6-11a, 6-12a and 6-13b), while the mean network signal is not effected by increasing microcrack length (Figure 6-10b and 6-11b).

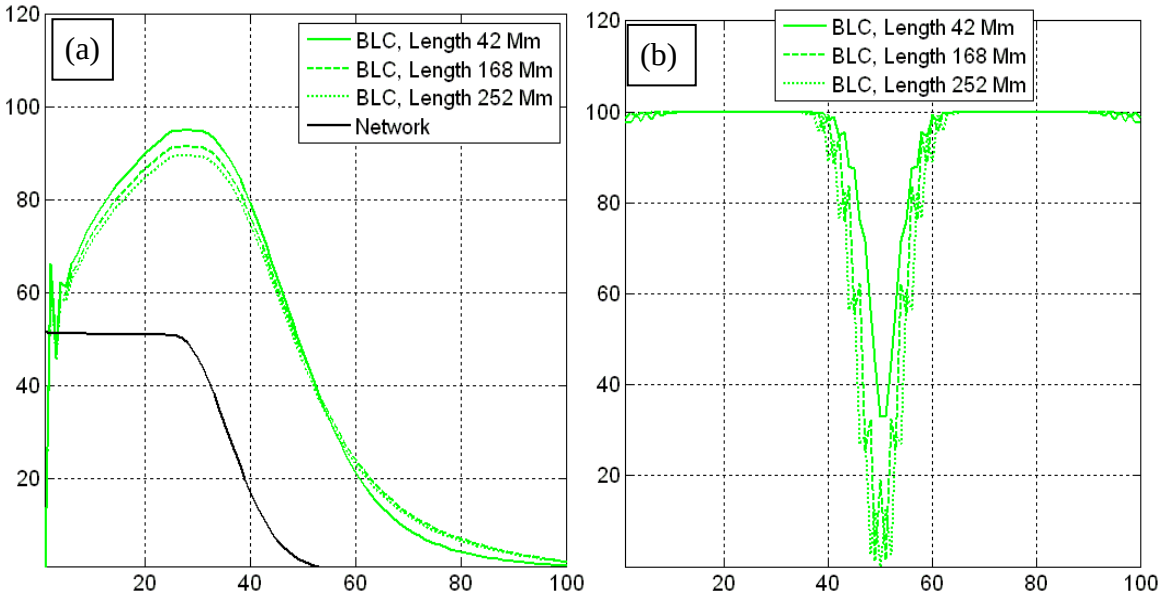

Figure 6-10: Mean BLC and network response with CD (a) and BLC activity across the top of the model, after 26 iterations for sample models (b) with variation of microcrack length at level A.

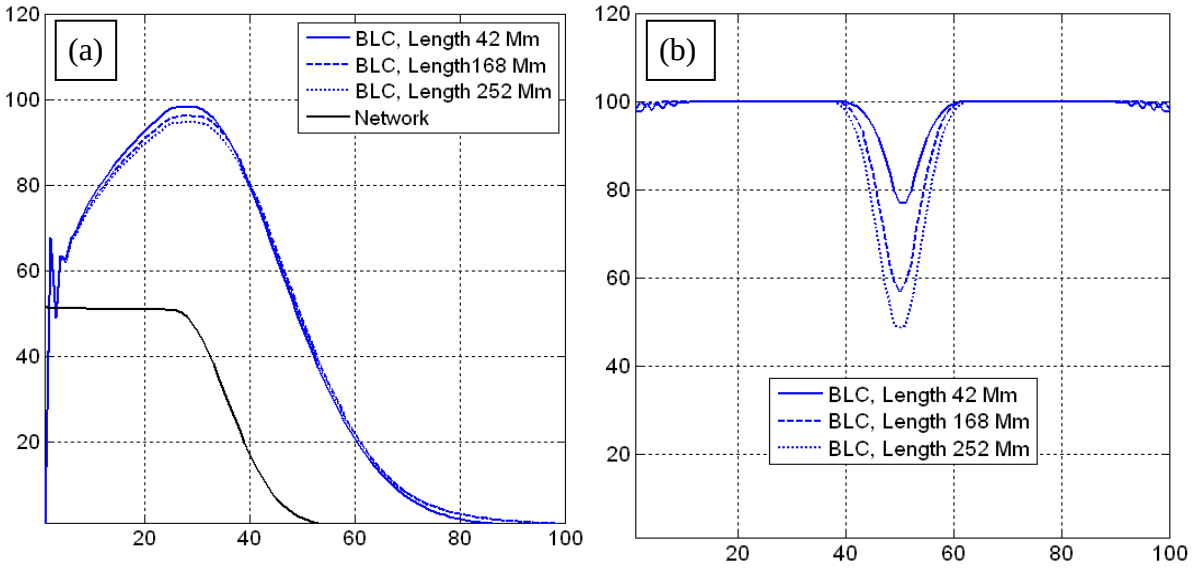

Figure 6-11: Mean and individual BLC response with CD (a) and BLC activity across the top of the model, after 26 iterations for sample models (b) with variation of microcrack length at level B.

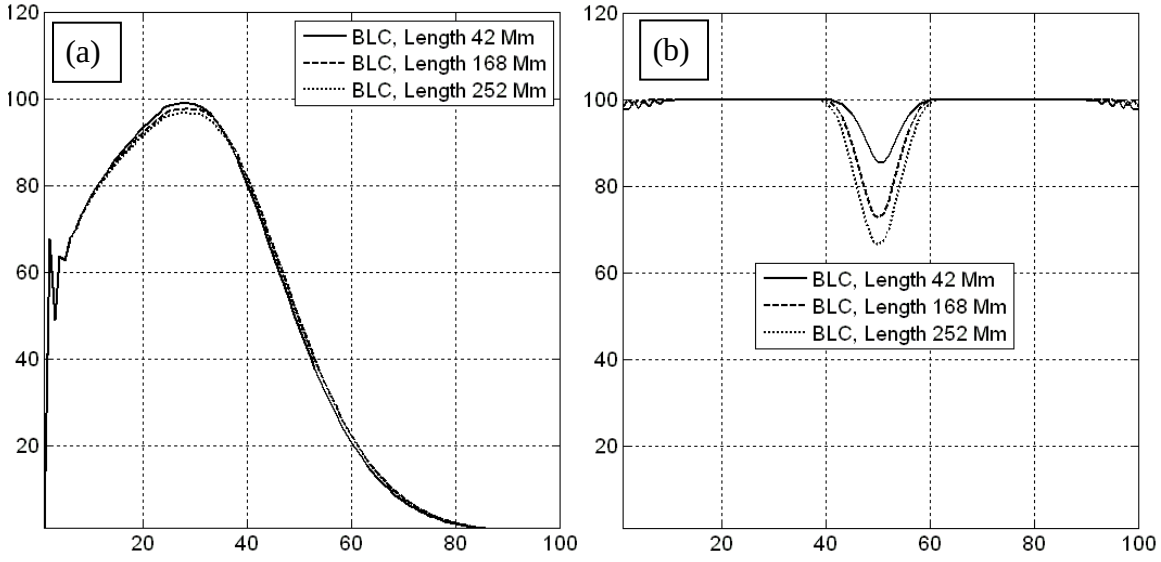

Figure 6-12: Mean BLC response with CD (a) and BLC activity across the top of the model, after 26 iterations for sample models (b) with variation of microcrack length at level C.

With a microcrack of 1mm, at level D (Figure 6-13c) BLC activity is reduced by almost 23%, a similar effect as observed in a microcrack of 42μm at level B, and the mean BLC activity with and without calcium decay also dropped by 6 % at 26 seconds after strain application (Figure 6-13a and b). A similar effect is seen in a microcrack of 42μm at point A (Figure 6-9c and d), and it follows a decline (Figure 6-13a and b).

No significant change to the radius of effected cells was observed as the length of the microcrack increased.

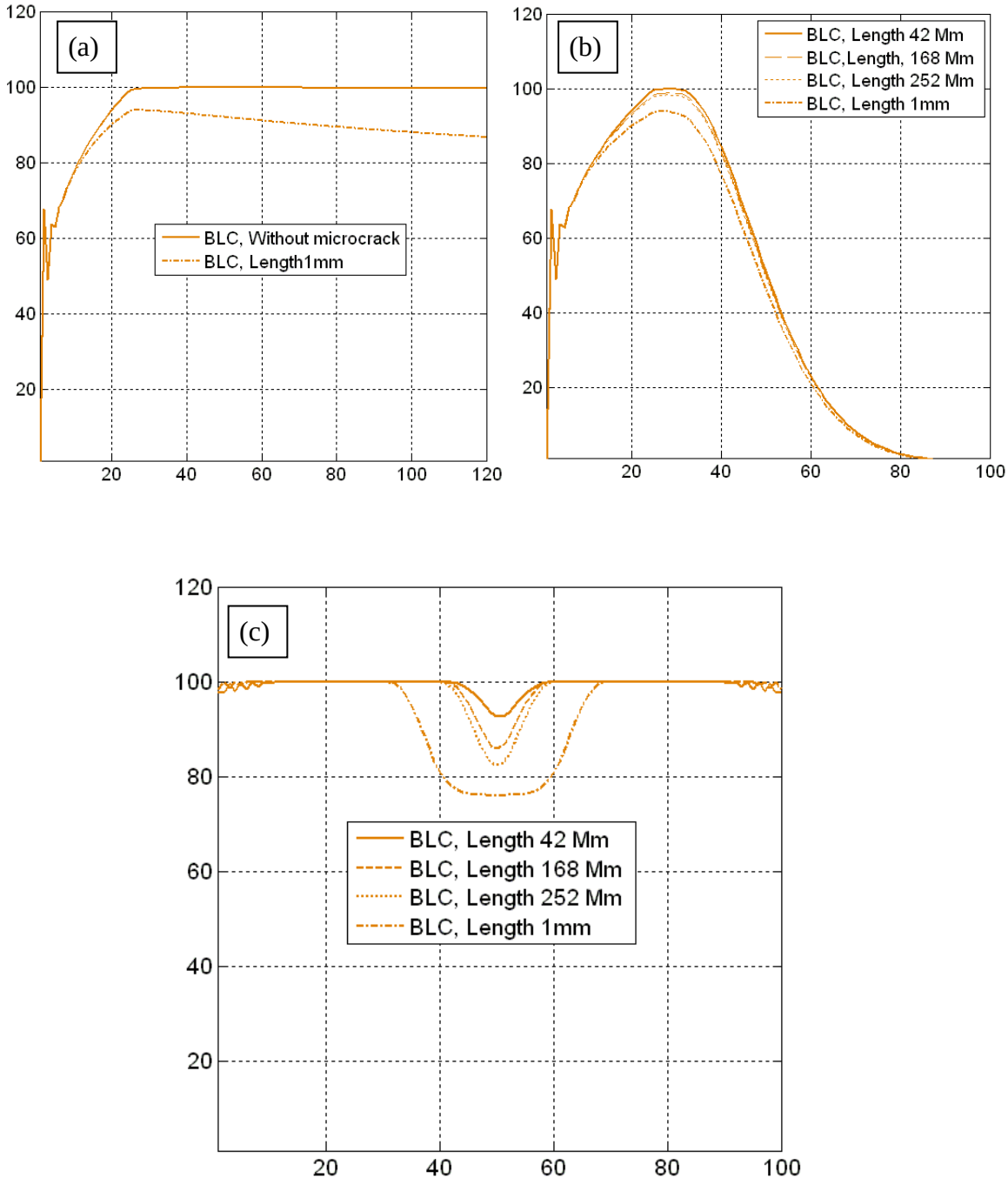

Figure 6-13: Mean BLC response without CD (a) and with CD (b) and BLC activity across the top of the model, after 26 iterations for sample models (c) with variation of microcrack length at level D.

6.3.3 Discussion

The sensitivity of the BLC and osteocyte network to increases in microcrack length and location was examined using a simple model. When there is no microcrack, the mean BLC response reaches 100% activity after 26 seconds (Figure 6-9c and d) and declines when the calcium decay factor is applied (Figure 6-9d). In simulations with microcracks, however, the peak BLC activity is reduced significantly with a tiny microcrack of just 42μm. When the microcrack located at 42μm below the surface, the signal is reduced by 67%, with or without calcium decay; with a continuing overall decline in network response (Figure 6-9c and d). The effect of variations in microcrack length at different locations on the BLC signal across the surface of the bone are examined in Figures 6-10, 6-11, 6-12 and 6-13: They show a decline in BLC signals, as the length of the microcrack increases at each location (Figures 6-10b, 6-11b, 6-12b and 6-13c) however, the decrease reduces as the distance from the bone surface increases (Figure 6-9). Although the average BLC activity levels decrease with the existence of a microcrack at any applied location (Figures 6-9d, 6-10a, 6-11a, 6-12a and 6-13b). No significant decline is observed in mean network activity with increasing length of microcrack even at 42 μm below the surface (Figures 6-10a and 6-11a). The radius of effected BLCs with a microcrack of 42μm in length is reduced as the distance of the microcrack from the bone surface increases. This ranges from 11 cells at A to 7 cells at D, and this change appears to be independent of microcrack length. This model also shows that the effect of cracks disappear as they appear deeper than 210μm below the surface in the bone, even if their length increases up to 2mm.

The greatest declines in BLC signals are observed when the microcracks occur nearest to the surface (Figure 6-9). This suggests that regions close to the surface are the most mechanically sensitive (Adachi et al., 2009a). It may be that remodelling is initiated near locations, where the BLC signal drops below a certain critical level, which would repair the crack and thereby return to 'normal' signal levels (Martin, 2000). Microcracks within 500 μm of the bone surface in compact bone are observed as was discussed in Chapter 3, Section 3.4, the corresponding effects on the BLC signalling have not yet been examined in any literature. However the results of current model suggest only a negligible effect in the signalling of BLC for the model with microcracks positioned deeper than 210μm below the bone surface. Thus, this study provides new information on the effects that microcracks may have on the initiation of bone remodelling by altering the BLC activity.

All simplifications and assumptions in the parameterisation of the cellular functions in this model were similar those in Chapter4. In conclusion, a simulation of the osteocyte-BLC network has been developed to investigate osteocyte signal propagation, the corresponding BLC signals, and the effect of microcracks with different properties on that signalling. The results clearly show that microcrack location has a marked effect on the signal at the BLCs on the bone surface.

Chapter 7 Discussion

7.1 Introduction

This chapter provides an overview of the work conducted throughout this project and describes how it supports and sheds more light on current theories of mechanotransduction. The main results are discussed here, as detailed discussions and analyses of the results have been conducted and validated in the corresponding chapters.

7.2 The basic model with asymmetrical communication and "calcium decay" factor

The importance of the osteocyte and bone lining cell network in the mechanotransduction processes of bone is well established, although the actual processes involved are still a matter of debate. Communication between osteocytes, via the inter-connecting lacuno-canalicular network through gap junctions, and between that network and bone lining cells seems high likely and a number of mechanisms have been proposed in the literature, and have been summarised in the earlier chapters of this thesis**.** Ausk et al. (2006) developed a simple model of the osteocyte network containing 81 osteocytes which were subjected to bending. In this model the osteocytes were activated by mechanical strain where the level of activity signal was dependent on the cell locations and according to specified activity thresholds. That signal was then radiated to neighbouring osteocytes to simulate intercellular communications through the

interconnecting canalicular and gap junctions. Ausk also examined the effect of heterogeneity for all the cellular functions. Based on these ideas, similar simulations of cell-to-cell communications are developed in Chapter 4 of this thesis to investigate osteocyte signal propagation, and the effect of heterogeneity on the signalling in a much more complex osteocyte network. The results confirm that inclusion of cell heterogeneity has a marked effect on the signal both at individual osteocytes and within the network as a whole, for instance, 15% heterogeneity led to an increase in mean network response signal of 27% after 100 seconds (iterations) (Figure 4-3). In addition to the figures presented in Chapter 4, the effect of heterogeneity is evident in the movies provided in Appendix C, the accompanying on CD. These short movies show the variation of the signals with different heterogeneities. They also run in real time during the simulation process. They clearly show that the network and mean BLC activity signals reach their maximum quicker as the degree of heterogeneity increased. Furthermore, the variations in the predicted mean network signals (as illustrated in Figure 4-2) compare well with the values reported in Ausk et al. (2006) (Figure 4-5). Apart from strain thresholds, secondary cell-cell communication thresholds were predefined in Ausk's model which indicated that activity signal from neighbours ($S_c(i,j,t)$) needed to surpass to initiate and maximally influence activity in the recipient cells. There is no evidence to support such a constraint on secondary cell-to-cell communication. Ausk also assumed that cell communication occurs between each osteocyte and all of its immediate neighbours, however, the concept of averaging cell activity within neighbourhoods is just a hypothesis. The activity

signals for each osteocyte in Ausk's model were governed by the comparison of two calculated signals, its own previous cell activity and the average signals from neighbours, but in the current research, the model was developed by applying a complex and bidirectional communication in the network (Chapter 5). In order to apply this bidirectional and asymmetrical communication in the network simulation, it was assumed that each cell could receive a signal from its neighbours ($S_g(i,j,t)$) while also simultaneously transmitting a signal ($S_l(i,j,t)$) to them. The activity signals ($S_0(i,j,t)$) of each osteocyte in current model in this thesis were calculated by propagation and transmission of signals from neighbours in addition to its own signal activity response to the strain at that point. Ausk's model was also limited in that it assumed symmetrical communication between only the osteocytes and totally ignored bone lining cells.

In the current research, once bone lining cells are also included in the model, on the surface of bone, attached to the osteocyte network. In the investigation in the effect of heterogeneity, the mean BLC signal increased rapidly to 100% activation with just 15% heterogeneity and an overall increase in mean BLC response of 34% (Figure 4-7). However, the results also show that homogenous simulations reach their maximal (albeit lower) activity signal level faster than the heterogeneous simulations. Moreover the trend for a rapid increase in mean BLC signal after stimulation compares well with the experiments ((Guo et al., 2006, Huo et al., 2010, Adachi et al., 2009a, Charras and Horton, 2002, Hung et al., 1996). They observed that osteoblasts respond to a mechanical stimulus with a dramatic increase in intracellular calcium signals, although in their experiments

single osteoblastic cells were stimulated rather than an entire osteocyte-BLC network.

The experiments performed by Adachi et al. (2009) indicated that the intercellular communications between osteocytes and bone surface cells are asymmetrical. They also measured the propagation factors, which are illustrated in Figure 5-1 and summarised in Table 5-1. In order to apply this bidirectional and asymmetrical communication in the network simulation, new equations were defined for the model, as discussed in Chapter 5. It was assumed that each cell is able to receive a signal from its neighbours while simultaneously transmitting a signal. The results of the simulation confirmed that the level of these propagation factors is critical and BLC activity could follow two different behaviours depending on the assumed values. Adachi's propagation factors scaled by 1.0905% were determined to be the critical values in the model (Figure 5-3). When less than these values, the mean BLC signal increased to reach a constant the maximum value (Figure 5-2), but, when more than these critical values, the mean BLC activity increased but declined again after peaks values were attained(Figure 5-3).

Charras and Horton (2002) also observed that when the stimulus was removed from the cell, intracellular calcium levels decreased, back to the baseline level. Based on this observation, it was assumed that over time different signals propagate throughout the osteocyte network to the bone lining cells, but gradually these signals decrease by a specified "calcium decay" (CD) at time 'T' where the calcium decay factor was applied to the model for all osteocytes. Thus, it appears

that the mean BLC activity, with the calcium decay factor included, reaches a peak then follows a significant decline. The same is true for the simulation where the applied propagation factor is greater than the critical value with different end point, however, the mean network signals decline considerably (Figure 5-4). The variations in the predicted mean BLC signals for different decay factors are illustrated in Figures 5-4 and 5-5a are similar to the observed intercellular calcium signals for BLC adjacent to the stimulated single osteocytes are predicted by Guo et al. (2006)(Figure 3-8) and Adachi et al. (2009) (Figure 5-5b) respectively. The variation in the predicted mean BLC signal with different CD factors also compares well, i.e. rapid increase after strain application , loading cycle duration (over 100 seconds) and a decrease after the CD application, with the some experiments *in vitro* and *in situ* (Charras and Horton, 2002, Hung et al., 1996, Huo et al., 2010). It seems that just by changing the value of the CD factor, the simulation can produce the mean BLC signal of different experiments. The results clearly show that the inclusion of asymmetrical communication and CD factor in the simulation, have a noticeable effect on the signal of the BLCs at the surface.

7.3 The effect of apoptosis and microcracks

Within the osteocyte and bone lining cell network there will inevitably be some osteocytes and their canalicular connections that function incorrectly due to the effects of apoptosis and microcracks. Apoptotic osteocytes can also occur in association with pathological conditions such as osteoporosis with 6% to 10% apoptosis (Qiu et al., 2003, Almeida et al., 2007). Furthermore, iliac cancellous bone

osteocyte density is reported to decline patients with vertebral fractures (Qiu et al., 2003, Almeida et al., 2007). There is evidence that in some diseases, such as osteoporosis, the number of apoptotic osteocytes is higher than normal, as discussed in Chapters 3 and 6. It seems likely that apoptosis and microcracks affect the functioning of the osteocyte network, explaining the higher rates of remodelling observed with osteoporosis. Furthermore microcrack formation followed by a disruption in the canalicular connections of the osteocyte network may possibly be the stimulus which initiates bone remodelling. It has been observed that a microcrack breaks the canaliculi of the lacunar network and induces osteocyte apoptotic death (Rochefort et al., 2010, Noble and Reeve, 2000, Seeman, 2006). Based on this observation, a "Life Coefficient" (LC) was introduced in the model for every osteocyte in the network to characterise the viability and allow the inclusion of effects such as microcracks and apoptotic osteocytes.

In the apoptotic simulations, the effect of the CD factor was assessed by running simulations with the calcium decay factor of 1% at 20 iterations (seconds) after strain application. All propagation factors are assumed to be exactly as they were measured by Adachi et al. (2009) as the corresponding results compared very well with the experiments discussed in Chapter 5. The effect of 1% CD factor was also examined at 26 seconds after strain application because in this case, the mean BLC activity could reach the maximum peak of 100% activity follow a great decline to baseline activity level. Where all cells are viable, the BLC response is relatively high and uniform (Figures 6-1a and 6-2a, at 20 seconds), reaching 100% activity after 26 seconds without calcium decay factor (Figure 6-4). In apoptotic

simulations, however, the BLC activity is reduced significantly. The simulations with 3% apoptosis led to a decline in peak BLC signal of 14% in the model without calcium decay factor and also with the CD factor at 26 seconds after strain application, but nearly a half of that decline was observed in the model with calcium decay, when it applied 20 seconds after strain application (Figures 6-4, 6-5 and 6-6). The variation in the BLC signal across the surface of the bone varies enormously (Figure 6-3), with mean surface signals varying by a standard deviation of 8% and 4.64% including CD factor in the model. The effect of apoptosis is demonstrated more clearly in the movies in the Appendix C on the CD. These short movies show the variation of the signals with different levels osteocyte apoptosis. They also run in real time during the simulation process. They clearly show that the network and mean BLC activity signals decreased as the degree of osteocyte apoptosis increased. The variations in the predicted mean BLC signals (Figures 6-4, 6-5 and 6-6) compare well with the general behaviour observed experimentally by Adachi et al. (2009a) (Figure 5-5b) and others (Charras and Horton, 2002, Guo et al., 2006, Hung et al., 1996, Huo et al., 2010). As expected, the greatest declines in BLC signal are observed when the apoptotic osteocytes occur nearest to the surface (Figures 6-3a and 6-3e). This also suggests that regions close to the surface are the most mechanically sensitive (Adachi et al., 2009a), and the location of the apoptotic osteocytes are more important than their density (Hedgecock et al., 2007, Qiu et al., 2003). It may be that remodelling is initiated at these locations, when the BLC signal drops below a certain critical level, which would remove and replace some of the most superficial osteocytes, but not those

deeper in the bone matrix, possibly making it vulnerable for further remodelling (Martin, 2000). The mean BLC activity signal decreased at peak by increasing the level of osteocyte apoptosis. It may refer to an increase the rate of bone remodelling in the study by Hedgecock et al. (2007) which showed that there was a direct relationship between the density of osteocyte apoptosis and the rate of remodelling. An increase in osteclast numbers with increasing osteocyte apoptosis was also reported in both cortical and trabecular bone by Clark et al. (2005) and Aguirre et al. (2006). Therefore, these findings and the results of the current model suggest that the rate of bone remodelling may be increased (by an increased the number of osteoclasts (bone resorption) as the degree of osteocyte apoptosis increase followed by decreasing of BLC activity signal on the bone surface. The results clearly show that the inclusion of apoptosis in the simulation has a marked effect on signalling at the BLCs on the bone surface. Most of the apoptotic osteocytes are in the bulk of the bone material, any resultant surface remodelling and replacement of affected osteocytes will therefore only have a minimal effect on the level of signalling at the surface. This may explain the mechanisms which lead to increased remodelling and the eventual bone loss observed in osteoporosis (Tatsumi et al., 2007).

In simulations with microcracks, the propagation factors were assumed to be exactly as they were measured by Adachi et al. (2009). The effect of the CD factor also added and was assessed by running simulations with the calcium decay factor of 1% at either 20 or 26 iterations (seconds) after strain application as the corresponding results compared very well with the experiments discussed in

Chapter 5. Then the effects of variety of microcracks with different length of 42μm, 168μm, 252μm and 1mm (Tables 3-2 and 3-3) at different positions of 42μm, 84μm, 126μm and 168μm below the surface (Figures 6-7 and 6-8) were examined on the signalling of BLCs and network. In simulations with microcracks, however, the peak BLC activity is reduced significantly with a tiny microcrack of just 42μm. When the microcrack located at 42μm below the surface, the signal is reduced by 67%, with or without calcium decay; with a continuing overall decline in network response (Figure 6-9c and d). The effect of variations in microcrack length at different locations on the BLC signal across the surface of the bone are examined in Figures 6-10, 6-11, 6-12 and 6-13: They show a decline in BLC signals, as the length of the microcrack increases at each location (Figures 6-10b, 6-11b, 6-12b and 6-13c) however, the decrease reduces as the distance from the bone surface increases (Figures 6-9). Although the average BLC activity levels decrease with the existence of a microcrack at any applied location (Figures 6-9d, 6-10a, 6-11a, 6-12a and 6-13b). No significant decline is observed in mean network activity with increasing length of microcrack even at 42 μm below the surface (Figures 6-10a and 6-11a). The radius of BLCs affected by a microcrack of 42μm in length is reduced as the distance of the microcrack from the bone surface increases. This ranges from 11 cells at 42μm below the surface to 7 cells at 168μm below the surface, and this change appears to be independent of microcrack length. The greatest declines in BLC signals are observed when the microcracks occur nearest to the surface (Figure 6-9). This suggests that regions close to the surface are the most mechanically sensitive (Adachi et al., 2009a). Furthermore, the computational

study of Gefen and Neulander (2007) suggested that a microcrack with minimal length of 48μm and minimal depth of 26μm from the bone surface is required to activate bone remodelling in trabecular bone. It may be that remodelling is initiated near locations, where the BLC signal drops, which would repair the crack and thereby return to 'normal' signal levels (Martin, 2000). Microcracks within 500 μm of the bone surface in compact bone (O'Brien et al., 2003) are observed as discussed in Chapter 3, Section 3.4, the corresponding effects on the BLC signalling have not yet been examined in any literature. However the results of current model suggest only a negligible effect on the signalling of BLC for the model with microcracks positioned deeper than 210μm below the bone surface. Thus, this study provides new information on the possible effects of microcracks and their ability to initiate bone remodelling by altering the BLC activity at the bone surface.

This is the first simulation of the osteocyte and bone lining cell network which has been used to examine the role of the network in mechanotransduction, and the effect of osteocyte apoptosis and microcrack on network signalling. Inevitably there are approximations and simplifications in the model that need further development.

Firstly, it was assumed that only osteocytes are sensitive to mechanical loading and generate the activity signal, however BLCs may also respond directly to strain (Cowin, 2002, Duncan and Turner, 1995). It was also assumed that the osteocytes, BLCs and network connections are distributed uniformly in two dimensions, while in actual bone of course, there is a very complex three

dimensional interconnecting lacuna-canalicular network, with differing numbers of neighbouring connections (Bonewald, 2011). In the simulation, the capacity of cells to communicate with each other was assumed to be unlimited, but *in vivo* it is known that cellular response declines during continuous activity due to the depletion of a variety of molecular stores (Berridge, 1993, Clapham, 1995, Hung et al., 1996). And finally, the effect of longitudinal microcracks was examined but transverse microcracks are also observed in cortical bones *in vivo* (Wasserman et al., 2008, Zioupos, 2001), the effects of which have yet to be considered.

Chapter 8 Conclusions and future work

8.1 Conclusions

The main aim of this thesis was to create and test a simulation of the osteocyte and BLC network to investigate osteocyte signal propagation, the corresponding BLC signals, and the effects of apoptosis and microcracks on the signalling. The results show that the inclusion of osteocyte apoptosis and microcracks in the model has a marked effect. Also, because the apoptotic osteocytes are located through the depth of the bone material, any resultant surface remodelling and resultant replacement of affected osteocytes will not fully restore the maximum level of signalling at the surface. This may explain the mechanism which leads to increased remodelling and the eventual bone loss observed in osteoporosis (Tatsumi et al., 2007). As discussed in Chapter 3 there is a limitation to the measure of depth of microcracks in *in vivo* experiments, this could be facilitated by using the computer simulation such as this research.

This study also shows how information about topography of microcracks in the osteocyte network of cortical bone can be proved based on the effects they have on the activity levels of bone lining cells, however, further development of this would be required. Also through the understanding of cell interactions and the genetic controls of bone cells particularly, functions such as osteocytic mechanosensing for detecting damage and signalling to the surface cells which activate appropriate responses have recently opened new pathways to drug

development for osteoporosis (Martin et al., 2008). The simulations developed here could provide a useful measurement to investigate such developments.

In brief, the main conclusions of this study are summarised below:

1. A basic simulation of cellular communication in the osteocyte and bone lining cell network has been developed, and the sensitivity to heterogeneity in cellular functions has been examined.
2. The simulation was integrated with asymmetric communications between osteocytes and bone lining cells and expanded to include calcium decay to simulate BLC response when the mechanical stimulus was removed.
3. The effect of osteocyte apoptosis on the signalling in the osteocyte-bone lining cell network was modelled.
4. Microcracks of various lengths and locations were considered and the effects of signalling on the bone surface and osteocyte network were modelled.

8.2 Future work

This simulation of the osteocyte-BLC network is far from complete and needs much further development.

It was assumed in the current model that the osteocytes, BLCs and network connections are distributed uniformly in two dimensions. The expansion of these simulations to actual bone with a very complex three dimensional interconnecting

lacuna-canalicular network, containing differing numbers of neighbourhood connections would be desirable, because osteocyte connectivity may also play a role in bone disease (Figure 2-6)(Knothe et al., 2004), as it discussed in Section 2.3.9.

Also, in the simulation, the capacity of the cells to communicate with each other was assumed to be unlimited, but *in vivo* it is known that cell response declines during continuous activity due to the depletion of a variety of molecular stores (Berridge, 1993, Clapham, 1995, Hung et al., 1996, Kabbara and Allen, 1999). This effect also needs to be included in future models.

Regarding microcrack examination, the effects of longitudinal microcracks only have been examined so far but transverse microcracks are also observed in cortical bones *in vivo* (Wasserman et al., 2008, Zioupos, 2001) so the effects of these transverse microcracks should also be considered in future work.

Since the activity signals of the mean BLC were found to be sensitive to values of propagation factors in Chapter5, a sensitivity study for the different propagation factors is required.

The effect of different loadings such as compression, should also be considered. Simulations with different strain distribution will also be modelled later. Furthermore, accurate strain values around microcrack should be included in future model.

The removal of a layer of bone to stimulate resorption then rebuilding with a new layer of healthy osteocytes would be one of the future model.

A further step is to combine the remodelling processes by osteoblasts and osteoclasts discussed earlier in this thesis, to produce a more realistic simulation of the mechanotransduction mechanism to represent the normal processes which bone undergoes together with mechanical loading on a large scale.

References

ADACHI, T., AONUMA, Y., ITO, S.-I., TANAKA, M., HOJO, M., TAKANO-YAMAMOTO, T. & KAMIOKA, H. 2009a. Osteocyte calcium signaling response to bone matrix deformation. *Journal of Biomechanics,* 42**,** 2507-2512.

ADACHI, T., AONUMA, Y., TAIRA, K., HOJO, M. & KAMIOKA, H. 2009b. Asymmetric intercellular communication between bone cells: Propagation of the calcium signaling. *Biochemical and Biophysical Research Communications,* 389**,** 495-500.

AGUIRRE, J. I., PLOTKIN, L. I., STEWART, S. A., WEINSTEIN, R. S., PARFITT, A. M., MANOLAGAS, S. C. & BELLIDO, T. 2006. Osteocyte apoptosis is induced by weightlessness in mice and precedes osteoclast recruitment and bone loss. *J Bone Miner Res,* 21**,** 605-15.

ALFORD, A. I., JACOBS, C. R. & DONAHUE, H. J. 2003. Oscillating fluid flow regulates gap junction communication in osteocytic MLO-Y4 cells by an ERK1/2 MAP kinase-dependent mechanism. *Bone,* 33**,** 64-70.

ALMEIDA, M., HAN, L., MARTIN-MILLAN, M., PLOTKIN, L. I., STEWART, S. A., ROBERSON, P. K., KOUSTENI, S., O'BRIEN, C. A., BELLIDO, T., PARFITT, A. M., WEINSTEIN, R. S., JILKA, R. L. & MANOLAGAS, S. C. 2007. Skeletal involution by age-associated oxidative stress and its acceleration by loss of sex steroids. *J Biol Chem,* 282**,** 27285-97.

ANDERSON, S. J., FURTH, M., WOLFF, L., RUSCETTI, S. K. & SHERR, C. J. 1982. Monoclonal antibodies to the transformation-specific glycoprotein encoded by the feline retroviral oncogene v-fms. *J Virol,* 44**,** 696-702.

AUBIN, J. E., LIU, F., MALAVAL, L. & GUPTA, A. K. 1995. Osteoblast and chondroblast differentiation. *Bone,* 17**,** 77S-83S.

AUBIN, J. E. & TRIFFITT, J. T. 2002. Chapter 4 - Mesenchymal Stem Cells and Osteoblast Differentiation. *In:* JOHN, P. B., LAWRENCE, G. R., GIDEON A. RODANA2 - JOHN P. BILEZIKIAN, L. G. R. & GIDEON, A. R. (eds.) *Principles of Bone Biology (Second Edition).* San Diego: Academic Press.

AUBIN, J. E. & TURKSEN, K. 1996. Monoclonal antibodies as tools for studying the osteoblast lineage. *Microsc Res Tech,* 33**,** 128-40.

AUSK, B. J., GROSS, T. S. & SRINIVASAN, S. 2006. An agent based model for real-time signaling induced in osteocytic networks by mechanical stimuli. *Journal of Biomechanics,* 39**,** 2638-2646.

AZARI, A., SCHOENMAKER, T., FALONI, A. P. D., EVERTS, V. & DE VRIES, T. J. 2011. Jaw and long bone marrow derived osteoclasts differ in shape and their response to bone and dentin. *Biochemical and Biophysical Research Communications,* 409**,** 205-210.

BARON, R., NEFF, L., ROY, C., BOISVERT, A. & CAPLAN, M. 1986. Evidence for a high and specific concentration of (Na+,K+)ATPase in the plasma membrane of the osteoclast. *Cell,* 46**,** 311-320.

BARRAGAN-ADJEMIAN, C., NICOLELLA, D., DUSEVICH, V., DALLAS, M. R., EICK, J. D. & BONEWALD, L. F. 2006. Mechanism by which MLO-A5 late

osteoblasts/early osteocytes mineralize in culture: Similarities with mineralization of lamellar bone. *Calcified tissue international,* 79**,** 340-353.

BASSO, N. & HEERSCHE, J. N. M. 2006. Effects of hind limb unloading and reloading on nitric oxide synthase expression and apoptosis of osteocytes and chondrocytes. *Bone,* 39**,** 807-814.

BATRA, N., KAR, R. & JIANG, J. X. Gap junctions and hemichannels in signal transmission, function and development of bone. *Biochimica et Biophysica Acta (BBA) - Biomembranes*.

BATRA, N., KAR, R. & JIANG, J. X. 2011. Gap junctions and hemichannels in signal transmission, function and development of bone. *Biochimica et Biophysica Acta (BBA) - Biomembranes*.

BÉLANGER, L. 1969. Osteocytic osteolysis. *Calcified tissue international,* 4**,** 1-12.

BELLIDO, T., ALI, A. A., GUBRIJ, I., PLOTKIN, L. I., FU, Q., O'BRIEN, C. A., MANOLAGAS, S. C. & JILKA, R. L. 2005. Chronic elevation of parathyroid hormone in mice reduces expression of sclerostin by osteocytes: a novel mechanism for hormonal control of osteoblastogenesis. *Endocrinology,* 146**,** 4577-83.

BELLIDO, T., ALI, A. A., PLOTKIN, L. I., FU, Q., GUBRIJ, I., ROBERSON, P. K., WEINSTEIN, R. S., O'BRIEN, C. A., MANOLAGAS, S. C. & JILKA, R. L. 2003. Proteasomal degradation of Runx2 shortens parathyroid hormone-induced anti-apoptotic signaling in osteoblasts. A putative explanation for why intermittent administration is needed for bone anabolism. *J Biol Chem,* 278**,** 50259-72.

BENNETT, M. V. L., CONTRERAS, J. E., BUKAUSKAS, F. F. & SAEZ, J. C. 2003. New roles for astrocytes: Gap junction hemichannels have something to communicate. *Trends in Neurosciences,* 26**,** 610-617.

BERRIDGE, M. J. 1993. Inositol trisphosphate and calcium signalling. *Nature,* 361**,** 315-325.

BIVI, N., LEZCANO, V., ROMANELLO, M., BELLIDO, T. & PLOTKIN, L. I. 2011. Connexin43 interacts with betaarrestin: a pre-requisite for osteoblast survival induced by parathyroid hormone. *J Cell Biochem,* 112**,** 2920-30.

BODINE, P. V. N., TRAILSMITH, M. & KOMM, B. S. 1996. Development and characterization of a conditionally transformed adult human osteoblastic cell line. *Journal of Bone and Mineral Research,* 11**,** 806-819.

BONEWALD, L. 2006a. Osteocytes as multifunctional cells. *J Musculoskelet Neuronal Interact,* 6**,** 331-3.

BONEWALD, L. F. 2004. Osteocyte biology: its implications for osteoporosis. *J Musculoskelet Neuronal Interact,* 4**,** 101-4.

BONEWALD, L. F. 2006b. Mechanosensation and Transduction in Osteocytes. *Bonekey Osteovision,* 3**,** 7-15.

BONEWALD, L. F. 2011. The amazing osteocyte. *Journal of Bone and Mineral Research,* 26**,** 229-238.

BONUCCI, E., BALLANTI, P., DELLA ROCCA, C., MILANI, S., LO CASCIO, V. & IMBIMBO, B. 1990. Technical variability of bone histomorphometric measurements. *bone Miner,* 11**,** 177-86.

BOYDE, A., JONES, S. J., PIPER, K. & KOMIYA, S. 1994. P16. Bigger is better is this true for osteoclasts? *Bone,* 15**,** 120-121.

BRONCKERS, A. L. J. J., GOEI, W., LUO, G., KARSENTY, G., DSOUZA, R. N., LYARUU, D. M. & BURGER, E. H. 1996. DNA fragmentation during bone formation in neonatal rodents assessed by transferase-mediated end labeling. *Journal of Bone and Mineral Research,* 11**,** 1281-1291.

BURGER, E. H. & KLEIN-NULEND, J. 1999. Mechanotransduction in bone--role of the lacuno-canalicular network. *The FASEB journal : official publication of the Federation of American Societies for Experimental Biology,* 13 Suppl**,** S101-12.

BURR, D. B., MILGROM, C., FYHRIE, D., FORWOOD, M., NYSKA, M., FINESTONE, A., HOSHAW, S., SAIAG, E. & SIMKIN, A. 1996. In vivo measurement of human tibial strains during vigorous activity. *Bone,* 18**,** 405-10.

BURR, D. B., TURNER, C. H., NAICK, P., FORWOOD, M. R., AMBROSIUS, W., HASAN, M. S. & PIDAPARTI, R. 1998. Does microdamage accumulation affect the mechanical properties of bone? *Journal of Biomechanics,* 31**,** 337-345.

BURR, S. T., IFJU, P. G. & MORRIS, D. H. 1995. A Method for Determining Critical Strain-Gauge Size in Anisotropic Materials with Large Repeating Unit Cells. *Experimental Techniques,* 19**,** 25-27.

BUSSE, B., DJONIC, D., MILOVANOVIC, P., HAHN, M., PUESCHEL, K., RITCHIE, R. O., DJURIC, M. & AMLING, M. 2010. Decrease in the osteocyte lacunar density accompanied by hypermineralized lacunar occlusion reveals failure and delay of remodeling in aged human bone. *Aging Cell,* 9**,** 1065-1075.

CHARRAS, G. T. & HORTON, M. A. 2002. Single cell mechanotransduction and its modulation analyzed by atomic force microscope indentation. *Biophysical Journal,* 82**,** 2970-2981.

CHENG, B. X., KATO, Y., ZHAO, S., LUO, J., SPRAGUE, E., BONEWALD, L. F. & JIANG, J. X. 2001a. PGE(2) is essential for gap junction-mediated intercellular communication between osteocyte-like MLO-Y4 cells in response to mechanical strain. *Endocrinology,* 142**,** 3464-3473.

CHENG, B. X., ZHAO, S. J., LUO, J., SPRAGUE, E., BONEWALD, L. F. & JIANG, J. X. 2001b. Expression of functional gap junctions and regulation by fluid flow in osteocyte-like MLO-Y4 cells. *Journal of Bone and Mineral Research,* 16**,** 249-259.

CHIBA, H., SAWADA, N., OYAMADA, M., KOJIMA, T., NOMURA, S., ISHII, S. & MORI, M. 1993. RELATIONSHIP BETWEEN THE EXPRESSION OF THE GAP JUNCTION PROTEIN AND OSTEOBLAST PHENOTYPE IN A HUMAN OSTEOBLASTIC CELL-LINE DURING CELL-PROLIFERATION. *Cell Structure and Function,* 18**,** 419-426.

CIVITELLI, R., BEYER, E. C., WARLOW, P. M., ROBERTSON, A. J., GEIST, S. T. & STEINBERG, T. H. 1993. CONNEXIN43 MEDIATES DIRECT INTERCELLULAR COMMUNICATION IN HUMAN OSTEOBLASTIC CELL NETWORKS. *Journal of Clinical Investigation,* 91**,** 1888-1896.

CLAPHAM, D. E. 1995. Replenishing the stores. *Nature,* 375**,** 634-635.

CONLON, I. & RAFF, M. 1999. Size Control in Animal Development. *Cell,* 96**,** 235-244.

COWIN, S. C. 1999. Bone poroelasticity. *J Biomech,* 32**,** 217-38.
COWIN, S. C. 2002. Mechanosensation and fluid transport in living bone. *Journal of musculoskeletal & neuronal interactions,* 2**,** 256-60.
COWIN, S. C., MOSS-SALENTIJN, L. & MOSS, M. L. 1991. Candidates for the mechanosensory system in bone. *J Biomech Eng,* 113**,** 191-7.
COWIN, S. C., WEINBAUM, S. & ZENG, Y. 1995. A case for bone canaliculi as the anatomical site of strain generated potentials. *J Biomech,* 28**,** 1281-97.
DALLAS, S. L. & BONEWALD, L. F. 2010. Dynamics of the transition from osteoblast to osteocyte.
DODD, J. S., RALEIGH, J. A. & GROSS, T. S. 1999. Osteocyte hypoxia: a novel mechanotransduction pathway. *American Journal of Physiology - Cell Physiology,* 277**,** C598-C602.
DONAHUE, H. J. 2000. Gap junctions and biophysical regulation of bone cell differentiation. *Bone,* 26**,** 417-22.
DOTY, S. B. & NUNEZ, E. A. 1985. ACTIVATION OF OSTEOCLASTS AND THE REPOPULATION OF BONE SURFACES FOLLOWING HIBERNATION IN THE BAT, MYOTIS-LUCIFUGUS. *Anatomical Record,* 213**,** 481-495.
DUCHER, G., DALY, R. M. & BASS, S. L. 2009. Effects of repetitive loading on bone mass and geometry in young male tennis players: a quantitative study using MRI. *J Bone Miner Res,* 24**,** 1686-92.
DUNCAN, R. L. & TURNER, C. H. 1995. Mechanotransduction and the functional response of bone to mechanical strain. *Calcified tissue international,* 57**,** 344-58.
DUNSTAN, C. R., EVANS, R. A., HILLS, E., WONG, S. Y. & HIGGS, R. J. 1990. Bone death in hip fracture in the elderly. *Calcified tissue international,* 47**,** 270-5.
EBIHARA, L. 2003. New roles for connexons. *News in Physiological Sciences,* 18**,** 100-103.
EL HAJ, A. J., MINTER, S. L., RAWLINSON, S. C., SUSWILLO, R. & LANYON, L. E. 1990. Cellular responses to mechanical loading in vitro. *J Bone Miner Res,* 5**,** 923-32.
ELMARDI, A. S., KATCHBURIAN, M. V. & KATCHBURIAN, E. 1990. Electron microscopy of developing calvaria reveals images that suggest that osteoclasts engulf and destroy osteocytes during bone resorption. *Calcified tissue international,* 46**,** 239-45.
EMERTON, K. B., HU, B., WOO, A. A., SINOFSKY, A., HERNANDEZ, C., MAJESKA, R. J., JEPSEN, K. J. & SCHAFFLER, M. B. 2010. Osteocyte apoptosis and control of bone resorption following ovariectomy in mice. *Bone,* 46**,** 577-583.
ERIKSEN, E. 2010. Cellular mechanisms of bone remodeling. *Reviews in Endocrine & Metabolic Disorders,* 11**,** 219-227.
FACCIO, R., CHOI, Y., TEITELBAUM, S. L. & TAKAYANAGI, H. 2011. 6 - The Osteoclast: The Pioneer of Osteoimmunology. *In:* JOSEPH, L., MD, YONGWON, C., PHD, MARK, H. & HIROSHI TAKAYANAGI, M. D. P. (eds.) *Osteoimmunology.* San Diego: Academic Press.
FERMOR, B., GUNDLE, R., EVANS, M., EMERTON, M., POCOCK, A. & MURRAY, D. 1998. Primary Human Osteoblast Proliferation and Prostaglandin E2 Release in Response to Mechanical Strain In Vitro. *Bone,* 22**,** 637-643.

FERMOR, B. & SKERRY, T. M. 1995. PTH/PTHrP receptor expression on osteoblasts and osteocytes but not resorbing bone surfaces in growing rats. *J Bone Miner Res,* 10**,** 1935-43.

FRITTON, J. C., MYERS, E. R., WRIGHT, T. M. & VAN DER MEULEN, M. C. H. 2005. Loading induces site-specific increases in mineral content assessed by microcomputed tomography of the mouse tibia. *Bone,* 36**,** 1030-1038.

FROST, H. M. 1960. In vivo osteocyte death. *J Bone Joint Surg Am,* 42-A**,** 138-43.

FROST, H. M. 1966. Bone dynamics in metabolic bone disease. *Bone Jt Surg,* 48**,** 1203.

FROST, H. M. 1992. Perspectives: Bone's mechanical usage windows. *Bone Miner,* 19**,** 257-271.

GALSON, D. L. & ROODMAN, G. D. 2011. 2 - Origins of Osteoclasts. *In:* JOSEPH, L., MD, YONGWON, C., PHD, MARK, H. & HIROSHI TAKAYANAGI, M. D. P. (eds.) *Osteoimmunology.* San Diego: Academic Press.

GOMEZ-HERNANDEZ, J. M., MIGUEL, M. C., LARROSA, B., GONZALEZ, D. & BARRIO, L. C. 2003. Molecular basis of calcium regulation in connexin-32 hemichannels. *Proceedings of the National Academy of Sciences of the United States of America,* 100**,** 16030-16035.

GOODENOUGH, D. A. & PAUL, D. L. 2003. Beyond the gap: Functions of unpaired connexon channels. *Nature Reviews Molecular Cell Biology,* 4**,** 285-294.

GRAMOUN, A., TREBEC, D. P., AZIZI, N., SODEK, J. & MANOLSON, M. F. 2009. Osteoclast activity is regulated by the extracellular matrix protein fibronectin eliciting different signaling pathways. *Bone,* 44, Supplement 2**,** S324.

GROSS, T. S., AKENO, N., CLEMENS, T. L., KOMAROVA, S., SRINIVASAN, S., WEIMER, D. A. & MAYOROV, S. 2001. Selected Contribution: Osteocytes upregulate HIF-1alpha in response to acute disuse and oxygen deprivation. *J Appl Physiol,* 90**,** 2514-9.

GROSS, T. S., KING, K. A., RABAIA, N. A., PATHARE, P. & SRINIVASAN, S. 2005. Upregulation of osteopontin by osteocytes deprived of mechanical loading or oxygen. *J Bone Miner Res,* 20**,** 250-6.

GUO, D. Y., KEIGHTLEY, A., GUTHRIE, J., VENO, P. A., HARRIS, S. E. & BONEWALD, L. F. 2010. Identification of osteocyte-selective proteins. *Proteomics,* 10**,** 3688-3698.

GUO, X. E., TAKAI, E., JIANG, X., XU, Q., WHITESIDES, G. M., YARDLEY, J. T., HUNG, C. T., CHOW, E. M., HANTSCHEL, T. & COSTA, K. D. 2006. Intracellular calcium waves in bone cell networks under single cell nanoindentation. *MCB Molecular and Cellular Biomechanics,* 3**,** 95-107.

H.J, D. 2000. Gap junctions and biophysical regulation of bone cell differentiation. *Bone,* 26**,** 417-422.

HAN, Y., COWIN, S. C., SCHAFFLER, M. B. & WEINBAUM, S. 2004. Mechanotransduction and strain amplification in osteocyte cell processes. *Proceedings of the National Academy of Sciences of the United States of America,* 101**,** 16689-94.

HARTER, L. V., HRUSKA, K. A. & DUNCAN, R. L. 1995. Human osteoblast-like cells respond to mechanical strain with increased bone matrix protein

production independent of hormonal regulation. *Endocrinology,* 136**,** 528-35.

HATTNER, R. & FROST, H. M. 1963. An Equation for the Mesenchymal Cell Activation Function in the Lamellar Bone Remodelling Equations. *Henry Ford Hosp Med Bull,* 11**,** 455-73.

HAZENBERG, J. G., FREELEY, M., FORAN, E., LEE, T. C. & TAYLOR, D. 2006. Microdamage: A cell transducing mechanism based on ruptured osteocyte processes. *Journal of Biomechanics,* 39**,** 2096-2103.

HEDGECOCK, N. L., HADI, T., CHEN, A. A., CURTISS, S. B., MARTIN, R. B. & HAZELWOOD, S. J. 2007. Quantitative regional associations between remodeling, modeling, and osteocyte apoptosis and density in rabbit tibial midshafts. *Bone,* 40**,** 627-637.

HEFTI, T., FRISCHHERZ, M., SPENCER, N. D., HALL, H. & SCHLOTTIG, F. 2010. A comparison of osteoclast resorption pits on bone with titanium and zirconia surfaces. *Biomaterials,* 31**,** 7321-7331.

HEINO, T. J., HENTUNEN, T. A. & VAANANEN, H. K. 2002. Osteocytes inhibit osteoclastic bone resorption through transforming growth factor-beta: enhancement by estrogen. *J Cell Biochem,* 85**,** 185-97.

HEINO, T. J., HENTUNEN, T. A. & VAANANEN, H. K. 2004. Conditioned medium from osteocytes stimulates the proliferation of bone marrow mesenchymal stem cells and their differentiation into osteoblasts. *Exp Cell Res,* 294**,** 458-68.

HEINO, T. J., KURATA, K., HIGAKI, H. & VÄÄNÄNEN, H. K. 2006. Development of a novel three-dimensional culture system to study the role of mechanically damaged osteocytes in the initiation of targeted bone remodeling. *Journal of Biomechanics,* 39, Supplement 1**,** S457.

HERNANDEZ, C. J., MAJESKA, R. J. & SCHAFFLER, M. B. 2004. Osteocyte density in woven bone. *Bone,* 35**,** 1095-1099.

HOFFLER, C. E., HANKENSON, K. D., MILLER, J. D., BILKHU, S. K. & GOLDSTEIN, S. A. 2006. Novel explant model to study mechanotransduction and cell-cell communication. *Journal of orthopaedic research : official publication of the Orthopaedic Research Society,* 24**,** 1687-98.

HUNG, C. T., ALLEN, F. D., POLLACK, S. R. & BRIGHTON, C. T. 1996. Intracellular Ca2+ stores and extracellular Ca2+ are required in the real-time Ca2+ response of bone cells experiencing fluid flow. *Journal of Biomechanics,* 29**,** 1411-1417.

HUO, B., KANG, Y. Y., HU, M. & LI, P. 2011. Advances of mechanical stimulation-induced calcium response and transfer in osteoblasts. *Yiyong Shengwu Lixue/Journal of Medical Biomechanics,* 26**,** 382-388.

HUO, B. B., LU, X. L. & GUO, X. E. 2010. Intercellular calcium wave propagation in linear and circuit-like bone cell networks. *Philosophical Transactions of the Royal Society A: Mathematical, Physical and Engineering Sciences,* 368**,** 617-633.

IMAI, S., KAKSONEN, M., RAULO, E., KINNUNEN, T., FAGES, C., MENG, X., LAKSO, M. & RAUVALA, H. 1998. Osteoblast recruitment and bone formation enhanced by cell matrix-associated heparin-binding growth-associated molecule (HB-GAM). *J Cell Biol,* 143**,** 1113-28.

ISHIHARA, Y., KAMIOKA, H., HONJO, T., UEDA, H., TAKANO-YAMAMOTO, T. & YAMASHIRO, T. 2008. Hormonal, pH, and calcium regulation of connexin 43-mediated dye transfer in osteocytes in chick calvaria. *J Bone Miner Res,* 23**,** 350-60.

JEDAMZIK, B., MARTEN, I., NGEZAHAYO, A., ERNST, A. & KOLB, H. A. 2000. Regulation of Lens rCx46-formed Hemichannels by Activation of Protein Kinase C, External Ca²⁺ and Protons. *Journal of Membrane Biology,* 173**,** 39-46.

JIANG, J. X., SILLER-JACKSON, A. J. & BURRA, S. 2007. Roles of gap junctions and hemichannels in bone cell functions and in signal transmission of mechanical stress. *Frontiers in Bioscience,* 12**,** 1450-1462.

JILKA, R. L., BELLIDO, T., ALMEIDA, M., PLOTKIN, L. I., O'BRIEN, C. A., WEINSTEIN, R. S. & MANOLAGAS, S. C. 2008. Chapter 13 - Apoptosis of Bone Cells. *In:* JOHN, P. B., LAWRENCE, G. R., T. JOHN MARTINA2 - JOHN P. BILEZIKIAN, L. G. R. & MARTIN, T. J. (eds.) *Principles of Bone Biology (Third Edition).* San Diego: Academic Press.

JILKA, R. L., WEINSTEIN, R. S., BELLIDO, T., ROBERSON, P., PARFITT, A. M. & MANOLAGAS, S. C. 1999. Increased bone formation by prevention of osteoblast apoptosis with parathyroid hormone. *Journal of Clinical Investigation,* 104**,** 439-446.

JILKA, R. L., WEINSTEIN, R. S., PARFITT, A. M. & MANOLAGAS, S. C. 2007. Quantifying osteoblast and osteocyte apoptosis: challenges and rewards. *J Bone Miner Res,* 22**,** 1492-501.

JOHNSON, L. C. 1966. The kinetics of skeletal remodeling in structural organization of the Skeleton. *Birth defects Original Article Series11***,** 66-142.

KABBARA, A. A. & ALLEN, D. G. 1999. The role of calcium stores in fatigue of isolated single muscle fibres from the cane toad. *Journal of Physiology,* 519**,** 169-176.

KAMIOKA, H., ISHIHARA, Y., RIS, H., MURSHID, S. A., SUGAWARA, Y., TAKANO-YAMAMOTO, T. & LIM, S. S. 2007. Primary cultures of chick osteocytes retain functional gap junctions between osteocytes and between osteocytes and osteoblasts. *Microscopy and Microanalysis,* 13**,** 108-117.

KANEHISA, J. & HEERSCHE, J. N. M. 1988. Osteoclastic bone resorption: In vitro analysis of the rate of resorption and migration of individual osteoclasts. *Bone,* 9**,** 73-79.

KATO, Y., BOSKEY, K., SPEVAK, L., DALLAS, M., HORI, M. & BONEWALD, L. F. 2001. Establishment of an osteoid preosteocyte-like cell MLO-A5 that spontaneously mineralizes in culture. *Journal of Bone and Mineral Research,* 16**,** 1622-1633.

KATO, Y., WINDLE, J. J., KOOP, B. A., MUNDY, G. R. & BONEWALD, L. F. 1997. Establishment of an osteocyte-like cell line, MLO-Y4. *Journal of Bone and Mineral Research,* 12**,** 2014-2023.

KIMMEL, D. B., FONG, T., AKHTER, M. P., COATS, J. & WRONSKI, T. 2011. Effects of PTH(1-34) and estrogen status on osteocyte lacunar properties in rats. *Bone,* 48**,** S97-S98.

KIMMEL, D. B., FONG, T., CANDELL, S., COATS, J., AKHTER, M. P. & WRONSKI, T. J. 2010. Estrogen status and PTH effects on osteocyte lacunae in rats. *Bone,* 47**,** S434-S434.

KLEINNULEND, J., SEMEINS, C. M., VELDHUIJZEN, J. P. & BURGER, E. H. 1993. Effect of Mechanical Stimulation on the Production of Soluble Bone Factors in Cultured Fetal Mouse Calvariae. *Cell and Tissue Research,* 271**,** 513-517.

KNOTHE TATE, M. & KNOTHE, U. 2000a. An ex vivo model to study transport processes and fluid flow in loaded bone. *J Biomech,* 33**,** 247 - 254.

KNOTHE TATE, M. L., ADAMSON, J. R., TAMI, A. E. & BAUER, T. W. 2004. The osteocyte. *The International Journal of Biochemistry & Cell Biology,* 36**,** 1-8.

KNOTHE TATE, M. L. & KNOTHE, U. 2000b. An ex vivo model to study transport processes and fluid flow in loaded bone. *Journal of Biomechanics,* 33**,** 247-254.

KNOTHE TATE, M. L., NIEDERER, P. & KNOTHE, U. 1998. In Vivo Tracer Transport Through the Lacunocanalicular System of Rat Bone in an Environment Devoid of Mechanical Loading. *Bone,* 22**,** 107-117.

KURATA, K., FUKUNAGA, T., MATSUDA, J. & HIGAKI, H. 2007. Role of mechanically damaged osteocytes in the initial phase of bone remodeling. *International Journal of Fatigue,* 29**,** 1010-1018.

LAKKAKORPI, P. T. & VÄÄNÄNEN, H. K. 1996. Cytoskeletal changes in osteoclasts during the resorption cycle. *Microsc Res Tech,* 33**,** 171-181.

LEE, S.-H., RHO, J., JEONG, D., SUL, J.-Y., KIM, T., KIM, N., KANG, J.-S., MIYAMOTO, T., SUDA, T., LEE, S.-K., PIGNOLO, R. J., KOCZON-JAREMKO, B., LORENZO, J. & CHOI, Y. 2006. v-ATPase V0 subunit d2-deficient mice exhibit impaired osteoclast fusion and increased bone formation. *Nature Medicine,* 12**,** 1403-1409.

LEE, T., STAINES, A. & TAYLOR, D. 2002. Bone adaptation to load: microdamage as a stimulus for bone remodelling. *J Anat,* 201**,** 437 - 446.

MANOLAGAS, S. C. 2000. Corticosteroids and fractures: a close encounter of the third cell kind. *J Bone Miner Res,* 15**,** 1001-5.

MANOLAGAS, S. C. 2006. Choreography from the tomb: An emerging role of dying osteocytes in the purposeful, and perhaps not so purposeful, targeting of bone remodeling. *BoneKEy-Osteovision,* 3.

MANOLAGAS, S. C. 2010. From estrogen-centric to aging and oxidative stress: A revised perspective of the pathogenesis of osteoporosis. *Endocrine Reviews,* 31**,** 266-300.

MANOLAGAS, S. C. & PARFITT, A. M. 2010. What old means to bone. *Trends in Endocrinology and Metabolism,* 21**,** 369-374.

MARIEB, E. N. & HOEHN, K. 2010. *Human anatomy & physiology*, Benjamin Cummings.

MARKS JR, S. C. & ODGREN, P. R. 2002. Chapter 1 - Structure and Development of the Skeleton. *In:* JOHN, P. B., LAWRENCE, G. R., GIDEON A. RODANA2 - JOHN P. BILEZIKIAN, L. G. R. & GIDEON, A. R. (eds.) *Principles of Bone Biology (Second Edition).* San Diego: Academic Press.

MAROTTI, G. 1996. The structure of bone tissues and the cellular control of their deposition. 101:25–79. *Ital J Anat Embryol=Arch Ital Anat,* 101**,** 25-79.

MAROTTI, G., FERRETTI, M., MUGLIA, M. A., PALUMBO, C. & PALAZZINI, S. 1992. A quantitative evaluation of osteoblast-osteocyte relationships on growing endosteal surface of rabbit tibiae. *Bone,* 13**,** 363-8.

MARTIN, R. B. 2000. Toward a unifying theory of bone remodeling. *Bone,* 26**,** 1-6.

MASON, D. J., HILLAM, R. A. & SKERRY, T. M. 1996. Constitutive in vivo mRNA expression by osteocytes of β-actin, osteocalcin, connexin-43, IGF-I, c-fos and c-jun, but not TNF-α nor tartrate-resistant acid phosphatase. *Journal of Bone and Mineral Research,* 11**,** 350-357.

MCNAMARA, L. M. & PRENDERGAST, P. J. 2007. Bone remodelling algorithms incorporating both strain and microdamage stimuli. *Journal of Biomechanics,* 40**,** 1381-1391.

MI, L. Y., BASU, M., FRITTON, S. P. & COWIN, S. C. 2005a. Analysis of avian bone response to mechanical loading, Part Two: Development of a computational connected cellular network to study bone intercellular communication. *Biomechanics and Modeling in Mechanobiology,* 4**,** 132-146.

MI, L. Y., FRITTON, S. P., BASU, M. & COWIN, S. C. 2005b. Analysis of avian bone response to mechanical loading - Part One: Distribution of bone fluid shear stress induced by bending and axial loading. *Biomechanics and Modeling in Mechanobiology,* 4**,** 118-131.

MILLER, S. C. 1987. THE BONE LINING CELL - A DISTINCT PHENOTYPE. *Calcified tissue international,* 41**,** 1-5.

MILLER, S. C., BOWMAN, B. M., SMITH, J. M. & JEE, W. S. S. 1980. CHARACTERIZATION OF ENDOSTEAL BONE-LINING CELLS FROM FATTY MARROW BONE SITES IN ADULT BEAGLES. *Anatomical Record,* 198**,** 163-173.

MILLER, S. C., SAINT-GEORGES, L. D., BOWMAN, B. M. & JEE, W. S. 1989. Bone lining cells: structure and function.

. *Scanning Microsc,* 3**,** 953-961.

MIYAUCHI, A., NOTOYA, K., OKABE, K., GOTO, M., TAKAGI, Y., MIKI, Y., TAKANO-YAMAMOTO, T., JINNAI, K., TAKAHASHI, K., KUMEGAWA, M., CHIHARA, K., FUJITA, T. & MIKUNI-TAKAGAKI, Y. 2000. PTH activates volume-sensitive calcium influx pathways through the activation of adenyl cyclase in mechanically loaded osteocytes. *Journal of Bone and Mineral Research,* 15**,** S224-S224.

MULLENDER, M. G. & HUISKES, R. 1997. Osteocytes and bone lining cells: Which are the best candidates for mechano-sensors in cancellous bone? *Bone,* 20**,** 527-532.

MULLENDER, M. G., HUISKES, R., VERSLEYEN, H. & BUMA, P. 1996. Osteocyte density and histomorphometric parameters in cancellous bone of the proximal femur in five mammalian species. *J Orthop Res,* 14**,** 972-9.

NICOLELLA, D. P., BONEWALD, L. F., MORAVITS, D. E. & LANKFORD, J. 2005. Measurement of microstructural strain in cortical bone. *Eur J Morphol,* 42**,** 23-9.

NICOLELLA, D. P., FENG, J. Q., MORAVITS, D. E., BONIVITCH, A. R., WANG, Y., DUSECICH, V., YAO, W., LANE, N. & BONEWALD, L. F. 2008. Effects of nanomechanical bone tissue properties on bone tissue strain: implications for osteocyte mechanotransduction. *J Musculoskelet Neuronal Interact,* 8**,** 330-1.

NICOLELLA, D. P., MORAVITS, D. E., GALE, A. M., BONEWALD, L. F. & LANKFORD, J. 2006. Osteocyte lacunae tissue strain in cortical bone. *Journal of Biomechanics,* 39**,** 1735-1743.

NIJHOUT, H. F. 2003. The control of body size in insects. *Developmental Biology,* 261**,** 1-9.

NIJWEIDE, P. J., VAN DER PLAS, A. & SCHERFT, J. P. 1981. Biochemical and histological studies on various bone cell preparations. *Calcified tissue international,* 33**,** 529-40.

NOBLE, B. 2008. The role of the osteocyte in bone turnover. *Bone,* 43**,** S22-S22.

NOBLE, B. S. 2000. Osteocyte death: Its biological significance. *Journal of Bone and Mineral Research,* 15**,** 823-823.

NOBLE, B. S., PEET, N., STEVENS, H. Y., BRABBS, A., MOSLEY, J. R., REILLY, G. C., REEVE, J., SKERRY, T. M. & LANYON, L. E. 2003. Mechanical loading: biphasic osteocyte survival and targeting of osteoclasts for bone destruction in rat cortical bone. *American Journal of Physiology-Cell Physiology,* 284**,** C934-C943.

NOBLE, B. S. & REEVE, J. 2000. Osteocyte function, osteocyte death and bone fracture resistance. *Mol Cell Endocrinol,* 159**,** 7-13.

NOBLE., PEET, N., STEVENS, H. Y., BRABBS, A., MOSLEY, J. R., REILLY, G. C., REEVE, J., SKERRY, T. M. & LANYON, L. E. 2003. Mechanical loading: biphasic osteocyte survival and targeting of osteoclasts for bone destruction in rat cortical bone. *Am J Physiol Cell Physiol,* 284**,** C934-43.

NONAKA, T., MATSUMOTO, H., SHIMADA, W., MIYAGI, I., OKADA, K., FUKAO, H., UESHIMA, S., KIKUCHI, H., TANAKA, S. & MATSUO, O. 1995. Effect of cyclic AMP on urokinase-type plasminogen activator receptor and fibrinolytic factors in a human osteoblast-like cell line. *Biochimica et Biophysica Acta (BBA) - Molecular Cell Research,* 1266**,** 50-56.

O'BRIEN, F. J., TAYLOR, D. & CLIVE LEE, T. 2005. The effect of bone microstructure on the initiation and growth of microcracks. *Journal of Orthopaedic Research,* 23**,** 475-480.

O'BRIEN, F. J., TAYLOR, D. & LEE, T. C. 2003. Microcrack accumulation at different intervals during fatigue testing of compact bone. *Journal of Biomechanics,* 36**,** 973-980.

OKADA, S., YOSHIDA, S., ASHRAFI, S. H. & SCHRAUFNAGEL, D. E. 2002. The canalicular structure of compact bone in the rat at different ages. *Microsc Microanal,* 8**,** 104-15.

PALUMBO, C., PALAZZINI, S. & MAROTTI, G. 1990a. Morphological-Study of Intercellular-Junctions during Osteocyte Differentiation. *Bone,* 11**,** 401-406.

PALUMBO, C., PALAZZINI, S., ZAFFE, D. & MAROTTI, G. 1990b. Osteocyte Differentiation in the Tibia of Newborn Rabbit: An Ultrastructural Study of the Formation of Cytoplasmic Processes. *Cells Tissues Organs,* 137**,** 350-358.

PARFITT, A. M. 1990. Bone forming cells in clinical conditions. *In:* BK, H. (ed.) *Bone: a treatise the osteoblast and osteocyte.* Caldwell: Telford Press.

PARFITT, A. M. 2002. Targeted and nontargeted bone remodeling: relationship to basic multicellular unit origination and progression. *Bone,* 30**,** 5-7.

PIENKOWSKI, D. & POLLACK, S. R. 1983. The origin of stress-generated potentials in fluid-saturated bone. *J Orthop Res,* 1**,** 30-41.

PIPER, K., BOYDE, A. & JONES, S. J. 1992. The relationship between the number of nuclei of an osteoclast and its resorptive capability in vitro. *Anat Embryol (Berl),* 186**,** 291-299.

PLOTKIN, L. I. & BELLIDO, T. 2001. Bisphosphonate-Induced, Hemichannel-Mediated, Anti-Apoptosis Through the Src/ERK Pathway: A Gap Junction-Independent Action of Connexin43. *Cell Communication and Adhesion,* 8**,** 377-382.

PLOTKIN, L. I., MANOLAGAS, S. C. & BELLIDO, T. 2002. Transduction of cell survival signals by connexin-43 hemichannels. *Journal of Biological Chemistry,* 277**,** 8648-8657.

QIU, S., RAO, D. S., PALNITKAR, S. & PARFITT, A. M. 2002. Relationships between osteocyte density and bone formation rate in human cancellous bone. *Bone,* 31**,** 709-11.

QIU, S., RAO, D. S., PALNITKAR, S. & PARFITT, A. M. 2003. Reduced iliac cancellous osteocyte density in patients with osteoporotic vertebral fracture. *J Bone Miner Res,* 18**,** 1657-63.

QUIST, A. P., RHEE, S. K., LIN, H. & LAL, R. 2000. Physiological role of gap-junctional hemichannels: Extracellular calcium-dependent isosmotic volume regulation. *Journal of Cell Biology,* 148**,** 1063-1074.

RANSJÖ, M., SAHLI, J. & LIE, A. 2003. Expression of connexin 43 mRNA in microisolated murine osteoclasts and regulation of bone resorption in vitro by gap junction inhibitors. *Biochemical and Biophysical Research Communications,* 303**,** 1179-1185.

RHEE, Y., BIVI, N., FARROW, E., LEZCANO, V., PLOTKIN, L. I., WHITE, K. E. & BELLIDO, T. 2011. Parathyroid hormone receptor signaling in osteocytes increases the expression of fibroblast growth factor-23 in vitro and in vivo. *Bone,* 49**,** 636-43.

ROBEY, P. G. 2002. Chapter 14 - Bone Matrix Proteoglycans and Glycoproteins. *In:* JOHN, P. B., LAWRENCE, G. R., GIDEON A. RODANA2 - JOHN P. BILEZIKIAN, L. G. R. & GIDEON, A. R. (eds.) *Principles of Bone Biology (Second Edition).* San Diego: Academic Press.

ROCHEFORT, G., PALLU, S. & BENHAMOU, C. 2010. Osteocyte: the unrecognized side of bone tissue. *Osteoporosis International,* 21**,** 1457-1469.

ROMANELLO, M. & D'ANDREA, P. 2001. Dual mechanism of intercellular communication in HOBIT osteoblastic cells: A role for gap-junctional hemichannels. *Journal of Bone and Mineral Research,* 16**,** 1465-1476.

ROODMAN, G. D. 1995. Osteoclast function in Paget's disease and multiple myeloma. *Bone,* 17**,** S57-S61.

ROODMAN, G. D. 1996. Paget's disease and osteoclast biology. *Bone,* 19**,** 209-212.

ROODMAN, G. D. 1999. Cell biology of the osteoclast. *Exp Hematol,* 27**,** 1229-1241.

ROSS, F. P. & TEITELBAUM, S. L. 2001. Chapter 3 - Osteoclast Biology. *In:* ROBERT, M., DAVID, F., JENNIFER KELSEYA2 - ROBERT MARCUS, D. F. & JENNIFER, K. (eds.) *Osteoporosis (Second Edition).* San Diego: Academic Press.

RUBIN, C. 1984. Skeletal strain and the functional significance of bone architecture. *Calcified tissue international,* 36**,** S11-S18.

RUIMERMAN, R., HILBERS, P., VAN RIETBERGEN, B. & HUISKES, R. 2005. A theoretical framework for strain-related trabecular bone maintenance and adaptation. *J Biomech,* 38**,** 931-41.

SAEZ, J. C., BERTHOUD, V. M., BRANES, M. C., MARTINEZ, A. D. & BEYER, E. C. 2003. Plasma membrane channels formed by connexins: Their regulation and functions. *Physiological Reviews,* 83**,** 1359-1400.

SCHIRRMACHER, K., NONHOFF, D., WIEMANN, M., PETERSONGRINE, E., BRINK, P. R. & BINGMANN, D. 1996. Effects of calcium on gap junctions between osteoblast-like cells in culture. *Calcified tissue international,* 59**,** 259-264.

SCHIRRMACHER, K., SCHMITZ, I., WINTERHAGER, E., TRAUB, O., BRUMMER, F., JONES, D. & BINGMANN, D. 1992. CHARACTERIZATION OF GAP-JUNCTIONS BETWEEN OSTEOBLAST-LIKE CELLS IN CULTURE. *Calcified tissue international,* 51**,** 285-290.

SCHNEIDER, P., MEIER, M., WEPF, R. & MÜLLER, R. 2010. Towards quantitative 3D imaging of the osteocyte lacuno-canalicular network. *Bone,* 47**,** 848-858.

SEEMAN, E. 2006. Osteocytes—martyrs for integrity of bone strength. *Osteoporosis International,* 17**,** 1443-1448.

SEEMAN, E. & DELMAS, P. D. 2006. Bone quality--the material and structural basis of bone strength and fragility. *N Engl J Med,* 354**,** 2250-61.

SISSONS, H. A., KELMAN, G. J., LING, L., MAROTTI, G., CANE, V. & MUGLIA, M. A. 1990. A light and scanning electron microscopic study of osteocyte activity in calcium-deficient rats. *Calcified tissue international,* 46**,** 33-7.

SKERRY, T. M., BITENSKY, L., CHAYEN, J. & LANYON, L. E. 1989. Early Strain-Related Changes in Enzyme-Activity in Osteocytes Following Bone Loading Invivo. *Journal of Bone and Mineral Research,* 4**,** 783-788.

SRINIVASAN, S. & GROSS, T. S. 2000. Canalicular fluid flow induced by bending of a long bone. *Med Eng Phys,* 22**,** 127-33.

SU, M., BORKE, J. L., DONAHUE, H. J., LI, Z., WARSHAWSKY, N. M., RUSSELL, C. M. & LEWIS, J. E. 1997. Expression of connexin 43 in rat mandibular bone and periodontal ligament (PDL) cells during experimental tooth movement. *Journal of Dental Research,* 76**,** 1357-1366.

SUZUKI, R., DOMON, T. & WAKITA, M. 2000. Some osteocytes released from their lacunae are embedded again in the bone and not engulfed by osteoclasts during bone remodeling. *Anat Embryol (Berl),* 202**,** 119-28.

TAKEDA, S., ELEFTERIOU, F., LEVASSEUR, R., LIU, X., ZHAO, L., PARKER, K. L., ARMSTRONG, D., DUCY, P. & KARSENTY, G. 2002. Leptin Regulates Bone Formation via the Sympathetic Nervous System. *Cell,* 111**,** 305-317.

TATSUMI, S., ISHII, K., AMIZUKA, N., LI, M., KOBAYASHI, T., KOHNO, K., ITO, M., TAKESHITA, S. & IKEDA, K. 2007. Targeted Ablation of Osteocytes Induces Osteoporosis with Defective Mechanotransduction. *Cell Metabolism,* 5**,** 464-475.

TAYLOR, A. F., SAUNDERS, M. M., SHINGLE, D. L., CIMBALA, J. M., ZHOU, Z. & DONAHUE, H. J. 2007. Mechanically stimulated osteocytes regulate osteoblastic activity via gap junctions. *American Journal of Physiology - Cell Physiology,* 292**,** C545-C552.

TEITELBAUM, S. L. 2007. Osteoclasts: What Do They Do and How Do They Do It? *Am J Pathol,* 170**,** 427-435.

TEITELBAUM, S. L. 2010. Stem Cells and Osteoporosis Therapy. *Cell Stem Cell,* 7**,** 553-554.

THI, M. M., KOJIMA, T., COWIN, S. C., WEINBAUM, S. & SPRAY, D. C. 2003. Fluid shear stress remodels expression and function of junctional proteins in cultured bone cells. *American Journal of Physiology-Cell Physiology,* 284**,** C389-C403.

TREBEC, D. P., CHANDRA, D., GRAMOUN, A., LI, K., HEERSCHE, J. N. & MANOLSON, M. F. 2007. Increased expression of activating factors in large osteoclasts could explain their excessive activity in osteolytic diseases. *Journal of Cellular Biochemistry,* 101**,** 205-20.

TURNER, C. 1998. Three rules for bone adaptation to mechanical stimuli. *Bone,* 23**,** 399 - 407.

TURNER, C., FORWOOD, M. & OTTER, M. 1994. Mechanotransduction in bone: do bone cells act as sensors of fluid flow? *The FASEB Journal,* 8**,** 875-878.

TURNER, C. & ROBLING, A. 2005. Mechanisms by which exercise improves bone strength. *J Bone Miner Metab,* 23**,** S16 - 22.

TURNER, C. H., YOSHIKAWA, T., FORWOOD, M. R., SUN, T. C. & BURR, D. B. 1995. High frequency components of bone strain in dogs measured during various activities. *J Biomech,* 28**,** 39-44.

VAANANEN, H. K., ZHAO, H., MULARI, M. & HALLEEN, J. M. 2000. The cell biology of osteoclast function. *J Cell Sci,* 113**,** 377-381.

VAN DER PLAS, A., AARDEN, E. M., FEIJEN, J. H. M., DE BOER, A. H., WILTINK, A., ALBLAS, M. J., DE LEIJ, L. & NIJWEIDE, P. J. 1994. Characteristics and properties of osteocytes in culture. *Journal of Bone and Mineral Research,* 9**,** 1697-1704.

VAN DER PLAS, A. & NIJWEIDE, P. J. 1992. Isolation and purification of osteocytes. *J Bone Miner Res,* 7**,** 389-96.

VAN HOVE, R. P., NOLTE, P. A., VATSA, A., SEMEINS, C. M., SALMON, P. L., SMIT, T. H. & KLEIN-NULEND, J. 2009. Osteocyte morphology in human tibiae of different bone pathologies with different bone mineral density — Is there a role for mechanosensing? *Bone,* 45**,** 321-329.

VASHISHTH, D., GIBSON, G., KIMURA, J., SCHAFFLER, M. B. & FYHRIE, D. P. 2002. Determination of bone volume by osteocyte population. *The Anatomical Record,* 267**,** 292-295.

VASHISHTH, D., VERBORGT, O., DIVINE, G., SCHAFFLER, M. B. & FYHRIE, D. P. 2000. Decline in osteocyte lacunar density in human cortical bone is associated with accumulation of microcracks with age. *Bone,* 26**,** 375-380.

VENO, P. A., ZHAO, J., GUTHRIE, J., KO, S., BONEWALD, L. F., DALLAS, M. R. & DALLAS, S. L. 2005. Osteocyte stimulation of chemotaxis and invasiveness of

breast cancer: A proteomic analysis. *Journal of Bone and Mineral Research,* 20**,** S215-S215.

WANG, L., WANG, Y., HAN, Y., HENDERSON, S., MAJESKA, R., WEINBAUM, S. & SCHAFFLER, M. 2005a. In situ measurement of solute transport in the bone lacunar-canalicular system. *Proc Natl Acad Sci,* 102**,** 11911 - 11916.

WANG, L., WANG, Y., HAN, Y., HENDERSON, S. C., MAJESKA, R. J., WEINBAUM, S. & SCHAFFLER, M. B. 2005b. In situ measurement of solute transport in the bone lacunar-canalicular system. *Proceedings of the National Academy of Sciences of the United States of America,* 102**,** 11911-11916.

WANG, Y., MCNAMARA, Y.L., SCHAFFLER, M.B., WEINBAUM,S. 2008. Strain amplification and intergin based signalling in osteocytes. *Journal of Musculoskeletal Neuronal Interactions,* 8**,** 332-334.

WASSERMAN, N., BRYDGES, B., SEARLES, S. & AKKUS, O. 2008. In vivo linear microcracks of human femoral cortical bone remain parallel to osteons during aging. *Bone,* 43**,** 856-861.

WEINBAUM, S., COWIN, S. C. & ZENG, Y. 1994. A model for the excitation of osteocytes by mechanical loading-induced bone fluid shear stresses. *Journal of Biomechanics,* 27**,** 339-360.

WEINSTEIN, R. S. & MANOLAGAS, S. C. 2000. Apoptosis and osteoporosis. *The American Journal of Medicine,* 108**,** 153-164.

WEINSTEIN, R. S., O'BRIEN, C. A., ALMEIDA, M., ZHAO, H., ROBERSON, P. K., JILKA, R. L. & MANOLAGAS, S. C. 2011. Osteoprotegerin prevents glucocorticoid-induced osteocyte apoptosis in mice. *Endocrinology,* 152**,** 3323-31.

WEINSTEIN, R. S., WAN, C., LIU, Q., WANG, Y., ALMEIDA, M., O'BRIEN, C. A., THOSTENSON, J., ROBERSON, P. K., BOSKEY, A. L., CLEMENS, T. L. & MANOLAGAS, S. C. 2010. Endogenous glucocorticoids decrease skeletal angiogenesis, vascularity, hydration, and strength in aged mice. *Aging Cell,* 9**,** 147-161.

WESTBROEK, I., DE ROOIJ, K. E. & NIJWEIDE, P. J. 2002a. Osteocyte-specific monoclonal antibody MAb OB7.3 is directed against Phex protein. *J Bone Miner Res,* 17**,** 845-53.

WESTBROEK, P., DE, S. J., DUBRUEL, P., TEMMERMAN, E. & SCHACHT, E. H. 2002b. Flow-through cell for on-line amperometric determination of Ce(lV) during polymerization reactions. *Anal Chem,* 74**,** 915-20.

WHITFIELD, J. F. 2003. Primary cilium - Is it an osteocyte's strain-sensing flowmeter? *Journal of Cellular Biochemistry,* 89**,** 233-237.

WILLECKE, K., EIBERGER, J., DEGEN, J., ECKARDT, D., ROMUALDI, A., GULDENAGEL, M., DEUTSCH, U. & SOHL, G. 2002. Structural and functional diversity of connexin genes in the mouse and human genome. *Biological Chemistry,* 383**,** 725-737.

WOLFF , J. D. 1892. Das Gesetz der Transformation der Knochen. Berlin: A. Hirschwald.

YAGI, M., MIYAMOTO, T., SAWATANI, Y., IWAMOTO, K., HOSOGANE, N., FUJITA, N., MORITA, K., NINOMIYA, K., SUZUKI, T., MIYAMOTO, K., OIKE, Y., TAKEYA, M., TOYAMA, Y. & SUDA, T. 2005. DC-STAMP is essential for cell–cell fusion in

osteoclasts and foreign body giant cells. *The Journal of Experimental Medicine,* 202**,** 345-351.

YAMAGUCHI, D. T., MA, D. F., LEE, A., HUANG, J. & GRUBER, H. E. 1994. ISOLATION AND CHARACTERIZATION OF GAP-JUNCTIONS IN THE OSTEOBLASTIC MC3T3-E1 CELL-LINE. *Journal of Bone and Mineral Research,* 9**,** 791-803.

YANG LI, C., MAJESKA, R. J., LAUDIER, D. M., MANN, R. & SCHAFFLER, M. B. 2005. High-dose risedronate treatment partially preserves cancellous bone mass and microarchitecture during long-term disuse. *Bone,* 37**,** 287-295.

YELLOWLEY, C. E., LI, Z., ZHOU, Z., JACOBS, C. R. & DONAHUE, H. J. 2000. Functional gap junctions between osteocytic and osteoblastic cells. *Journal of Bone and Mineral Research,* 15**,** 209-217.

YINGLING, V. R., DAVIES, S. & SILVA, M. J. 2001. The effects of repetitive physiologic loading on bone turnover and mechanical properties in adult female and male rats. *Calcified tissue international,* 68**,** 235-239.

YOU, L. D., TEMIYASATHIT, S., LEE, P. L., KIM, C. H., TUMMALA, P., YAO, W., KINGERY, W., MALONE, A. M., KWON, R. Y. & JACOBS, C. R. 2008. Osteocytes as mechanosensors in the inhibition of bone resorption due to mechanical loading. *Bone,* 42**,** 172-179.

ZHANG, D. Q. & MCMAHON, D. 2001. Gating of retinal horizontal cell hemi gap junction channels by voltage, Ca2+, and retinoic acid. *Molecular Vision,* 7**,** 247-252.

ZHANG, K. Q., BARRAGAN-ADJEMIAN, C., YE, L., KOTHA, S., DALLAS, M., LU, Y. B., ZHAO, S. J., HARRIS, M., HARRIS, S. E., FENG, J. Q. & BONEWALD, L. F. 2006a. E11/gp38 selective expression in osteocytes: Regulation by mechanical strain and role in dendrite elongation. *Mol Cell Biol,* 26**,** 4539-4552.

ZHANG, P., SU, M., TANAKA, S. & YOKOTA, H. 2006b. Knee loading stimulates cortical bone formation in murine femurs. *BMC Musculoskeletal Disorders,* 7**,** 73.

ZHAO, S., KATO, Y., ZHANG, Y., HARRIS, S., AHUJA, S. S. & BONEWALD, L. F. 2002. MLO-Y4 osteocyte-like cells support osteoclast formation and activation. *Journal of Bone and Mineral Research,* 17**,** 2068-2079.

ZHAO, W. G., BYRNE, M. H., WANG, Y. M. & KRANE, S. M. 2000. Osteocyte and osteoblast apoptosis and excessive bone deposition accompany failure of collagenase cleavage of collagen. *Journal of Clinical Investigation,* 106**,** 941-949.

ZHAO, Y. & GRIGORIADIS, A. E. 2002. The effects of c-fos overexpression on osteoclast differentiation in transgenic mice. *Journal of Bone and Mineral Research,* 17**,** 1340-1340.

ZIOUPOS, P. 2001. Accumulation of in-vivo fatigue microdamage and its relation to biomechanical properties in ageing human cortical bone. *J Microsc,* 201**,** 270-8.

Appendix A: A sample of MATLAB codes

```
%---- Cell activity based on Strain ----
for i=n:-1:1
   for j=m:-1:1
      E(i,j) =LC(i,j) * E(i,j);
      if HTmin(i,j)==HTmax(i,j)
         if E(i,j)>=HTmax(i,j)
          S(i,j)=100;
         else
           S(i,j)=0;
         end
      elseif E(i,j)<= HTmin(i,j)
        S(i,j)=0;
      elseif E(i,j)>=HTmin(i,j) && E(i,j)<HTmax(i,j)
        S(i,j)=100*(E(i,j)-HTmin(i,j))/(HTmax(i,j)-HTmin(i,j));
      else
       S(i,j)=100 ;
      end
       if E(i,j)==0
        S(i,j)=0;
       end
   end
end
%---- Neighbourhood ----
```

Appendix B: Publications

JAHANI, M., AHWAL, F., JI, B., PATTON, R., GENEVER, P., FAGAN, MJ. 2010. Simulation of osteocyte apoptosis on signalling in the osteocyte-bone lining cell network and implications for osteoporosis. Osteoporosis International 21:3, 514.

JAHANI, M., AHWAL, F., PATTON, R., GENEVER, P., FAGAN, MJ. 2010. The effect of osteocyte apoptosis on the signalling in the osteocyte network and at the bone lining cell surface: a computer simulation. Bone 47:1, 145-146,

JAHANI, M., AHWAL, F., PATTON, R., GENEVER, P., FAGAN, MJ. 2010. Simulation of osteocyte network signalling and the effect of osteocyte apoptosis. 17th Congress of the European Society of Biomechanics, Edinburgh, 5-8 July.

JAHANI, M., AHWAL, F., PATTON, R., GENEVER, P., FAGAN, MJ. 2011. The implications of apoptosis and microcracks in osteocyte-bone lining cell networks – a computer simulation, ISB Conference Brussels, 3-5 July.

JAHANI, M., AHWAL, F., PATTON, R., GENEVER, P., FAGAN, MJ. 2012. The effect of osteocyte apoptosis on signalling in the osteocyte- and bone lining cell network: a computer simulation, a paper submitted to the *Journal of Biomechanics*, February 2012

Appendix C: Videos on the CD